NAVAL POSTGRADUATE SCHOOL

MONTEREY, CALIFORNIA

THESIS

FLIGHT QUALIFICATION OF A TERAHERTZ IMAGING CAMERA AS A CUBESAT PAYLOAD

by

Sarah J. Kline

June 2018

Thesis Advisor: Wenschel D. Lan
Co-Advisor: James H. Newman

THIS PAGE INTENTIONALLY LEFT BLANK

REPORT DOCUMENTATION PAGE			*Form Approved OMB No. 0704-0188*

1. AGENCY USE ONLY *(Leave blank)*	**2. REPORT DATE** June 2018	**3. REPORT TYPE AND DATES COVERED** Master's thesis

4. TITLE AND SUBTITLE FLIGHT QUALIFICATION OF A TERAHERTZ IMAGING CAMERA AS A CUBESAT PAYLOAD	**5. FUNDING NUMBERS** RGM42
6. AUTHOR(S) Sarah J. Kline	
7. PERFORMING ORGANIZATION NAME(S) AND ADDRESS(ES) Naval Postgraduate School Monterey, CA 93943-5000	**8. PERFORMING ORGANIZATION REPORT NUMBER**
9. SPONSORING / MONITORING AGENCY NAME(S) AND ADDRESS(ES) DoD Space	**10. SPONSORING / MONITORING AGENCY REPORT NUMBER**

11. SUPPLEMENTARY NOTES The views expressed in this thesis are those of the author and do not reflect the official policy or position of the Department of Defense or the U.S. Government.

12a. DISTRIBUTION / AVAILABILITY STATEMENT Approved for public release. Distribution is unlimited.	**12b. DISTRIBUTION CODE** A

13. ABSTRACT (maximum 200 words)

This thesis builds on the existing research of the Sensor Research Laboratory and the Space Systems Academic Group (SSAG) at the Naval Postgraduate School (NPS) to integrate an 80-micron terahertz (THz) imaging camera (TIC) as a CubeSat payload. This research investigates the potential utility of THz imaging and long-wave infrared (IR) imaging at room-temperature (20°C) cooling for applications of national interest like space situational awareness (SSA). Long-wave IR imaging capability already exists, and typically requires a large cryocooler to maintain cryogenic temperatures (3–70 K); efficient IR imaging at room temperature is an emerging technology. Additionally, this thesis examines the integration and test effort associated with flight qualifying the TIC engineering development unit (EDU) onto the SSAG-developed High Altitude Balloon (HAB) bus. This thesis contributes to the overall objective of integrating and flight qualifying the TIC as a payload compatible with a variety of buses. Integrating and testing the TIC EDU on a CubeSat attains focused research objectives of national interest and supports Department of Defense Space efforts in the utilization of very small satellites.

14. SUBJECT TERMS terahertz imaging camera, TIC, CubeSat, High Altitude Balloon, HAB	**15. NUMBER OF PAGES** 125
	16. PRICE CODE

17. SECURITY CLASSIFICATION OF REPORT	**18. SECURITY CLASSIFICATION OF THIS PAGE**	**19. SECURITY CLASSIFICATION OF ABSTRACT**	**20. LIMITATION OF ABSTRACT**
Unclassified	Unclassified	Unclassified	UU

NSN 7540-01-280-5500 Standard Form 298 (Rev. 2-89) Prescribed by ANSI Std. 239-18

THIS PAGE INTENTIONALLY LEFT BLANK

Approved for public release. Distribution is unlimited.

FLIGHT QUALIFICATION OF A TERAHERTZ IMAGING CAMERA AS A CUBESAT PAYLOAD

Sarah J. Kline
Lieutenant, United States Navy
BA, Duke University, 2014

Submitted in partial fulfillment of the
requirements for the degree of

MASTER OF SCIENCE IN SPACE SYSTEMS OPERATIONS

from the

NAVAL POSTGRADUATE SCHOOL
June 2018

Approved by: Wenschel D. Lan
Advisor

James H. Newman
Co-Advisor

James H. Newman
Chair, Department of Space Systems Academic Group

THIS PAGE INTENTIONALLY LEFT BLANK

ABSTRACT

This thesis builds on the existing research of the Sensor Research Laboratory and the Space Systems Academic Group (SSAG) at the Naval Postgraduate School (NPS) to integrate an 80-micron terahertz (THz) imaging camera (TIC) as a CubeSat payload. This research investigates the potential utility of THz imaging and long-wave infrared (IR) imaging at room-temperature (20°C) cooling for applications of national interest like space situational awareness (SSA). Long-wave IR imaging capability already exists, and typically requires a large cryocooler to maintain cryogenic temperatures (3–70 K); efficient IR imaging at room temperature is an emerging technology. Additionally, this thesis examines the integration and test effort associated with flight qualifying the TIC engineering development unit (EDU) onto the SSAG-developed High Altitude Balloon (HAB) bus. This thesis contributes to the overall objective of integrating and flight qualifying the TIC as a payload compatible with a variety of buses. Integrating and testing the TIC EDU on a CubeSat attains focused research objectives of national interest and supports Department of Defense Space efforts in the utilization of very small satellites.

THIS PAGE INTENTIONALLY LEFT BLANK

TABLE OF CONTENTS

LIST OF FIGURES

LIST OF TABLES

THIS PAGE INTENTIONALLY LEFT BLANK

LIST OF ACRONYMS AND ABBREVIATIONS

A	Amperes
C&DH	Command and Data Handling
CAD	Computer-Aided Design
COTS	Commercial off-the-Shelf
DoD	Department of Defense
EDU	Engineering Development Unit
EPS	Electrical Power System
FPA	Focal Plane Array
GEO	Geostationary Orbit
GEVS	General Environmental Verification Standard
HFOV	Horizontal Field of View
I^2C	Inter-integrated Circuit
IP	Internet Protocol
IR	Infrared
NPS	Naval Postgraduate School
POL	Point of Load
RPO	Rendezvous and Proximity Operations
SSA	Space Situational Awareness
SSAG	Space Systems Academic Group
THz	Terahertz
TIC	Thermal Imaging Camera
TLYF	Test-Like-You-Fly
V	Volts
W	Watts
XSS-11	Experimental Satellite System 11

THIS PAGE INTENTIONALLY LEFT BLANK

ACKNOWLEDGMENTS

With immense gratitude and sincere appreciation, my first acknowledgement goes to Dr. Wenschel Lan, my thesis advisor. Thank you for allowing me to work on this project and for all your guidance along the way. Your time, patience, and energy spent toward helping me succeed and driving this project forward made the entire process immensely enjoyable. Truly, thank you.

Dr. James Newman, it is impossible to say thank you enough for all the opportunities you have made available to me. I feel extremely fortunate to have had the chance to complete a class, directed study, and thesis with you.

To all the staff of the SSAG, I can honestly say each one of you have stopped your day to help me complete a task when I know there was other work to be done. Dan Sakoda, David Rigmaiden, Alex Savattone, Giovanni Minelli, Jim Horning, Lara Magallanes, Ron Phelps, Levi Owen … thank you.

This thesis would not have come to be without the encouragement and support of the Starbucks at the Dudley Knox Library, Alison Scharmota at the Graduate Writing Center, and my classmates working alongside me in the Small Satellite Laboratory. Thank you.

And last, but certainly not least, I would like to thank my mother, Betsy Bates, for always being a phone call away with love, support, and encouragement. Without you, none of this would have happened.

THIS PAGE INTENTIONALLY LEFT BLANK

I. INTRODUCTION

This thesis is the culmination and exploitation of two feats of current scientific research and development. The first is the proliferation of the CubeSat platform and the second is the development of sensors and detectors to access the terahertz (THz) portion of the electromagnetic spectrum. Both fields have experienced an exponential increase in acceptance and use within the last five years. The ability to put a satellite on-orbit and the technological advancements to detect terahertz radiation creates an opportunity to put the world's first terahertz imaging camera (TIC) into space as a CubeSat payload.

This thesis contributes to an overall objective of flight qualifying a TIC as a CubeSat payload through two different areas of research. The first area of research investigates the potential uses and applications of terahertz imaging in space. Specifically, it examines the utility of a TIC payload as a means of on-orbit satellite inspection and far away space object detection. The second area of research commences the flight qualification process of integrating a TIC as a CubeSat payload. The effort begins with development testing of a TIC engineering development unit (EDU) through vibration and thermal vacuum testing. While the High Altitude Balloon (HAB) bus developed by the Space Systems Academic Group (SSAG) serves as a baseline for integration and testing, compatibility with other CubeSat buses will be maintained. The expected results include attaining a greater understanding of the potential applications of terahertz imaging in space and demonstrating the utility of the CubeSat and HAB platforms in testing evolving technologies.

A. TERAHERTZ IMAGING BACKGROUND

Terahertz imaging is a cutting-edge technology currently unused in space. Imaging in the terahertz region has the potential to reveal physical phenomena never seen before in that region of the electromagnetic spectrum. Characteristics of the wavelength include the ability to penetrate common materials such as clothing, cardboard, walls, and plastic, while not being able to penetrate metals [1]. Absorption of water vapor in the atmosphere restricts terahertz wave propagation and, consequently, limits applications on the Earth to a range

of meters to tens of meters. Space, on the other hand, is a medium with very little atmosphere and vast amounts of terahertz radiation being emitted from the sun.

Until recently, the terahertz region of the electromagnetic spectrum has been "almost inaccessible because of the lack of efficient sources and detectors" [2]. The first terahertz images were taken by B. B. Hu and M. C. Nuss in 1995 [3] and, since then, continued research has shown the utility of terahertz radiation in medical diagnostic purposes [4], law enforcement applications [5], and quality control [1]. Although interest in the terahertz range has grown in recent years, it is still the "least well-explored region of the electromagnetic spectrum" [1]. The natural progression of the evolving technology leads to the opportunity for those in the space community to test terahertz imaging in space.

The TIC developed by the Sensor Research Laboratory at the Naval Postgraduate School (NPS) includes an uncooled (room temperature), metamaterial-based micro-electro-mechanical system (MEMS) focal plane array (FPA). The FPA absorbs terahertz radiation (80-micron, far infrared), and a micro-bolometer is used to create images in the long-wave infrared (IR) region (8-14 microns), which can be captured by an IR camera. The objective of the SSAG at NPS is to integrate the TIC as a CubeSat payload and reinforce the CubeSat and HAB platform as an operationally responsive capability effective in demonstrating advanced technologies.

B. CUBESAT BACKGROUND

The classification of small satellites called "CubeSats" refers to a satellite whose volume is a multiple of a cube measuring 10 x 10 x 10 centimeters (cm) [6]. This baseline standard is defined as a "1U" CubeSat. A "2U" CubeSat is 10 x 10 x 20 cm, a "3U" CubeSat is 10 x 10 x 30 cm, and as expected, additional sizes follow by a form factor of 10. Additional sizes like 6U, 12U, and 27U are proliferating as well. While a CubeSat is defined by volume, small satellites can also be classified by mass with nomenclature such as picosatellite, nanosatellite, microsatellite, and minisatellite. CubeSats span across different types of small satellite names depending on the weight, visually represented by Figure 1.

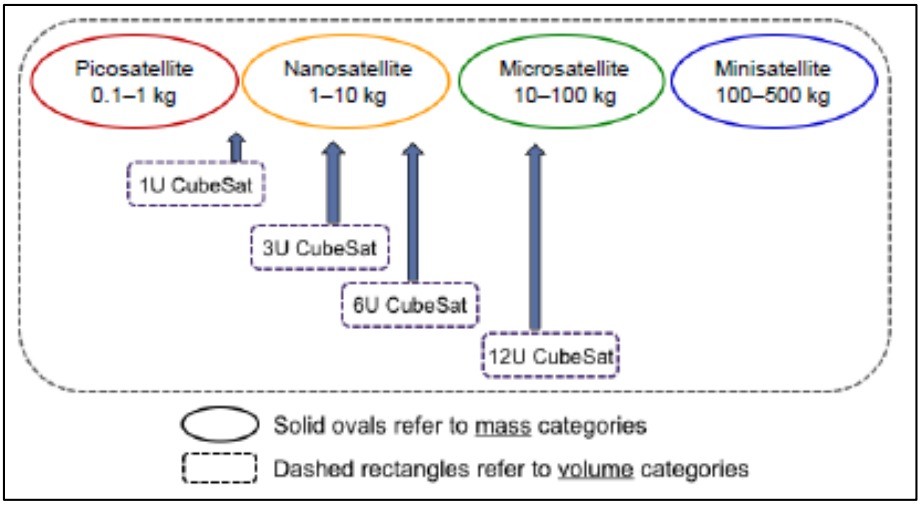

Figure 1. Small Satellite Nomenclature. Source: [6].

The first CubeSat was launched in 2000; since then, the platform has revolutionized how academia, the commercial industry, and the military interact with space [7]. As shown in Figure 2, the number of CubeSat launches per year exponentially increased in 2013, the "breakout year" for CubeSats [6]. Now, CubeSat launches commonly occur due to U.S. and foreign launch rideshare opportunities and launches from the International Space Station [6].

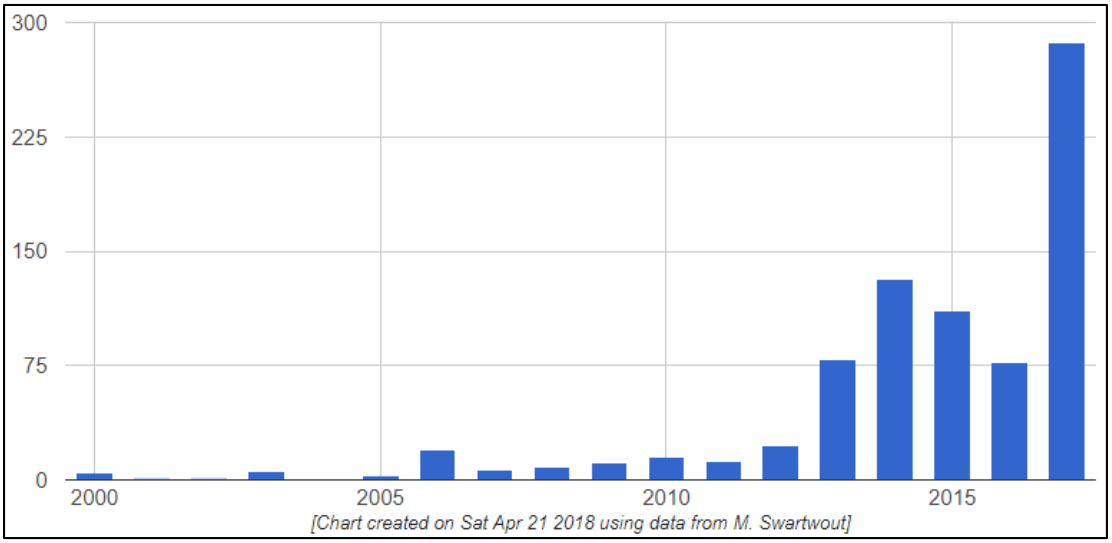

Figure 2. Small Satellites Launched from 2000–2018. Source: [7].

Unique to the CubeSat platform is the ability to create a relatively low-cost, minimally complex satellite in a relatively short amount of time. Without requiring big budgets, timelines, or resources, CubeSats allow for a whole new populace of users to access space. Additionally, it allows for even the big space users, like the military, to use space in a different way than before. The exquisite satellite constellations produced by the military cost billions of dollars and take decades to produce [8]. Commonly described as "quick" and "responsive" [9], CubeSats can be developed and positioned on-orbit considerably more quickly than a standard, large satellite. The flexible nature of CubeSats provides a platform to test and integrate a TIC for space-based purposes.

C. HAB BACKGROUND

Similar to how CubeSats can provide a low-cost, responsive means to demonstrate technologies in space, the HAB platform delivers an even cheaper and faster method to simulate a "near-space" environment through hoisting a bus and payload using a balloon. Within the SSAG at NPS, HAB flights provide hands-on experience to students in designing, testing, and operating a satellite. Without actually launching a satellite into orbit, students can fly a HAB to "near-space," around 100,000 feet, and interact with the hoisted bus and payload from ground stations, simulating an over-head satellite pass. The selection of the HAB bus for testing purposes leverages the experience and hardware availability within the SSAG.

The SSAG-developed HAB consists of a bus and payload designed within the CubeSat standard. The bus includes the major subsystems such as Command and Data Handling (C&DH), Communications, and the Electrical Power System (EPS), pictured in Figure 3 and Figure 4. The C&DH subsystem uses a Raspberry Pi Zero single-board computer to accomplish telemetry and data processing. The Communications subsystem consists of a radio mount attached to the Raspberry Pi Zero single-board computer and a monopole antenna for directional signal transmission. The EPS supplies power to the bus through batteries and solar panels. Additional bus components include two parachutes, one Global Positioning System (GPS) receiver (BYONICS GPS4), one Satellite Position and Tracker (SPOT) Trace, one Raspberry Pi camera, one thermistor, and two Firgelli motors

to release one of the parachutes and the balloon. One parachute is released by command, and the second parachute is released automatically at a predetermined altitude set before the HAB flight. Figure 5 visually depicts the HAB structure in flight hoisted by a balloon, and Figure 6 shows a HAB structure with both parachutes deployed for landing.

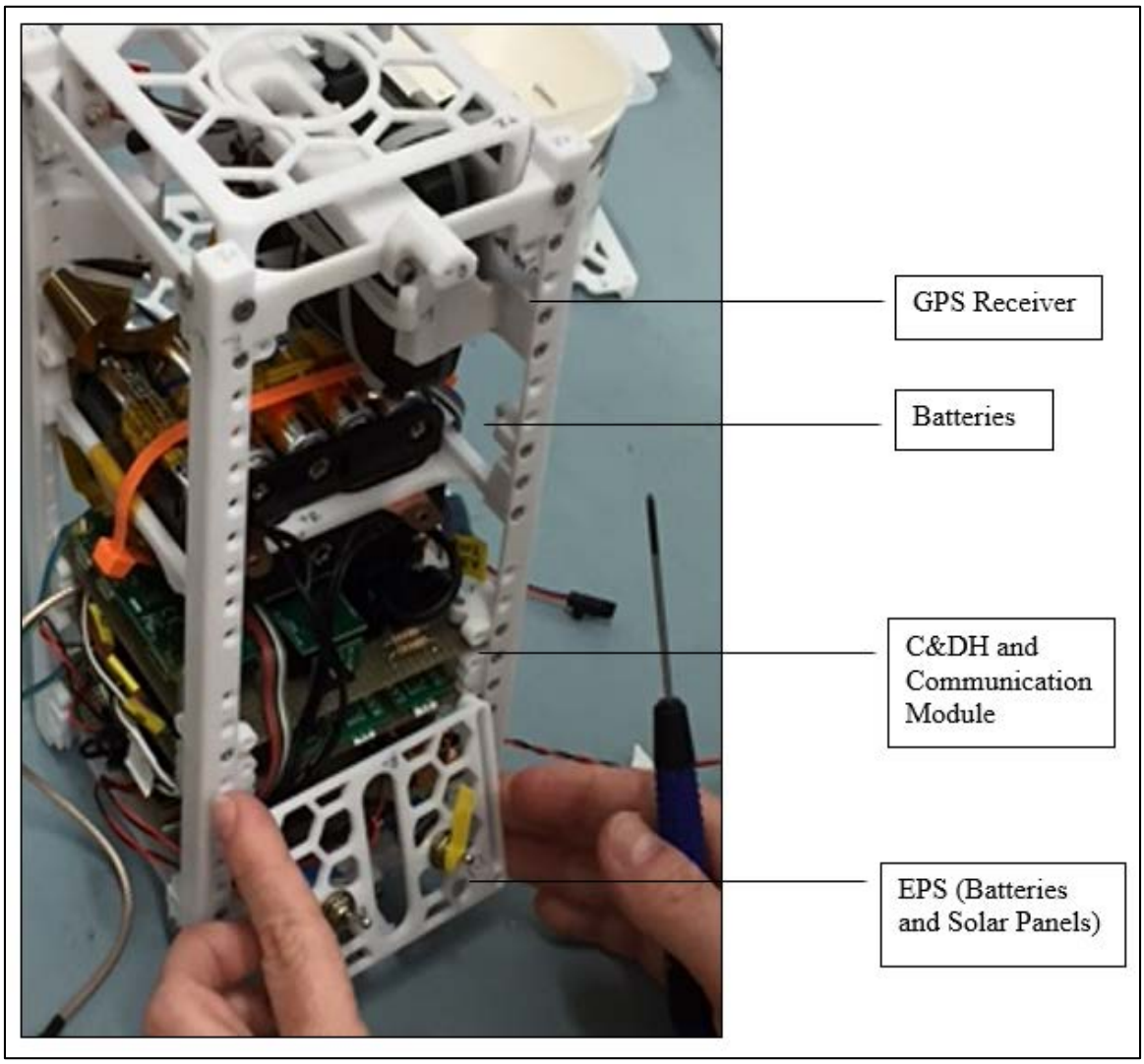

Figure 3. 2U CubeSat HAB Structure and Basic Components.
Adapted from [10].

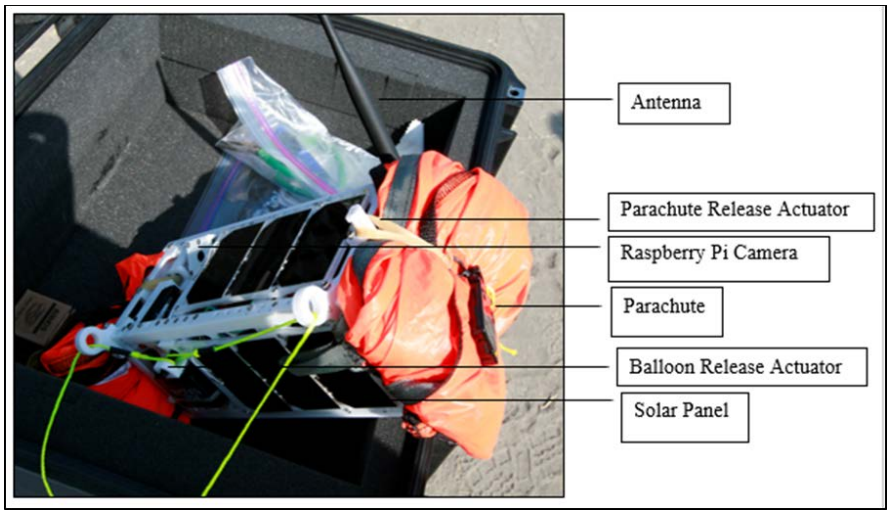

Figure 4. 2U CubeSat HAB Structure and Basic Components Continued. Adapted from [10].

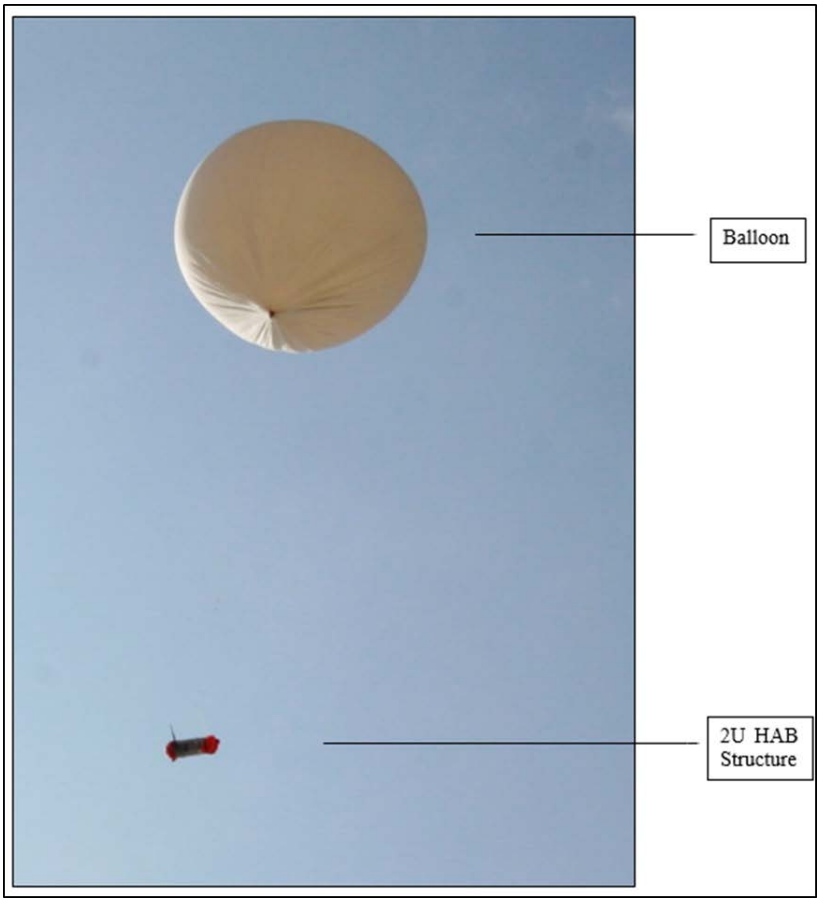

Figure 5. 2U HAB in Flight. Adapted from [10].

Figure 6. HAB Landing with Two Parachutes Deployed. Source: [10].

D. THESIS PURPOSE AND OBJECTIVE

The first objective of this thesis is to explore the utility of terahertz imaging in space. A satellite with a TIC payload may provide a non-destructive, non-invasive means of inspection and analysis by scanning the interior components on a non-functioning satellite. Furthermore, as the sun radiates significant energy in the terahertz range, a satellite with a TIC payload may see other objects in space, like satellites and debris, from far away. Another objective of this thesis is to perform developmental testing, in support of the flight qualification effort of integrating a TIC as a CubeSat payload, through vibration and thermal vacuum testing of the TIC EDU on the HAB bus.

This thesis builds on the existing research of the Sensor Research Laboratory and the SSAG at NPS, and future master's thesis students will contribute to the overall objective of putting a TIC payload in space. Lt Col Marcello Correa de Souza of the Brazilian Air Force conducted two HAB flights with the TIC EDU [11]. His work started the integration process of the TIC EDU onto the HAB bus. In continuation of the existing research, this thesis explores the potential applications of a TIC payload in space and begins the flight qualification process by conducting developmental tests on the TIC EDU. Future work includes conducting a HAB flight with the TIC payload, completing integration and acceptance testing on the payload flight unit, and integrating the TIC with the CubeSat bus

to perform system-level acceptance testing. Table 1 shows the past, current, and future work of the SSAG to achieve the objective of putting a TIC in space as a CubeSat payload. Overall, the integration and testing of the TIC on a CubeSat attains focused research objectives of national interest and supports DoD Space efforts in the utilization of very small satellites.

Table 1. Summary of Master's Thesis Work in the SSAG for Overall Objective of Putting a Terahertz Imaging Camera in Space as a CubeSat Payload

Topic	**Student Name**	**Scope of Thesis**	**Future Work**
NPS Terahertz Project: IR HAB Flight Testing and Integration [11]	Marcello Correa de Souza, Lt Col, Brazilian Air Force	Conducted two HAB flights with TIC EDU	Conduct a HAB flight with TIC payload
Flight Qualification of a Terahertz Imaging Camera as a CubeSat Payload [12]	Sarah Kline, LT, USN	Explored potential applications of a TIC payload & began flight qualification process by conducting developmental tests of TIC EDU	Integration and acceptance testing on payload Flight Unit & integrate payload Flight Unit with CubeSat bus to perform system-level acceptance testing

II. SPACE OPERATIONS OF THE TIC PAYLOAD

This chapter explores the characteristics of terahertz imaging and the potential applications of a TIC in space. Currently, according to the best knowledge of the author, no terahertz imaging payloads exist in space. However, the terahertz portion of the electromagnetic spectrum exhibits unique characteristics that may have practical applications for use in space, such as on-orbit satellite inspection and far away detection of space objects by reflected terahertz radiation.

A. CHARACTERISTICS OF TERAHERTZ IMAGING

Until the late 1990s, the field of terahertz science and technology faced significant challenges due to "a lack of suitable sources, sensitive detectors, and other components for the manipulation of radiation in this wavelength range" [1]. Within the past decade, the research field has dramatically evolved due to technological advancements and "the promise of valuable new applications" [1]. The terahertz region of the electromagnetic spectrum lies between the IR and the microwave, or between 30 micron meters and 3 millimeters in wavelength and 10^{11} to 10^{13} Hz in frequency, as shown in Figures 7 and 8.

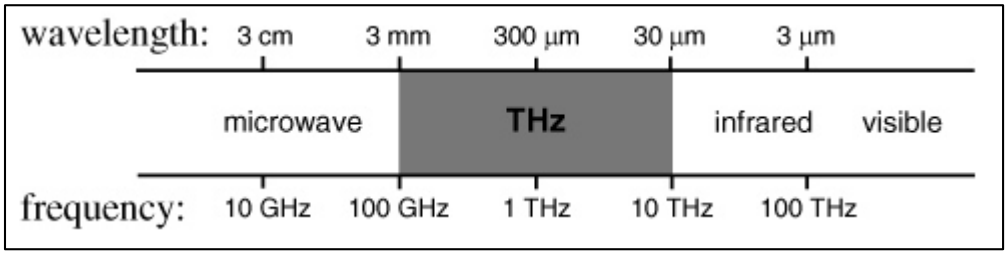

Figure 7. The Terahertz Region of the Electromagnetic Spectrum. Source: [1].

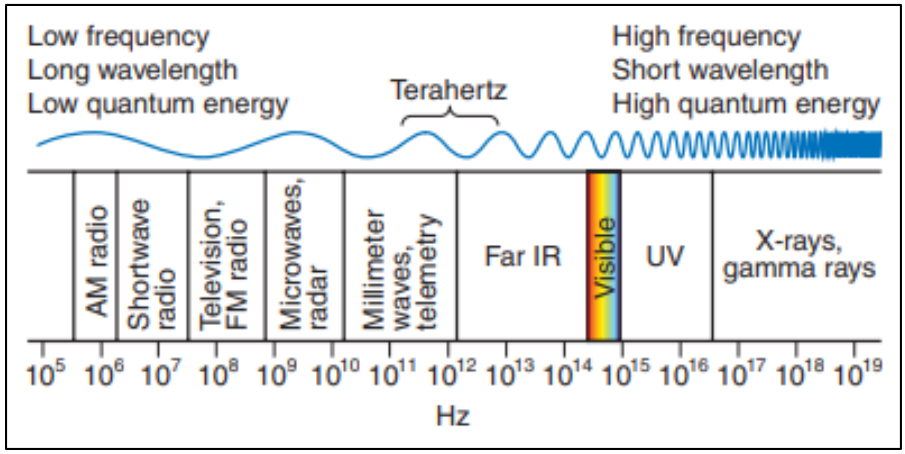

Figure 8. The Electromagnetic Spectrum from AM Radio to Gamma Rays. Source: [2].

Because of the location of the THz region, the techniques developed for terahertz imaging mirrored technologies from the IR and microwave fields of study. While at first borrowing concepts from established disciplines like synthetic aperture radar and x-rays, scientists and scholars have since developed methods unique to terahertz imaging [2].

Terahertz imaging occurs through passive radiation and the terahertz radiation can penetrate paper, textiles, plastics, wood, ceramics, semiconductors, frozen materials, clothing, cardboard, and walls as well as characterize powders and electronics [2]. Terahertz and x-ray waves are similar in that they both penetrate most solid materials, but unlike x-ray imaging, terahertz imaging can use passive radiation. The passive nature of terahertz radiation parallels characteristics of IR imaging. A distinct difference between the two, though, is terahertz radiation's ability to penetrate these many solid materials [2]. Scientists in the biomedical field recognize the benefits of terahertz radiation in medical applications [13]. Although still in the early stages of developing terahertz instrumentation, terahertz spectroscopy and imaging show promise in identifying "abnormal tissues faster and more accurately" than current methods, including x-ray systems [13]. In comparison to other inspection techniques, terahertz is unique in its nondestructive, nonhazardous ability to penetrate a wide variety of materials.

Although no terahertz imaging payloads have been launched into space, terahertz imaging applications are quickly developing on the earth. For example, in 2013, the New

York City Police Department (NYPD) received a "T-Ray machine" in order to assist in identifying concealed weapons [5]. Since terahertz radiation cannot penetrate metals, the terahertz imaging device could scan a person's body and reveal knives, guns, and other metallic-based weapons hidden under clothing, in book bags, or inside suitcases. Primarily, terahertz imaging applications remain in scientific labs. However, practical applications like counterfeit electronic identification [4], drug detection and identification through packaging materials [1], and concealed weapon detection [5], to name a few, seem promising. The evolving technology allows the opportunity to test the application of terahertz imaging in space, specifically for on-orbit satellite inspection and far away object detection.

B. ON-ORBIT SATELLITE INSPECTION

The material penetration characteristics of terahertz imaging opens the door for a state-of-the-art, on-orbit satellite inspection capability. Ideally, the TIC payload captures images in close proximity to the object requiring inspection, necessitating rendezvous and proximity operations (RPO). Due to the proliferation of RPO in the last decade, the required proficiency and technology to conduct proximity operations is readily available. The following sections present the current research of terahertz imaging as a means of material inspection, examine the history of RPO, and introduce a case study of a TIC payload conducting an on-orbit satellite inspection of a non-functioning satellite through proximity operations.

1. Terahertz Imaging as a Means of Material Inspection

Scholars from the University of Connecticut's Department of Electrical and Computer Engineering found that terahertz radiation performed excellently in comparison to current x-ray techniques in the ability to "image the interior structures and constituent materials of a wide variety of objects including Integrated circuits (ICs)" [4]. Terahertz radiation penetrated the electronic materials and subsequently allowed for the observation of different layers of the electronic components, including die and lead geometries. Researchers at the Department of Materials Science and Engineering from the Graduate School of Engineering at Tohoku University in Japan found that terahertz radiation

provided “quantitative detection” of disconnected aluminum electrical wires [14]. Additionally, according to a summary of current terahertz radiation applications from the Department of Electrical and Computer Engineering at Rice University, terahertz emission techniques successfully identified damaged electrical circuits through the characterization of the electrical field of the component [1]. Each study commented on the passive nature of terahertz imaging. The non-destructive means of inspection may be important for such applications as materials inspection and the characterization of electrical components.

2. History and Background of Rendezvous and Proximity Operations

Advanced capabilities and technologies are a critical component to space safety and sustainability. As space becomes increasingly congested, contested, and competitive, activities like RPO are increasingly vital in minimizing vulnerabilities of U.S. military, civil, and commercial sector assets. Proximity operations, the maneuvering of one satellite alongside a second satellite, enable debris removal and on-orbit servicing, refueling, and docking. Although spacecraft design was once viewed as a one-shot product, technology now supports on-orbit adjustments or maintenance. Space security expert and former United States Air Force (USAF) officer, Brian Weeden, asserts that RPO activity will only increase in the coming years, especially in the international community and commercial sector [15]. With the proliferation of the RPO capability, particularly within the commercial sector, now is the time to incorporate a new technology, like terahertz imaging, with the available maneuver. The commercial sector has not always proficiently conducted RPO, though, and throughout the past five decades, the United States military dominated RPO technology [15].

The first RPO in space occurred over fifty years ago, on December 15, 1965, between two manned NASA spacecraft, the Gemini VI-A and the Gemini VII [16]. Gemini VI-A launched into orbit on December 14th and conducted a series of maneuvers to rendezvous with Gemini VII, which launched into orbit on December 4th [16]. While orbiting 185 miles above the Earth [17], the Gemini spacecraft and the astronauts inside them maintained a “nose-to-nose” distance for approximately five hours [16]. Although the Soviet Union, in 1962 and 1963, launched manned spacecraft into orbit within miles of

each other, the spacecraft did not have any maneuvering abilities to conduct proximity operations. Therefore, the Soviet Union could not claim the first RPO in space [16]. Since 1965, RPO technologies and capabilities have proliferated throughout the commercial, civil, and military sectors in the United States and have allowed the United States to maintain superiority in its execution [15].

The U.S. military owns several programs which have "demonstrated far more advanced RPO technologies and capabilities than Russia or China" [15]. The Geosynchronous Space Situational Awareness Program (GSSAP), declassified in 2014, includes satellites in geosynchronous orbit (GEO) that conduct maneuvers to "provide characterization of other satellites in orbit around Earth" [18]. The Automated Navigation and Guidance Experiment for Local Space (ANGELS) program also provides a space situational awareness capability to the GEO belt that involves proximity operations, although rarely discussed since its launch in 2014 because of its classification [19]. Additionally, the Experimental Satellite System 11 (XSS-11) program utilizes small, micro satellites in LEO to conduct "in-space servicing and repair as well as close-up inspection" of other satellites [20].

Particularly within the last decade, the U.S. commercial and civil sectors are active and interested in RPO maneuvers in order to deliver capabilities such as debris removal, on-orbit satellite inspection, and on-orbit servicing to spacecraft. The company ViviSat intends to begin servicing satellites in GEO with a Mission Extension Vehicle (MEV) by 2018 [21] to provide on-orbit "mission life extension and protection services" [22]. Defense Advanced Research Projects Agency (DARPA) selected Space Systems/Loral (SS/L) in 2012 to determine how to "repurpose … valuable components, such as antennas" from one satellite to another [23]. The use of RPO maneuvers in the commercial sector is growing and continues to gain momentum as the applications of proximity operations become more desirable and lucrative. Now is the time to utilize the commercial sector's experience and to conduct on-orbit satellite inspection with terahertz imaging through RPO.

3. Case Study of a TIC Payload Conducting On-Orbit Satellite Inspection

After a satellite launches into space, the first task is to establish communications for command and control purposes. In some cases, communications with the satellite cannot be established, and typically, when the communication link fails, the reason is unknown. Without a communications link, satellite operators cannot establish command and control, cannot conduct altitude control maneuvers, and consequently, cannot save the satellite from de-orbiting from space. What if there was a way to inspect the satellite before it de-orbits? An inspection could provide a means to identify any anomalies and fix the errors, or at least understand what went wrong before the satellite burns up in the atmosphere. Furthermore, not just a visual inspection is possible, but a characterization of materials and wires. This case study proposes that a terahertz imaging camera payload could provide an on-orbit satellite inspection capability that achieves a level of analysis never-before seen in space.

Losing communications with a satellite is not uncommon, especially within the first moments in orbit. In April of 2018, India lost communications with its "most powerful communications satellite" in the final stage of the satellite's launch [24]. The reason for the loss in link, if known, was not specified. The satellite, known as GSAT 6A, showed no signs of failure before it suddenly went silent [25]. For small satellites, around 1–5% of CubeSats are unable to establish a communications link after launch and are considered dead on arrival [6].

Depending on the value of the satellite, various courses of actions occur. One option, the most common, is to continue attempting a communications link. Upon exhausting all troubleshooting on the ground, the satellite and its mission are determined a loss. A second solution is to take pictures of the non-functioning satellite in an attempt to determine the fault, achievable through programs like XSS-11 designed for close-up satellite inspection. Obtaining and analyzing imagery is currently the best solution available in space to determine anomalies on a spacecraft. Images, though, only help if the fault is superficial or visually apparent. What if the issue relates to faulty wiring, broken

circuits, or damaged materials? A means of on-orbit materials inspection is required to identify such issues.

A terahertz imaging payload provides a means to inspect and resolve anomalies on a defunct satellite beyond what the eyes can see. The solution is non-invasive, non-destructive, and completely passive. Although not yet tested in space, applications on earth show terahertz radiation's utility in materials inspection, circuit characterization, and wire health analysis, as discussed earlier in this chapter. Similar to having a broken bone hidden inside a human body, the outside appearance of a satellite does not always reveal the health of the equipment inside. Through use of RPO, a terahertz imaging payload can scan a defunct satellite at a distance in the order of tens of kilometers [15]. Terahertz imaging enables a more in-depth and extensive means of analysis and inspection, allowing for a greater understanding of a satellite's anomalies than ever before.

In the case of India's communications satellite, GSAT 6A, a terahertz imaging payload could potentially change the fate of this silent, non-functioning satellite or similar ones like it. Ideally, the terahertz imaging payload resides in multiple orbital regimes. For GSAT 6A, a GEO satellite, the terahertz imaging satellite would conduct a series of RPO maneuvers in the GEO-belt to close within tens of kilometers of the defunct satellite. Upon rendezvousing with GSAT 6A, the terahertz imaging payload would scan the satellite throughout multiple passes. The results of the scan could potentially reveal damaged cabling to externally mounted equipment like deployable systems, antennas, solar panels, and gimbals or discontinuities in a telescope or camera lens. While the detection of a fault might lead to correlating and identifying the issue, it might not necessarily be feasible to correct the anomaly on-orbit. Whether the fate of GSAT 6A could be changed or not, the lessons learned by identifying the error has the potential to affect the next flight vehicle. Terahertz imaging in space provides a means to increase the chance of survival for malfunctioning satellites or to learn valuable lessons for follow-on missions, potentially lowering the total program cost.

C. IMAGING OF OBJECTS ILLUMINATED BY TERAHERTZ RADIATION IN SPACE

The concept of imaging objects in space illuminated by terahertz radiation brings up two critical questions: How will the medium of space with the absence of water vapor affect terahertz imaging, and what will space looks like in the terahertz region of the electromagnetic spectrum? In essence, what will we see? Because the field of terahertz science and technology is relatively new and the sensors and detectors to image terahertz radiation were only recently developed, the terahertz region of the electromagnetic spectrum in space is, currently, an unused realm with potentially unobserved physical phenomena.

The sun emits all types of energy throughout its solar cycle that spans the electromagnetic spectrum from radio waves to gamma rays [26]. Without the presence of water vapor to restrict terahertz wave propagation, a terahertz imaging camera will potentially be able to detect objects illuminated by terahertz radiation from far away. For matters of Space Situational Awareness (SSA), a TIC payload not only aids in the examination of objects at close distances, it also serves a potential purpose in detecting reflected terahertz radiation from objects at far distances. Such identification aids in providing useful information that can be queued to other SSA assets, potentially even a TIC payload, for further classification and identification. Whereas visible light imagery requires resolution, terahertz radiation imagery requires reflection and could potentially span much greater distances. The imaging of objects illuminated by terahertz radiation from far away leverages the space medium and energy emitted by the sun to create a potential application of a TIC payload in space.

D. OTHER POTENTIAL APPLICATIONS OF TERAHERTZ IMAGING IN SPACE

As the field of terahertz science and technology continues to grow, space enthusiasts speculate on numerous other potential applications of terahertz imaging in space. A research and development team called StarTiger at the European Space Agency (ESA) believes “observations from space may be on the verge of a revolution with the possibility of looking into the terahertz frequency range” [27]. In September of 2003, the

StarTiger team used terahertz imaging technology to capture the “world’s first terahertz picture of a human hand.” StarTiger predicts potential applications of terahertz imaging in space may include “astronomy, atmospheric physics, and Earth and environmental monitoring.” Specifically, terahertz imaging can aid in monitoring global climate changes and studying ozone depletion mechanisms by observing the troposphere and stratosphere. Many other scientists, like those at Picometrix, Inc. and NDE Sciences Branch, share StarTiger’s excitement for terahertz imaging in space [28].

In 2005, the American Institute of Physics published an article by a group of scientists from Picometrix, Inc. and NDE Sciences Branch at NASA Langley Research Center [28] describing how a terahertz imager shows “great promise” in the inspection of sprayed on foam insulation on the Space Shuttle. The research finds that terahertz imaging performs well as means of “non-destructive evaluation” and “non-contact inspection of non-conductive materials such as plastics, foam, composites, ceramics, paper, wood and glass.” Specifically, the research demonstrates terahertz imaging can detect “voids and disbands intentionally incorporated within the sprayed on foam insulation of a space shuttle external tank mock-up.” The researchers used a terahertz imager attached to a 30-meter fiber optic umbilical and conducted the tests on a mock-up segment in a testing facility. Current advancements in technology now allow for the opportunity to test an on-orbit terahertz imaging payload. Scholars and scientists alike agree that terahertz imaging has the potential to revolutionize and improve the space environment.

In conclusion, the terahertz portion of the electromagnetic spectrum presents unique characteristics that create the opportunity for new applications in the space environment. Potential space operations of a TIC payload include on-orbit satellite inspection and far away space object detection. The technological advancements to detect terahertz radiation creates an opportunity to put the world’s first terahertz imaging camera (TIC) into space as a CubeSat payload.

THIS PAGE INTENTIONALLY LEFT BLANK

III. INTEGRATION AND FLIGHT QUALIFICATION PROCESS

The integration and flight qualification process of a satellite ranges anywhere from six months to decades. Many factors influence the timeline, including the size of the spacecraft, the scope of the mission, and the level of risk acceptable to the particular program. A typical integration process is represented in Figure 9. A piece of hardware, like the TIC, for example, is tested individually according to testing standards and then integrated with the rest of the bus.

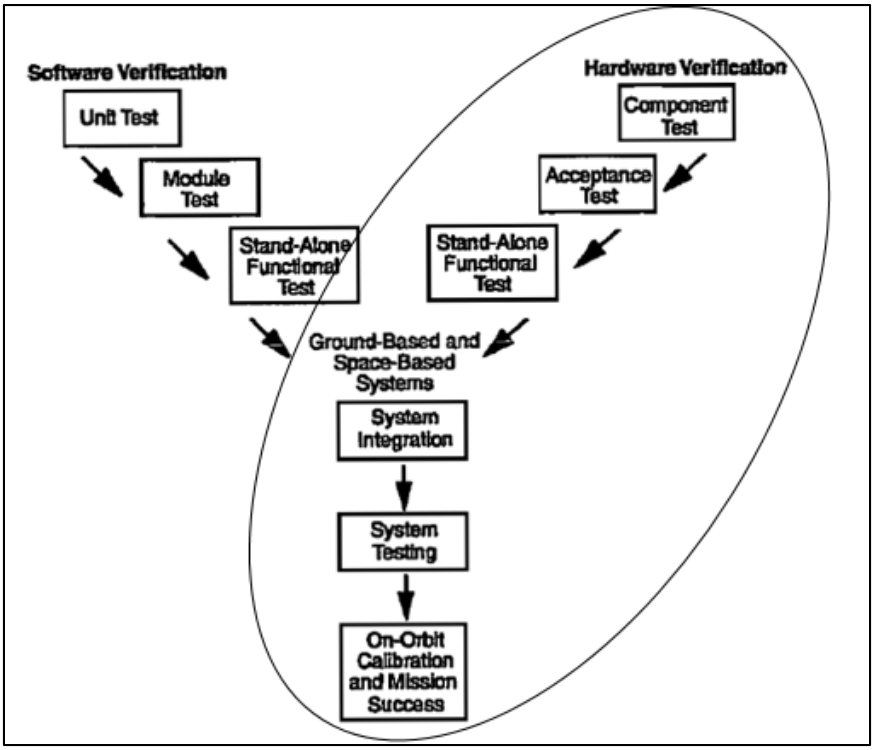

Figure 9. The Testing Process for Flight Qualifying a Satellite. Adapted from [29].

A piece of hardware is considered “flight qualified” when it has been tested at or above levels comparable to the expected environment. Testing standards ensure the piece of hardware survives the launch and space environment. This thesis begins the flight qualification process for integrating a TIC as a CubeSat payload.

The testing conducted for this thesis aimed to expose the TIC EDU to extreme conditions to ensure the feasibility of achieving the mission's requirements and to vet the qualification procedures for the flight hardware. Generally, for small satellites and more particularly in academic institutions, student education is the primary metric of success, and programs take big risks in the lack of testing and overall spacecraft design. Due to the focus on education and willingness to take risks, the failure rate is around 15% for 1U to 27U satellites according to a study done by the U.S. Space Program Mission Assurance Improvement Workshop of the Boeing Company. The study recommends extensive testing to mitigate the chance of failure [6]. This thesis recognizes and accounts for the common pitfall of accepting big risks by conducting vibration and thermal vacuum testing to industry-accepted testing standards and worst-case environmental factors.

Determining requirements and adhering to testing standards directly influences the integration and flight qualification process as well as increases the satellite's likelihood of success by mitigating risks. This chapter discusses the testing standards used for this thesis, examines the utility of developmental testing, presents the best practices of payload integration, and summarizes the HAB bus requirements. These areas of research set the foundation for the development tests conducted on the TIC EDU in support of achieving the ultimate goal of integrating the TIC as a CubeSat payload in the near future.

A. TESTING STANDARDS

Testing standards minimize the risk in a satellite program by creating requirements and guidelines for environmental verification. Greater adherence to the testing standards correlates directly with cost and greater success in the satellite's survival throughout the launch and space environment. The primary testing standard for this thesis is GSFC-STD-7000, the General Environmental Verification Standard (GEVS) from NASA Goddard Space Flight Center [30]. Additionally, this thesis references SMC-S-016, the Air Force Space Command's Space and Missile Systems Center Standard [31]. Familiarization with both documents provides an understanding of both commercial and military standards, which differ slightly in some areas. For example, the NASA GEVS requirement for the

duration of a qualification random vibration test is 2 minutes per axis [30], where the SMC-S-016 requires 3 minutes per axis [30].

The SMC-S-016 defines six different types of test categories: developmental tests, qualification tests, protoqualification tests, acceptance tests, prelaunch validation tests, and post-launch validation tests [31]. The testing accomplished for this thesis is developmental, meaning, as stated in the SMC-S-016, the tests were conducted on "representative articles to characterize engineering parameters, gather data, and validate the design approach." Development tests serve a variety of purposes, all of which primarily focus on confirming a certain design or requirement can be accomplished. This thesis utilizes development tests in order to develop and validate qualification and acceptance test procedures. The development tests of the TIC EDU serve as a means to evaluate new design concepts and reduce the risk in the qualification of the actual flight hardware.

In a paper written by W. F. Tosney and S. Pavlica of The Aerospace Corporation [32], the authors stressed the importance of using development tests to "subject hardware to the worst-case design conditions expected." Numerous examples exist in literature of prototypes not performing the same as the flight model, but the paper proposes mitigating the pitfall through rigorous environmental testing. Similarly, the SMC-S-016 refers to development testing as an "especially important ingredient to the mission success" that must be done "over a range of operating conditions that exceed the design limits" [31]. Overall, when used appropriately, development tests provide a lot of data, establish procedures, and validate the design concepts of engineering development units.

B. PAYLOAD INTEGRATION AND BEST PRACTICES

Payload integration refers to the testing, characterization, and installation of a payload onto a bus. A payload is defined as the combination of hardware and software that accomplishes the satellite's mission objectives [33]. Typically, the payload is unique and is the "fundamental reason that the spacecraft is flown" [33]. The bus is defined as the "rest of the spacecraft," which enables the payload to function as designed [33]. The term "best practices" refers to the methods used to avoid "downstream design, production and operational problems" [32]. Prior to payload integration, the payload is often tested as a

stand-alone unit before being integrating onto the bus. Then, the payload and the bus are tested together to ensure survivability of all the subsystems and parts. Best practice methods verify the testing process aligns with mission requirements. Without proper payload integration and the use of best practices, the overall satellite mission is at a high risk of mission failure.

The U.S. Space Mission Assurance Improvement Workshop derived eight recommendations from their study of small satellite mission success, one of which stressed the importance of planning time for extensive integration, verification, and testing (IV&T) [6]. The workshop also identified the lack of testing to be one of the eight major themes seen throughout failed missions [6]. Furthermore, the study highlighted the value of thermal vacuum testing, emphasizing its importance as the test that best simulates the space environment [6]. When it comes to preparing a spacecraft for the space environment, the value of testing cannot be understated. In particular, payload integration plays a vital role in the overall testing process because the payload is the fundamental component of the satellite which accomplishes the mission. A critical aspect of payload integration includes the "test-like-you-fly" methodology, a type of best practice that focuses on preparing the satellite for the space environment.

The "test-like-you-fly" (TLYF) philosophy stresses that the type of ground testing conducted on the satellite components must resemble the expected on-orbit environment as much as possible. TLYF is more of a "philosophy" than a "test-specific" methodology because it is a form of verification [32]. Although not an official term found in government standards or handbooks, the TLYF idea is conceptualized in a functional test commonly referred to as "day-in-the-life" (DITL) testing [32]. Testing of this type includes controlling the component with the software and bus expected to operate it when fielded, running the component in a mission-like environment, and exposing the component to mission-like levels of vibration, temperature, and radiation. Another type of TLYF functional test, "first-day-in-the-life" (FDITL), simulates the environment in which the satellite functions once deployed. The TLYF philosophy assumes if the component can survive environment-like testing on the ground, it increases the likelihood of survival in the actual environment.

A combination of following testing standards and using TLYF methodology makes for a robust payload integration process. Balancing testing standards with the expected environment allows for a low-risk, middle ground solution for testing. While TLYF is "necessary to attempt," it is also important to acknowledge "the inability to completely do so" [32]. The GEVS endorses the approach where "the entire payload is tested or verified under conditions that simulate the flight operations and flight environment as realistically as possible," but also acknowledges that "there may be unavoidable exceptions" and conditions that require lower levels of testing [30]. The best practice for payload integration is to follow testing standards and replicate the on-orbit environment as much as possible.

C. HAB INTERFACE REQUIREMENTS

For this thesis, the HAB bus was selected as the baseline bus for interface and testing purposes to leverage the experience and hardware availability within the SSAG. The following sections describe the mechanical and electrical interface requirements that shaped the testing setup and integration process.

1. Mechanical Interface

The payload attaches by means of mounting brackets with a symmetrical bolt pattern of #4-40 threaded holes 10 mm apart. The footprint must be within the dimensions of a 95 mm x 95 mm square. Any arrangement of components within the frame is allowable as long as the hardware connects to the hole locations on the frame. Ideally, the weight stays under 4 lbs. or 1.8 kg to remain within HAB weight limits. A HAB under 4 lbs. is exempt from the Code of Federal Regulations (CFR) for Unmanned Free Balloons [34]. Figure 10 shows the basic HAB structure, based off a 3U CubeSat volume. Figure 11 shows the HAB payload envelope from a top view.

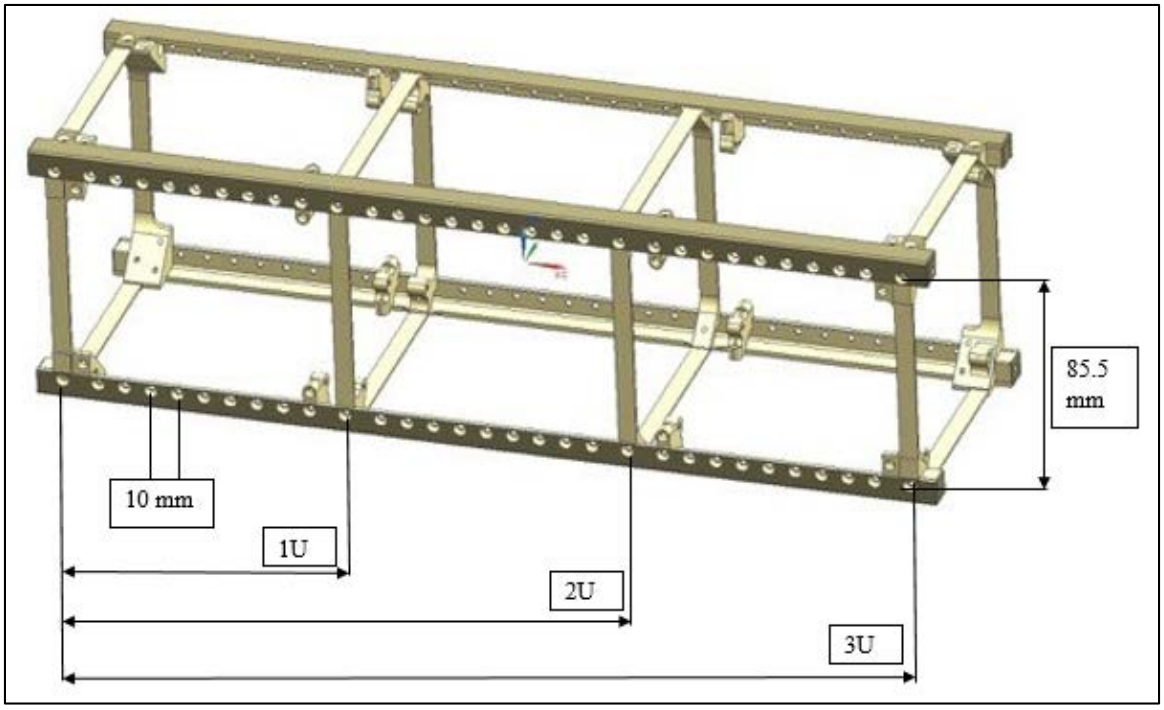

Figure 10. 3U HAB Structure with Measurements. Adapted from [35].

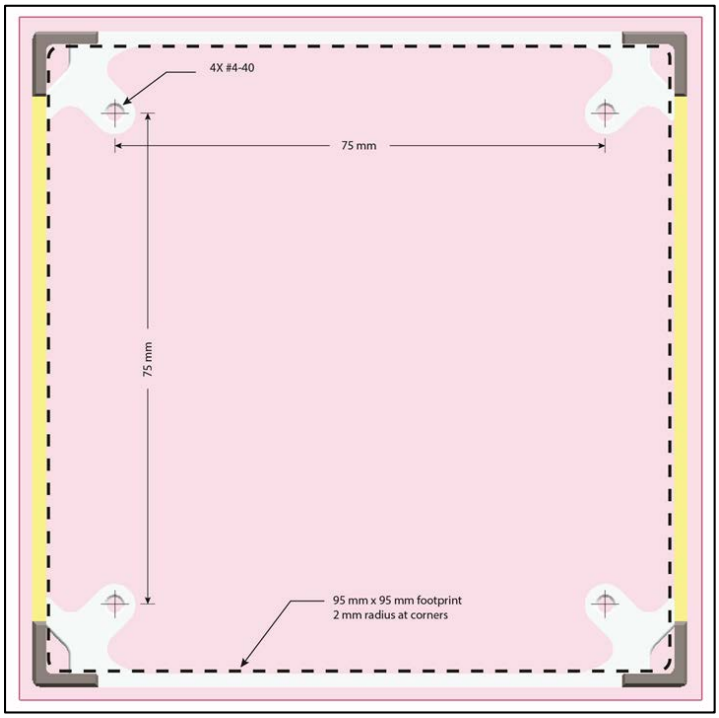

Figure 11. Top View of HAB Structure with Measurements. Source: [35].

2. Electrical Interface

a. Power Requirement

The SSAG-developed HAB bus nominally supplies 5 volts (V) of power to the payload [34]. The EPS subsystem consists of batteries and solar panels. The power supply from the batteries defines the voltage, and the solar panels supplement the power supply independently. The independent, yet supplementary, power supply from the solar panels proves its importance during flight. If the batteries fail because of cold temperatures, the EPS maintains consistent power supply through the solar panels. The TIC EDU uses 3.3 V of power from the EPS, well within the available power supply.

b. Raspberry Pi Board

Standard to the SSGA-developed HAB bus for the software, electrical, and power interface is a Raspberry Pi board. The Raspberry Pi essentially serves as the brain of the bus, the primary piece of hardware for C&DH. The TIC EDU communicates with the C&DH using Inter-Integrated Circuit (I^2C) protocol with a Raspberry Pi. Figure 12 shows the block diagram and interfaces of the EPS, C&DH, and payload.

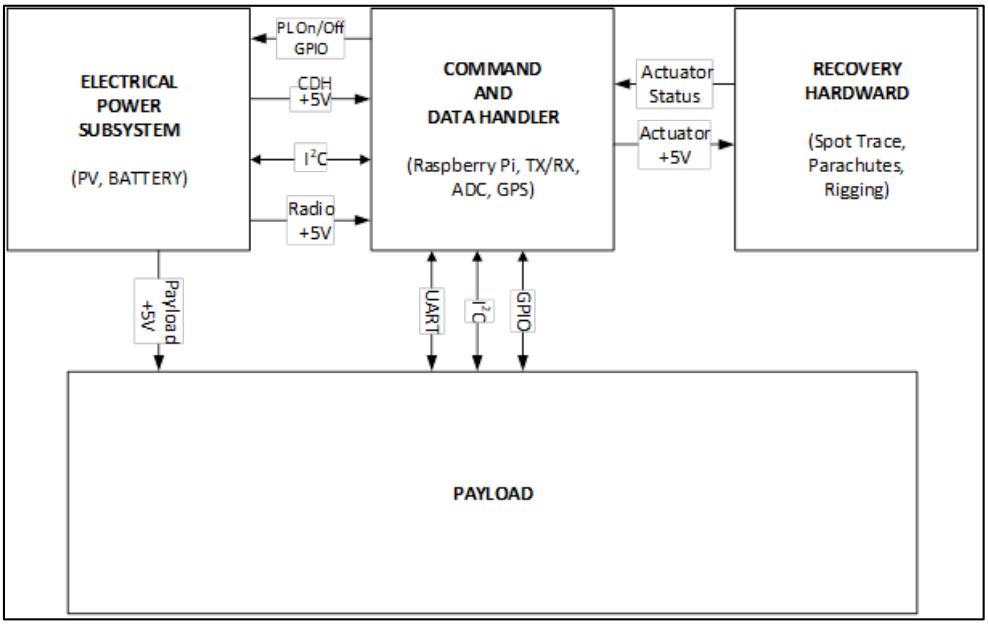

Figure 12. EPS, C&DH, Recovery Hardware, and Payload Interface Block Diagram for the SSAG-Developed HAB Bus. Source: [35].

The interface with the TIC EDU occurred through a Raspberry Pi Zero during the initial stages of familiarization with the camera. The Raspberry Pi interfaced with a desktop computer screen through USB and HDMI and the data from the camera saved onto a secure digital (SD) card, shown in Figure 13 and Figure 14. For the development testing phase, the TIC EDU and Raspberry Pi Zero were treated as a separate, standalone entity from the bus; therefore, external power sources such as a wall outlet power cord and a power supply provided power to the Raspberry Pi board and TIC EDU, respectively.

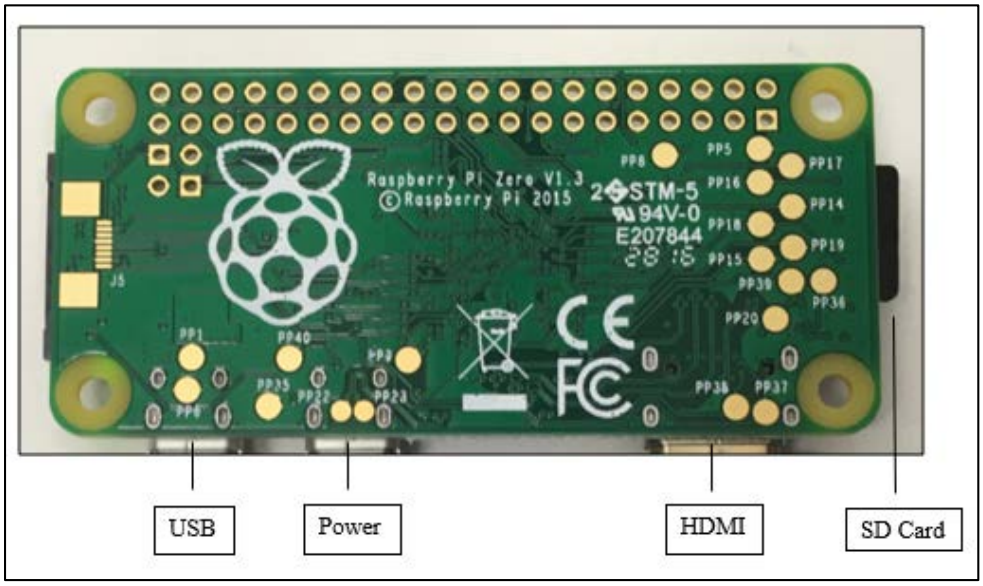

Figure 13. Interfaces of the Raspberry Pi Board

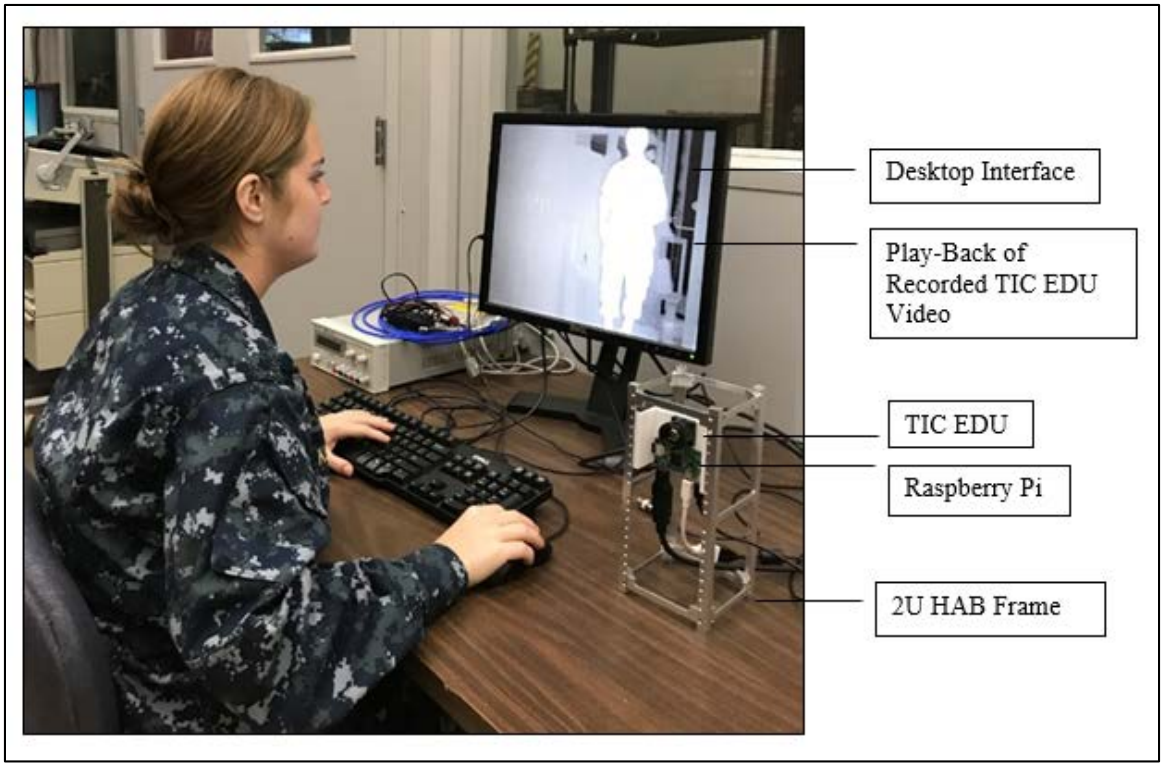

Figure 14. Desktop Setup for Initial Familiarization with the HAB Bus and TIC EDU

D. SUMMARY OF INTEGRATION AND FLIGHT QUALIFICATION PREPARATION

A knowledge of the testing standards and the best practices for payload integration set the foundation for the development tests conducted on the TIC EDU. The integration and flight qualification process for this thesis began by testing the TIC EDU individually. The vibration and thermal vacuum testing adhered to GEVS as well as incorporated TLYF methodology. The SSAG-developed HAB served as the baseline bus for the payload integration. In summary, this thesis began the integration and qualification process through development testing to support the overall mission objective of integrating a TIC as a CubeSat payload.

THIS PAGE INTENTIONALLY LEFT BLANK

IV. TIC EDU DEVELOPMENT TESTING

This chapter discusses the reasoning behind the selection of the IR camera used as the TIC EDU, the computer-aided design (CAD) model designed for mounting the TIC EDU, and the methodology and results of the vibration and thermal vacuum testing. The TIC EDU served as the dedicated hardware for design verification. Intrinsic to development testing at qualification standards, the TIC EDU underwent a testing environment "more severe than anything [expected for] the flight hardware" [36], as discussed in Chapter III. Clearly defined test objectives and pass/fail criteria established the intent for the vibration and thermal vacuum testing. The TIC EDU's success and survival through the development testing established confidence in the design and mission of integrating a TIC as a CubeSat payload.

A. TIC EDU BACKGROUND

The camera acquired as the TIC EDU is the FLIR BOSON 320 18 millimeter (mm) lens thermal imaging camera. Characteristics of the camera include a 320 x 256 array format, 12-degree horizontal field of view (HFOV), 18 mm focal length, 12-micron meter pixel pitch micro-bolometer, 9 Hz frame rate, temperature rating of -40°C to 80°C, 19.8 centimeter cubed (cm^3) volumetric camera body, and shock rating of 1,500 g at 0.4 milliseconds [37]. All development testing conducted on the TIC EDU remained within the manufacturer's specifications. The camera was selected by the previous Master's thesis student, Lt Col Marcello Correa de Souza, for its compliance with the SSAG-developed HAB bus by its "dimensions, weight, thermal sensitivity, effective focal length, operation temperature range, resolution, power consumption, and cost" [11]. Figure 15 presents the Interface Description Document (IDD) of the FLIR BOSON 320 18mm camera and Figure 16 shows the manufacturer's specifications.

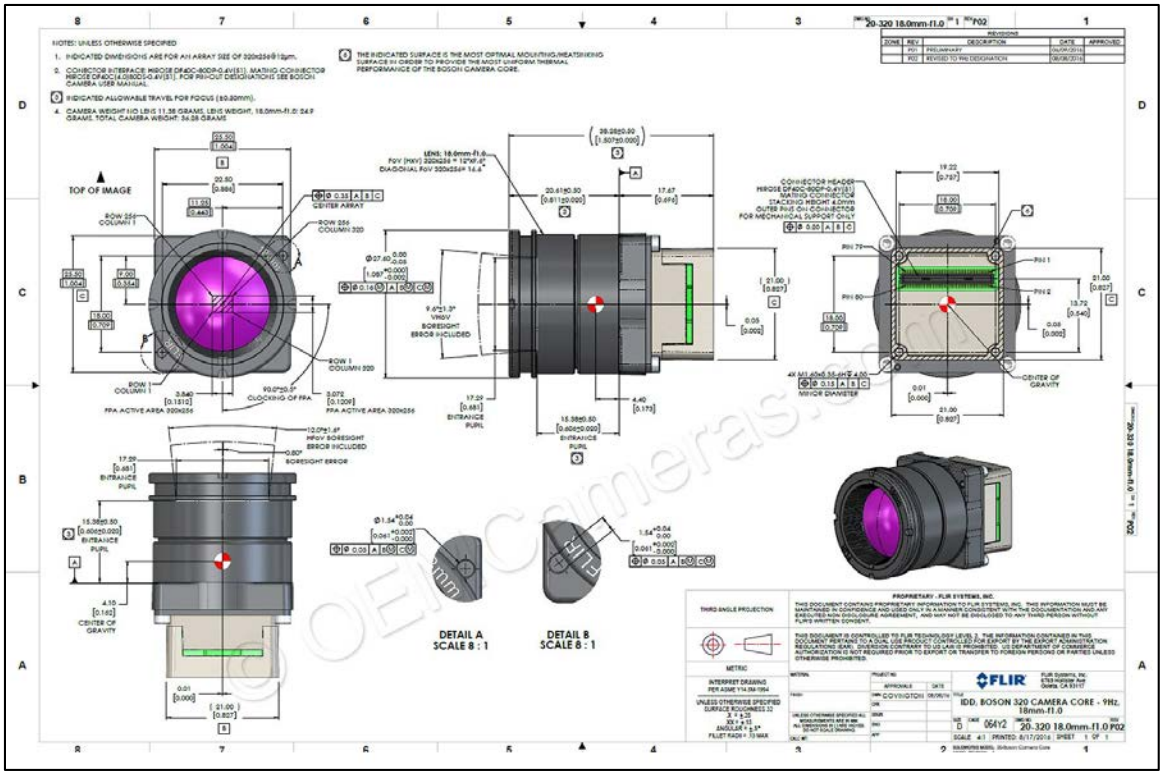

Figure 15. Interface Description Document (IDD) for the FLIR BOSON Camera. Source: [37].

Figure 16. FLIR BOSON Camera Specifications. Source: [37].

The selection of an IR camera as the EDU correlates to the on-going work of the Sensor Research Laboratory at NPS to develop a THz-to-IR imaging system [11]. The THz-to-IR conversion "involves a readout based on the heat generated by THz absorption using an IR camera" [11]. The ability to utilize a commercial off-the-shelf (COTS) IR camera allows for a relatively cheap and expendable means to codify the concept and to support on-going THz-to-IR research. While still closely resembling the meta-materials of a THz imaging camera, an IR camera provides a test bed for determining the initial integration challenges and testing limitations of a TIC onto a CubeSat.

B. CAD MODEL FOR TESTING

The CAD model created with NX product design software from Siemens PLM Software mounted the TIC EDU onto a 2U CubeSat HAB frame for testing. The CAD mounted both the TIC EDU and Raspberry Pi, then attached them onto the CubeSat HAB frame. The CAD model included four #0 holes to mount the TIC EDU, four #4-40 holes to mount a Raspberry Pi, and 12 #2-56 holes to attach to the CubeSat HAB frame. Figures 17, 18, and 19 show the front, side, and isometric view of the CAD model with the TIC EDU, Raspberry Pi, and CubeSat HAB frame interface holes. Figures 20 and 21 show the front, side, and isometric view of the CAD model aligned on a 2U CubeSat HAB frame with the TIC EDU.

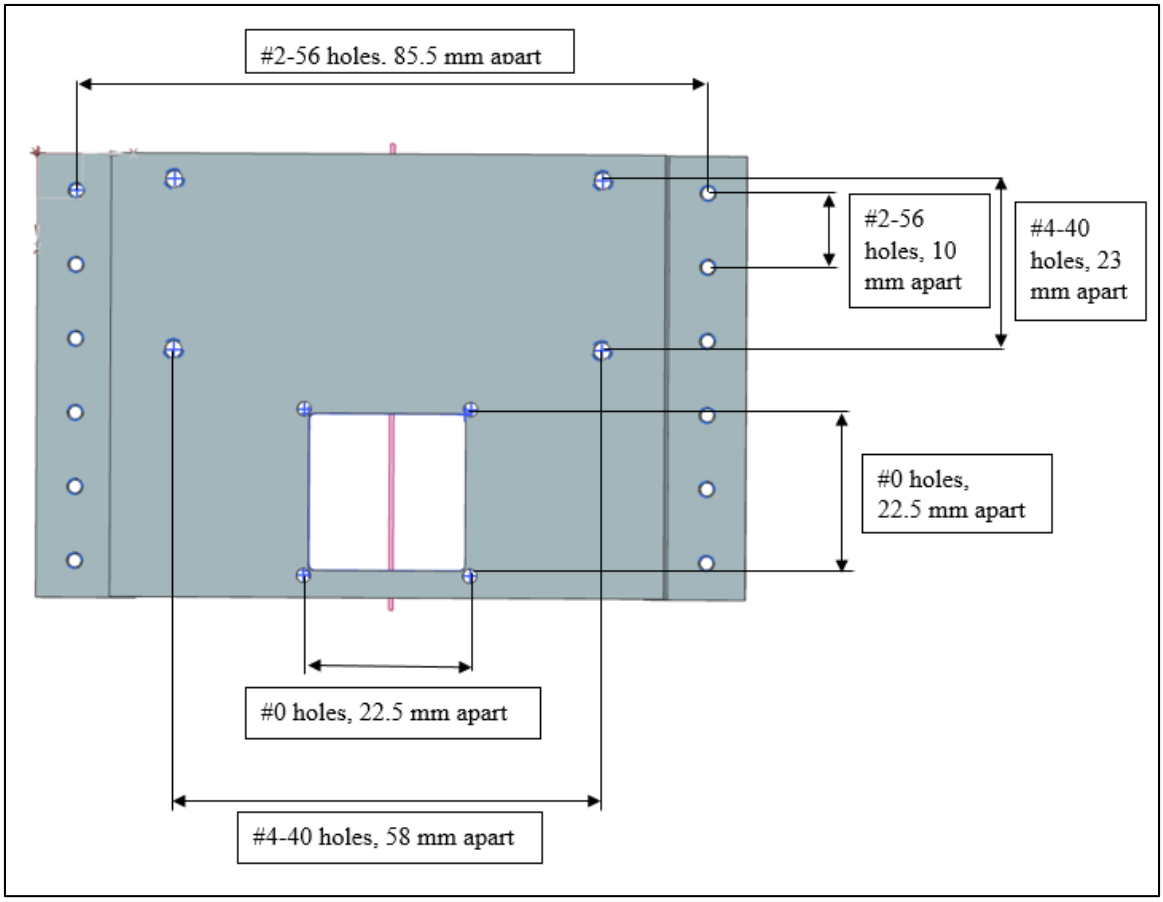

Figure 17. Front View of CAD Model with TIC EDU, Raspberry Pi, and CubeSat HAB Frame Interface Holes

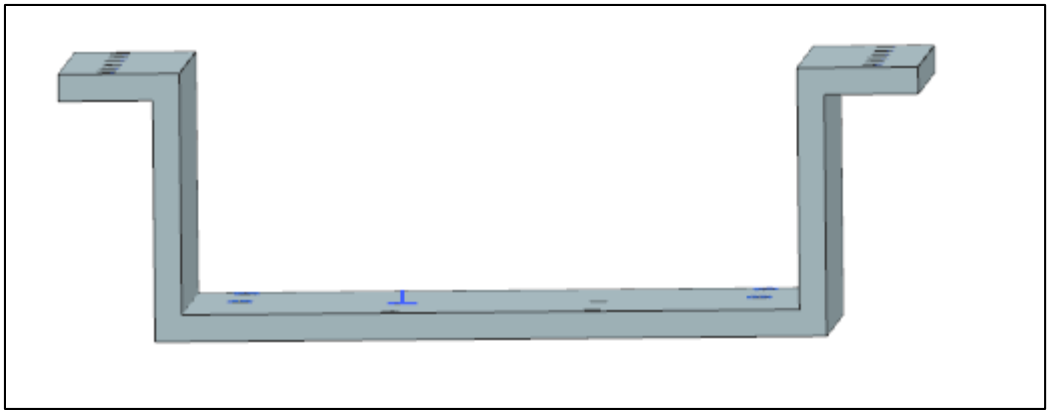

Figure 18. Side View of CAD Model with TIC EDU, Raspberry Pi, and CubeSat HAB Frame Interface Holes

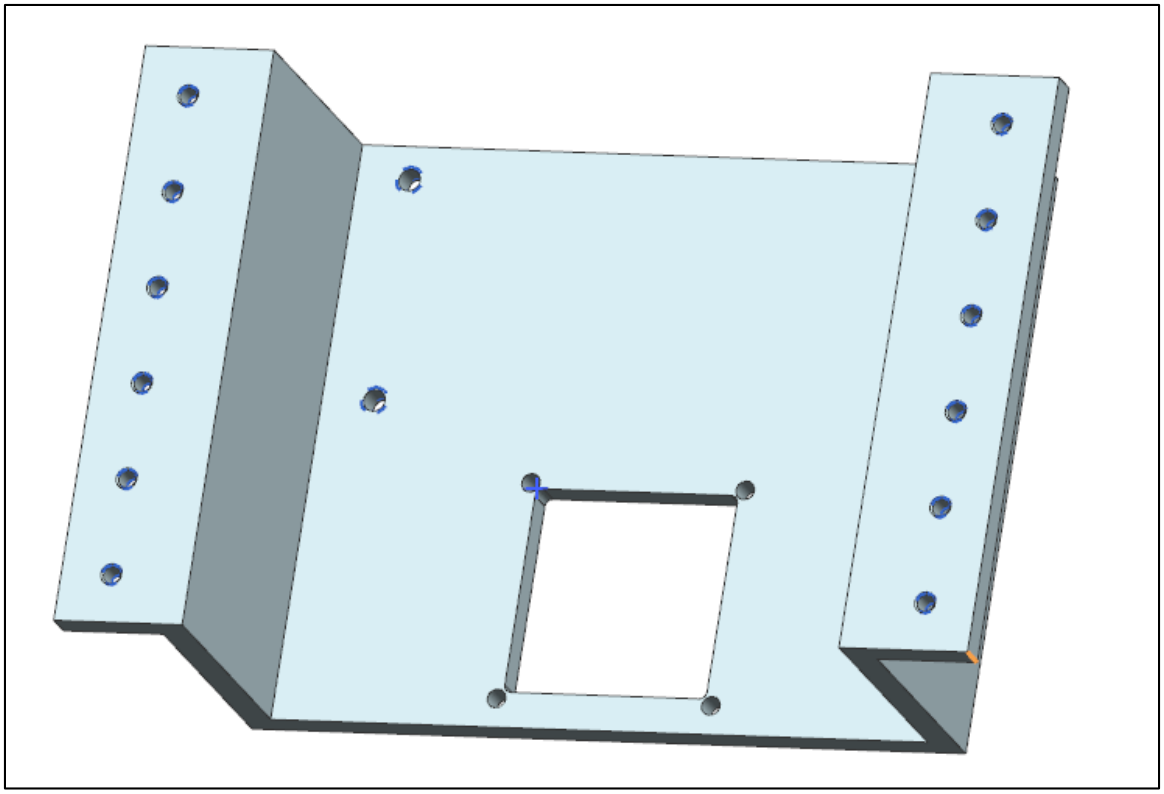

Figure 19. Isometric View of CAD Model with TIC EDU, Raspberry Pi, and CubeSat HAB Frame Interface Holes

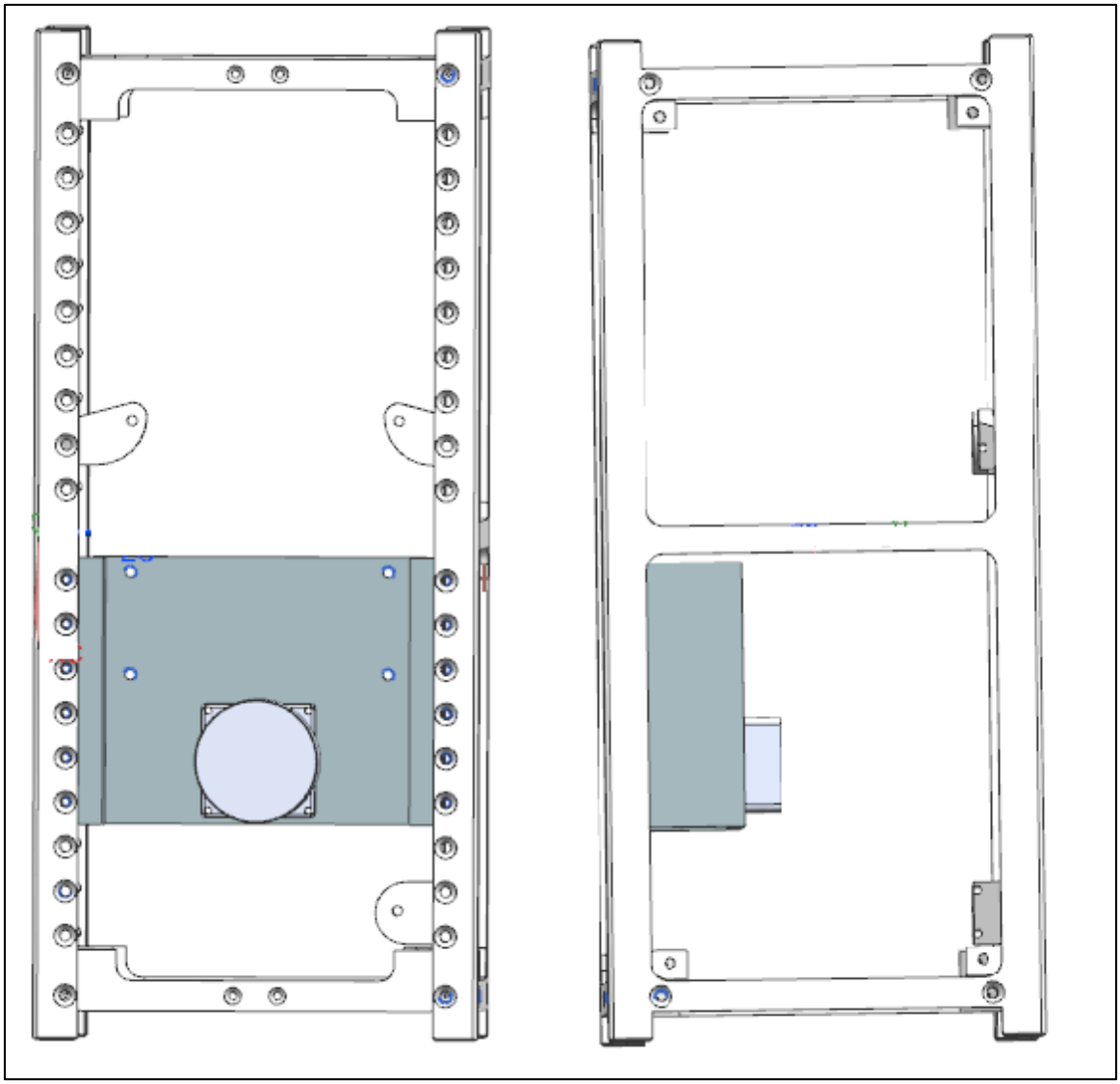

Figure 20. Front and Side View of CAD Model Mounting TIC EDU onto a 2U CubeSat HAB Frame

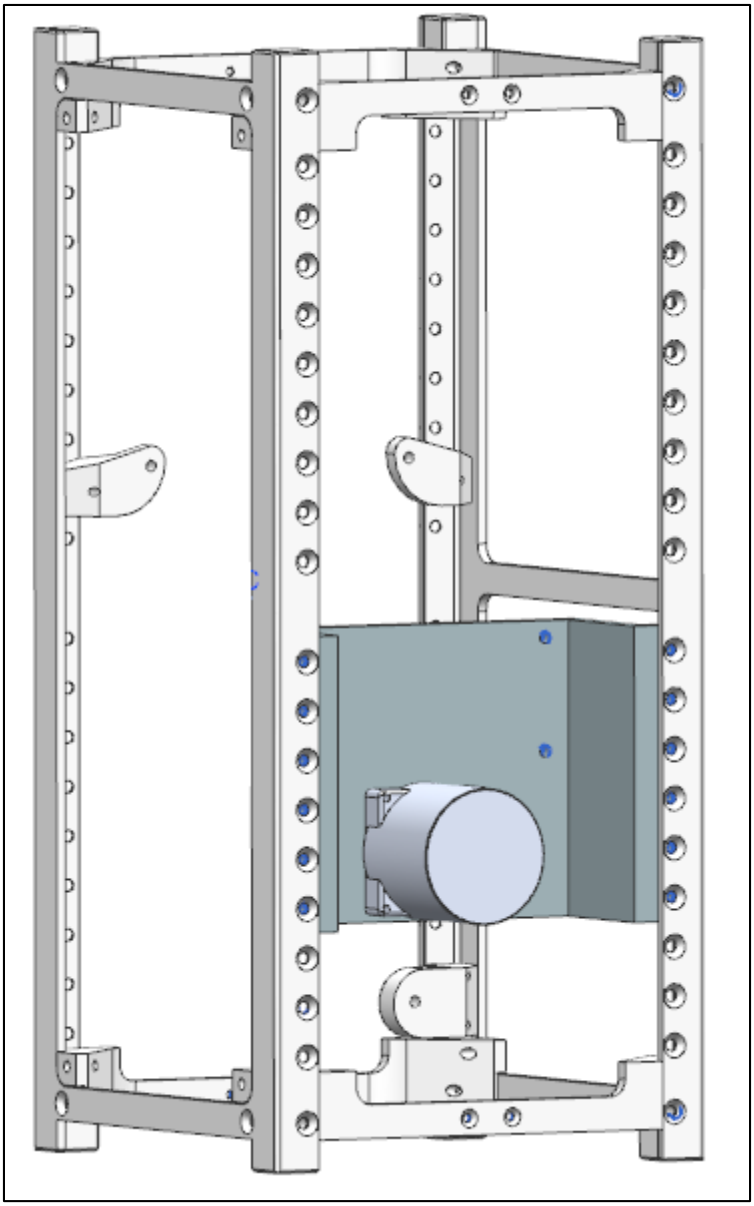

Figure 21. Isometric View of CAD Model Mounting TIC EDU onto a 2U CubeSat HAB Frame

C. VIBRATION TEST

The TIC EDU performed well and, overall, passed the criteria established for the vibration test. The data and imagery acquired from the testing reflects that the TIC EDU incurred little to no damage throughout the testing. The testing setup and the parameters used for the test correlate to the worst-case environment expected for the TIC EDU. The TIC EDU's success established confidence in the TIC payload's ability to survive the launch environment.

1. Test Objective

The primary objective of the vibration test was to verify the TIC EDU complied with the NASA GEVS random vibration requirements for prototype qualification. A secondary objective was to establish procedures and guidelines for future qualification, acceptance, and workmanship testing of the TIC payload.

2. Pass/Fail Criteria

The quality of the TIC EDU imagery needed to remain the same after the random vibration of the X, Y, and Z-axis for the TIC EDU to pass vibration testing. A failure meant the TIC EDU functioned abnormally or showed signs of degradation in its ability to take imagery.

3. Testing Plan

The testing plan comprised of five steps. First, the vibration test began with a visual inspection and functional test of the TIC EDU. Second, a low-level sine sweep was conducted on the first axis to establish a baseline signature; this is referred to as the "pre-sine sweep." Third, the random vibration was conducted. Fourth, a second baseline low-level sine sweep was conducted; this is referred to as the "post-sine sweep." Fifth, a visual inspection and functional test was conducted to assess any damage to the TIC EDU. The same process was repeated for the X, Y, and Z-axes. A visual inspection consisted of looking at the camera to identify any superficial signs of damage. A functional test consisted of ensuring the TIC EDU turned on and recorded video without qualitative degradation. Qualitative degradation entailed loss of resolution, an inability to image the

IR source, or pixel damage. Table 2 reflects the steps of a functional test, and Figure 22 shows the overall testing plan of the vibration test.

Table 2. Steps to Conduct a Functional Test on the TIC EDU

Step	Action
1	Open “Terminal” from Raspberry Pi desktop
2	If first time opening terminal, type ‘scudo kill all python’. Hit enter
3	If first time opening terminal, type ‘cd /home/pi/ir_tests’. Hit enter
4	Type the following command to run video, then hit enter: sudo /usr/bin/avconv –t 15 –f video4linux2 –I /dev/video0 –qscale 0 /home/pi/ir_tests/test1.avi
5	Type command ‘omxplayer test1.avi’, then hit enter, to play video
6	Ensure video quality is the same, with no signs of degradation

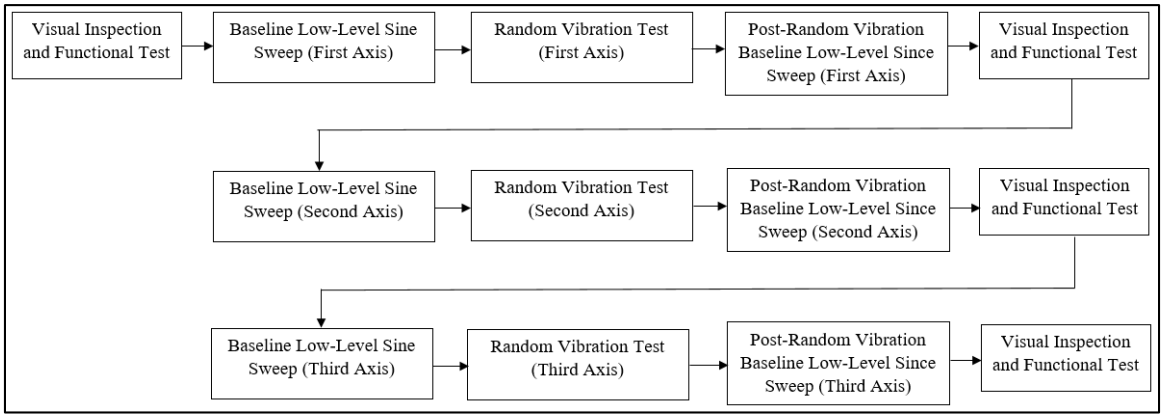

Figure 22. Overall Vibration Test Plan

4. Testing Parameters

The parameters for the sine sweeps originated from D. J. Ewins' book "Modal testing: theory, practice, and application" [38], used for its general vibration test guidelines and modal test parameters. The parameters for the random vibration originated from GEVS [30], selected for its rigorous testing standard to ensure survival through the launch environment. Tables 3, 4, and 5 reflect the parameter values used for this test, including the sine sweep parameters, the random vibration test parameters, and the random vibration test profile parameters. Figure 23 shows the random vibration test profile plot.

Table 3. Sine Sweep Parameters

Test Parameter	**Value**
Frequency Range	20 Hz – 2000 Hz
Acceleration	0.25 g
Sweep Rate	3 octaves/min

Table 4. Random Vibration Test Parameters

Test Parameter	**Value**
Frequency Range	20 Hz – 2000 Hz
Acceleration	14.1 G_{rms}
Test Duration	2 min/axis

Table 5. Random Vibration Test Profile Parameters

Frequency (Hz)	**Acceleration (g^2/Hz)**
20	0.026
50	0.16
800	0.16
2000	0.026
Overall	14.1 G_{rms}

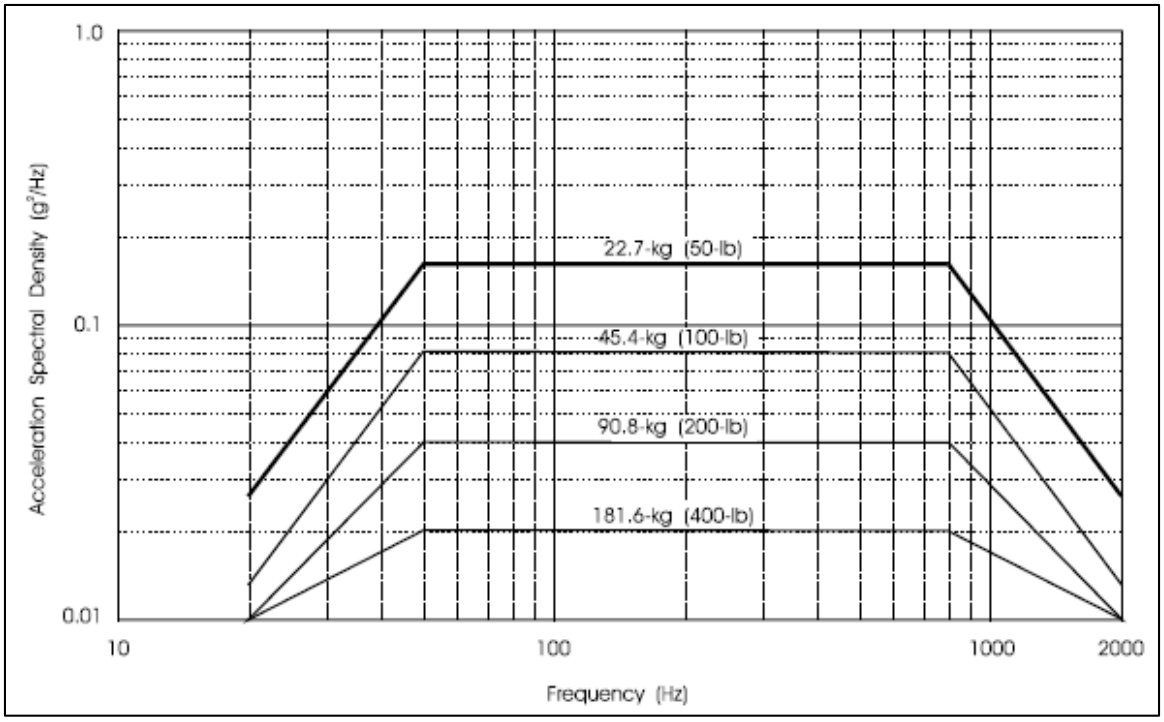

Figure 23. Random Vibration Test Profile Plot. Source: [30].

5. Test Setup

The TIC EDU, attached to the 2U HAB frame, interfaced with the vibration table through the #4-40 holes along the HAB frame. Accelerometers were placed close to the TIC EDU in order to measure the vibration response at the camera. One accelerometer was named "+Y accelerometer" and the second accelerometer was named "-Y accelerometer." The names were based off the accelerometers' location in relation to the coordinates of the HAB frame. Figure 24 shows the test setup of the TIC EDU on the vibration table.

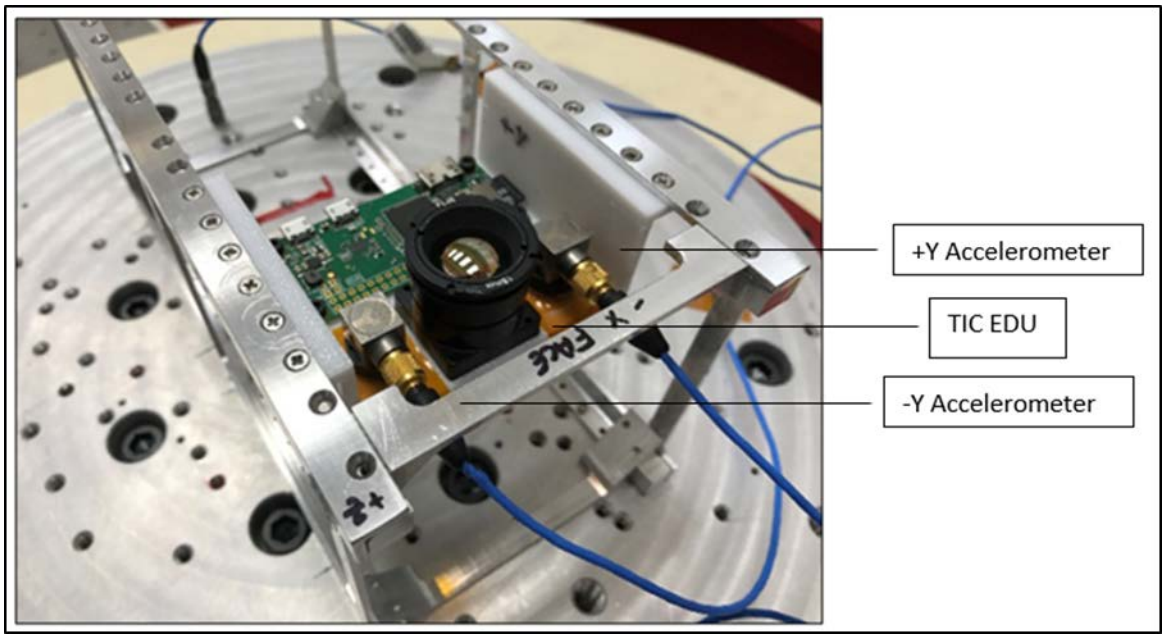

Figure 24. Testing Setup of TIC EDU on the Vibration Table

A 60 W incandescent lightbulb was used as the IR source for the TIC EDU functional tests. A tripod, which mounted a block with two #4-40 holes to attach the 2U HAB frame, was located approximately 13 feet from the IR source. The HAB mount provided positioning consistency for imaging. After the baseline sine sweep, random vibration, and post sine sweep of an axis, the TIC EDU was removed from the vibration table and mounted onto the tripod. The TIC EDU was powered on and the steps of the functional test were conducted. Upon completion of the functional test, the 2U HAB frame was mounted back onto the vibration table for testing of the next axis. Figure 25 shows the incandescent lightbulb attached to a light stand and Figure 26 shows the overall functional test setup.

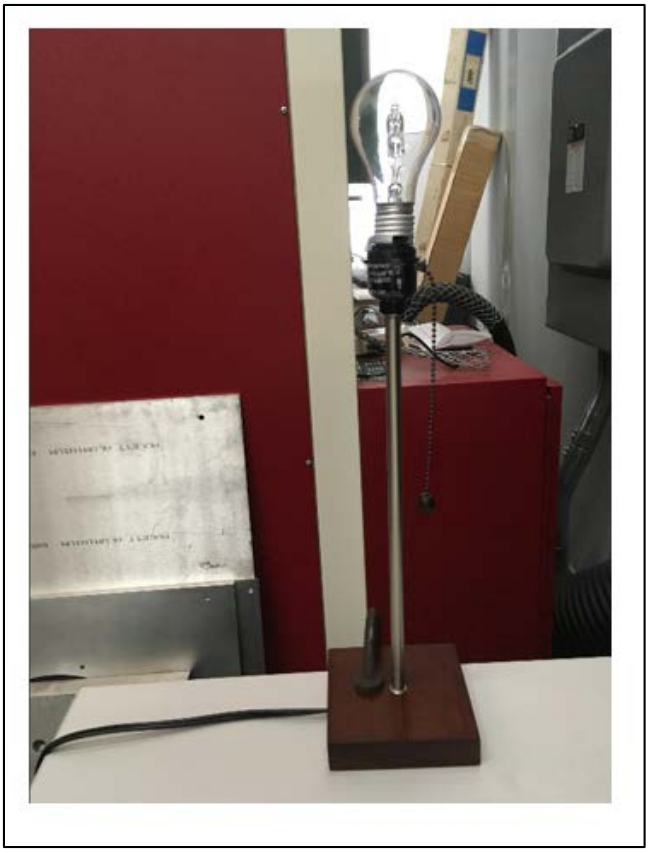

Figure 25. 60W Incandescent Lightbulb on a Stand as the IR Source

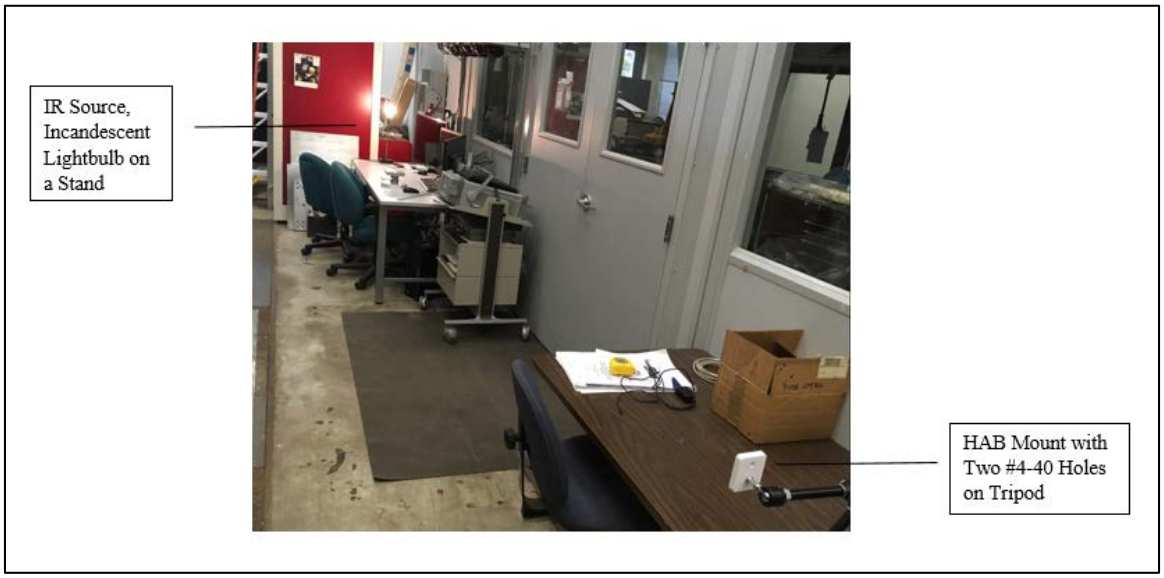

Figure 26. Vibration Test Functional Test Setup with HAB Mount and IR Source

6. Discussion

This section presents the data from the pre-sine and post-sine sweeps as well as the data from the random vibration test. All the data reflects the -Y accelerometer information. At the onset of the random vibration of the Z-Axis, the +Y accelerometer dislodged from the TIC EDU mount. For this reason, the data from the -Y accelerometer is presented for consistency.

a. Pre-sine and Post-sine Sweep Overlay Plots

The pre-sine and post-sine sweep overlay plot is used to assess if damage occurred to the test article during the random vibration test. The most important comparison is of the maximum peaks, which represents the test article's resonant frequency before and after the random vibration. An overlay plot easily compares the resonant frequencies from the pre-sine and post-sine sweep. Ideally, the difference in the peak values is minimal because a large percent difference suggests potential damage to the test article. The difference in peaks is calculated by the following equation, where "pre" refers to pre-sine resonant frequency and "post" refers to post-sine resonant frequency:

$$Difference\ in\ \% = \frac{|pre - post|}{pre} * 100$$

Overall, the percent differences were below 6% for each axis, and the overlay plots visually reflect the consistency in the maximum peaks. The low percent difference values provide confidence that the TIC EDU did not break or sustain any damage during the random vibration testing. Figures 27, 28, and 29 present the pre-sine and post-sine overlay plots with the resonant frequencies highlighted by a black vertical line at the frequency of peak acceleration. The blue plot shows the pre-sine sweep and the orange plot shows the post-sine sweep. The most important take-away remains the similarity in maximum peaks, showing the TIC EDU sustained little to no damage. Table 6 summarizes the resonant frequencies of the pre-sine and post-sine sweeps and the resulting percent differences for the X, Y, and Z-axes.

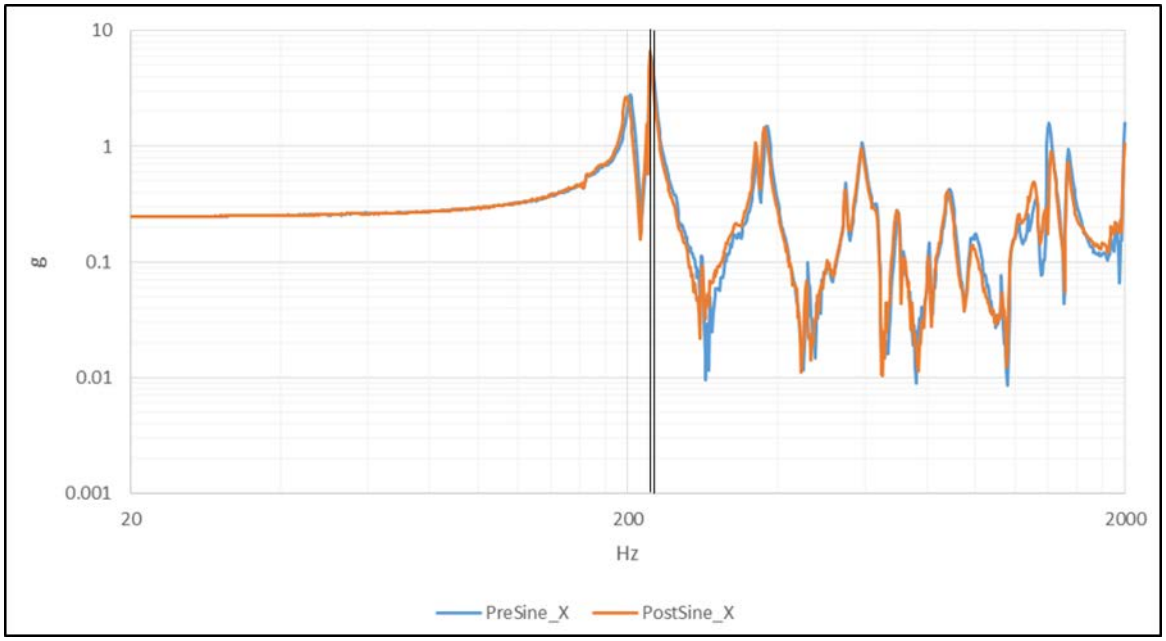

Figure 27. X-Axis Pre-sine and Post-sine Sweep Overlay Plot

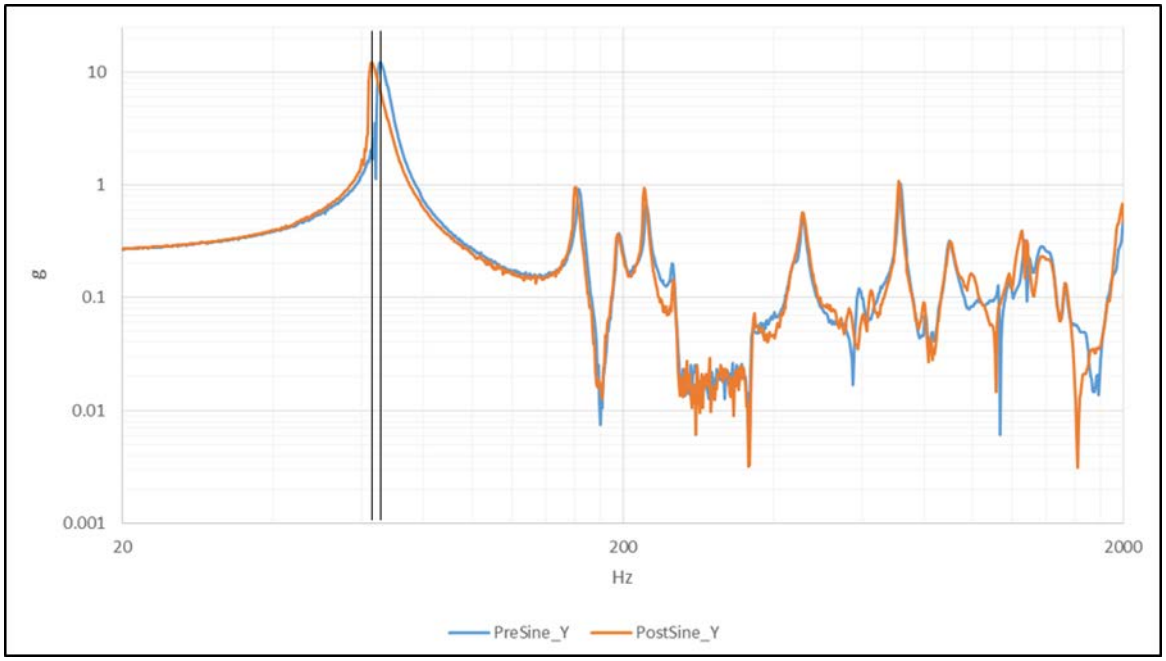

Figure 28. Y-Axis Pre-sine and Post-sine Sweep Overlay Plot

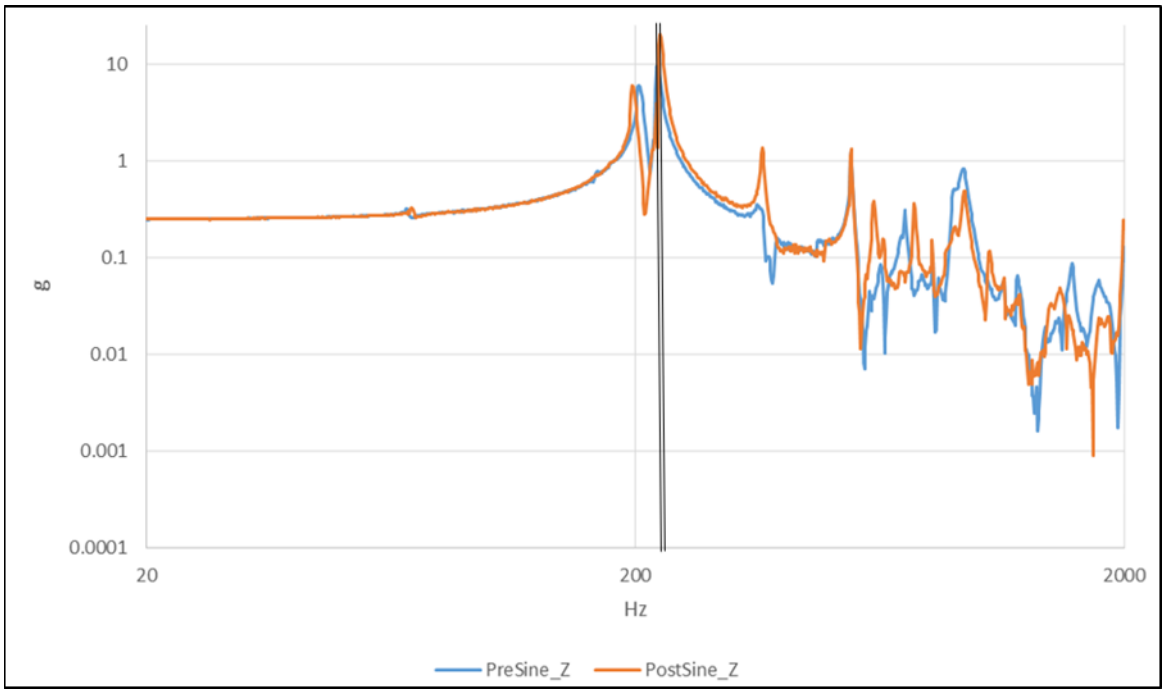

Figure 29. Z-Axis Pre-sine and Post-sine Sweep Overlay Plot

Table 6. Percent Differences between Pre-sine and Post-sine Resonant Frequencies for X, Y, and Z-Axis

Axis	**X**	**Y**	**Z**
Pre-Sine Resonant Frequency (Hz)	222	66	221
Post-Sine Resonant Frequency (Hz)	223	62	224
Percent Difference (%)	***0.5***	***5.9***	***1.4***

b. Random Vibration Overlay Plots

The random vibration overlay plots show the TIC EDU's response to the vibration environment in the X, Y, and Z direction for each axis. The most important measurement for assessing the overall response is the root-mean-square acceleration (G_{rms}), which reflects the energy of the area under the curve. The reference or input G_{rms} value is 14.1 G_{rms}, which corresponds to the qualification profile for GEVS shown in Table 5. By using GEVS prototype qualification standards and testing the payload without the bus, the random vibration test simulates a worst-case launch scenario. When affixed to a CubeSat with a bus, the payload encounters less vibration due to the increased stiffness of the

structure with the added boards and components. Since the test was only of the payload, it is expected that the amplitude of the fundamental peak would be higher than what would be seen when affixed with a bus.

Figures 30, 31, and 32 display the overlay plots for the X, Y, and Z-axes random vibration. Each plot shows the input G_{rms} value in yellow, the fundamental frequency peaks identified by a black vertical line, and the responses of the X, Y, and Z directions in blue, orange, and gray, respectively. Of note, the responses in the X, Y, and Z directions remain relatively similar between 400 and 2000 Hz. For each axis, the cross axis responses closely correlate in each plot. The correlation suggests a successful reading by the accelerometers of the responses in each direction. The frequency peaks below 400 Hz closely match for each axis, indicating the fundamental modes of the payload in this particular setup reside around 200 Hz. Table 7 summarizes the fundamental frequencies for each axis, showing the Z-axis responds with the highest amplitude. Specifically, for the Y-Axis overlay plot, although the cross-axis (X and Z) G_{rms} data appears low, the significantly lower values can be attributed to the absence of energy both below 200 Hz and above 400 Hz. The distinct peaks at approximately 70 Hz indicate that there are no issues with the test equipment. Table 8 summarizes the G_{rms} values for the X, Y, and Z directions for each axis.

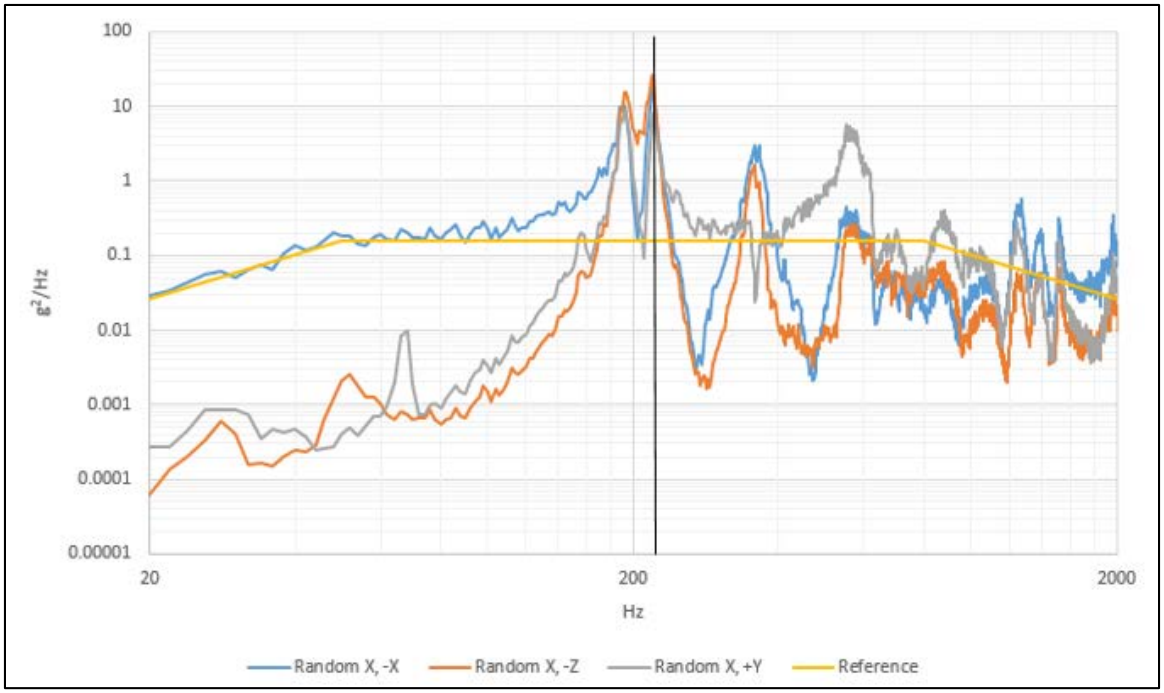

Figure 30. X-Axis Random Vibration Overlay Plot

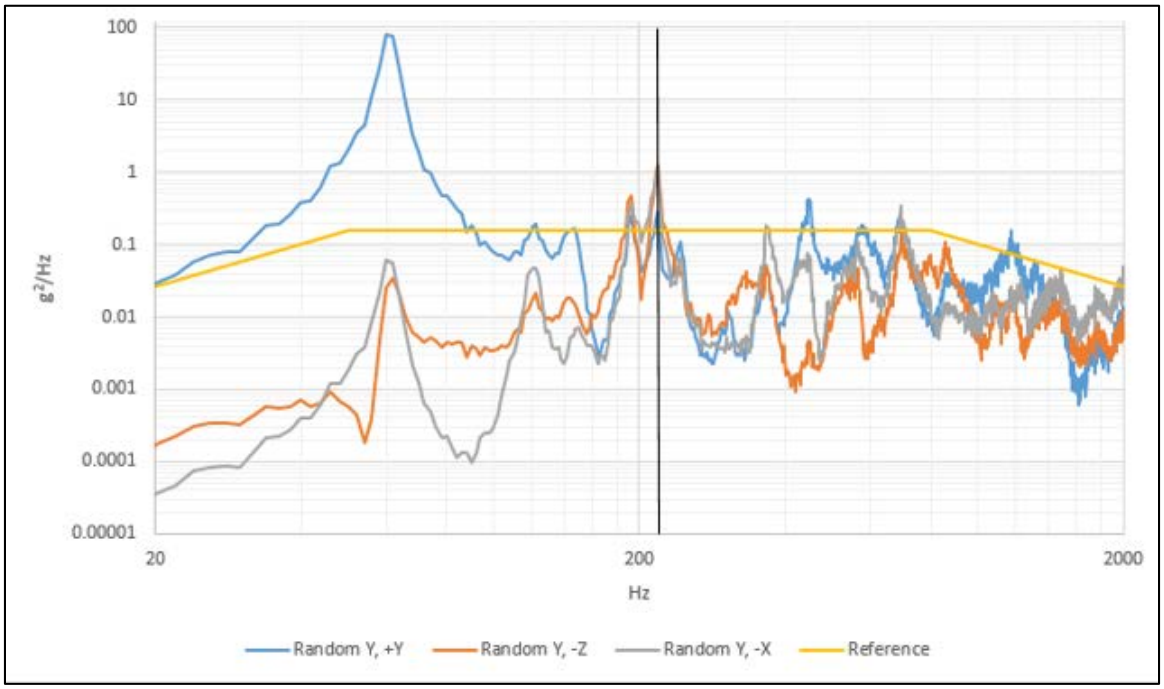

Figure 31. Y-Axis Random Vibration Overlay Plot

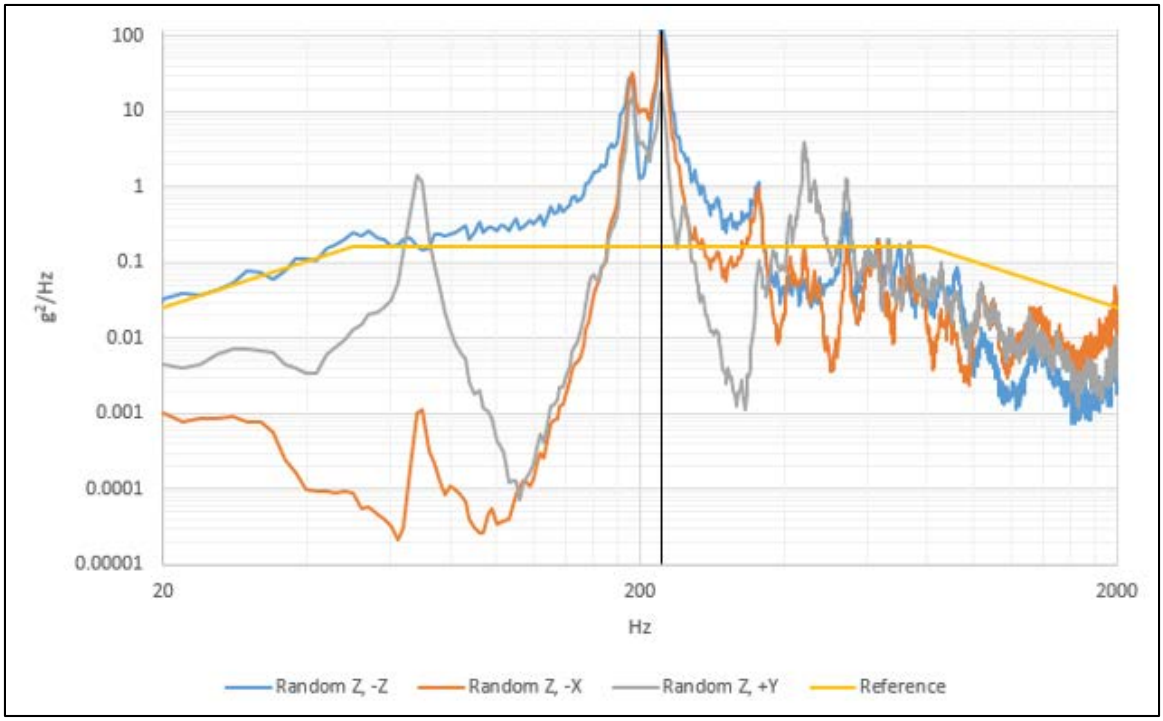

Figure 32. Z-Axis Random Vibration Overlay Plot

Table 7. Fundamental Frequencies for the X, Y, and Z Directions of Each Axis

Test Axis	**X**			**Y**			**Z**		
Response Axis	X	Y	Z	X	Y	Z	X	Y	Z
Fundamental Frequency (Hz)	220	220	220	218	218	218	222	220	222

Table 8. G_{rms} Values for the X, Y, and Z Directions of Each Axis

Test Axis	**X**			**Y**			**Z**		
Response Axis	X	Y	Z	X	Y	Z	X	Y	Z
G_{rms}	23	25	22	8	24	7	38	22	43

c. TIC EDU Imagery Comparison

The TIC EDU successfully recorded video during each function test. A functional test occurred after the baseline low-level sine sweep, random vibration, and post low-level sine sweep for each axis. A qualitative analysis of the imagery compared its appearance to the baseline imagery taken before the vibration test commenced. The TIC EDU passed the functional test if it imaged the IR radiation of the incandescent light bulb. Figure 33 shows the baseline imagery taken of the IR source while turned off and turned on before the start of the vibration test. Figure 34 shows the imagery from the functional test after each axis. The imagery captured by the TIC EDU after the vibration testing of each axis indicated the camera survived testing, establishing confidence in the design and survivability of a TIC in the launch environment.

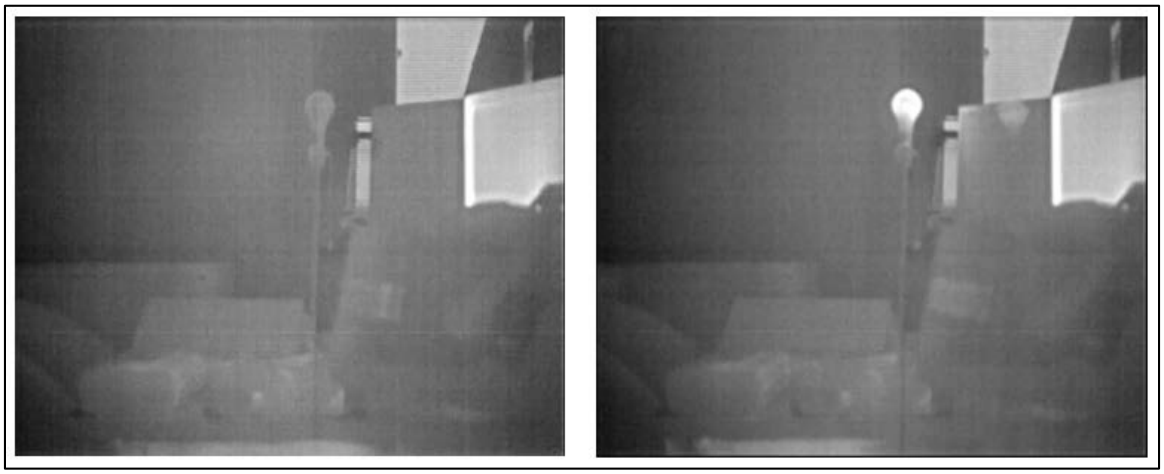

Figure 33. Baseline Imagery of IR Source

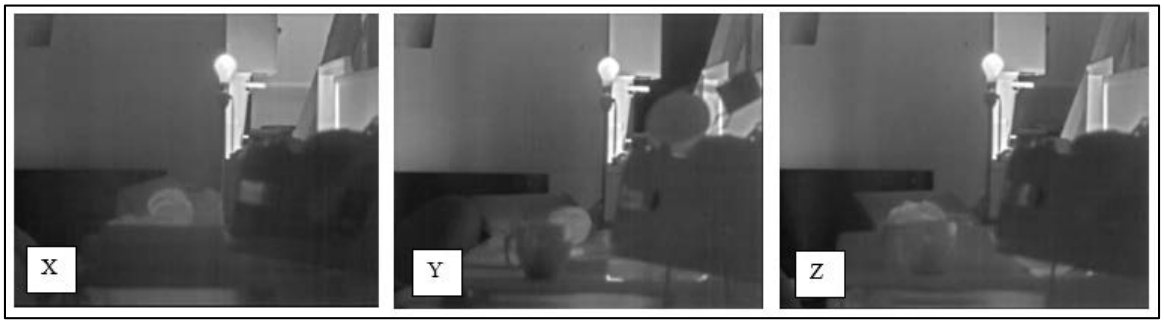

Figure 34. Imagery of IR Source after X, Y, and Z-Axis Vibration Testing

7. Results and Recommendations

The results of the random vibration test of the TIC EDU show the payload survived an average of 24 G_{rms} in response to the vibration environment. The amplitude of the response frequency indicates the payload was subjected to considerable amounts of energy. The payload endured a worst-case qualification testing because it was tested individually. The addition of the bus would potentially reduce the amplification by increasing the rigidity of the structure, and, thus, create a better vibration environment for the payload. Additionally, the results establish confidence in a COTS camera's ability to survive the launch environment. Future flight hardware testing can focus on workmanship of the terahertz lens, not the camera itself.

Overall, the TIC EDU successfully passed the vibration test. The TIC EDU recorded imagery after every test at the same quality as the baseline. Additionally, the pre-sine and post-sine data comparisons showed no dramatic change in the dynamic properties of the payload. Furthermore, the random vibration test provided G_{rms} data, with responses within reasonable limits for worst-case scenario testing. Without the presence of a bus and by testing to GEVS prototype qualification standards, the random vibration test simulated a worst-case environment. Although the amplitude of the frequency peak is high in the X, Y, and Z-axis random vibration plots, the high amplitude was expected due to the lack of rigidity in the 2U CubeSat frame without the bus. The standards and parameters used to conduct the vibration test developed the procedures for future flight qualification testing. The survival of the TIC EDU through the vibration test gives confidence for the flight hardware TIC's ability to survive a worst-case launch environment.

D. FIRST THERMAL VACUUM TEST

The TIC EDU did not perform as expected, and, overall, failed the criteria established for the thermal vacuum test. The TIC EDU stopped functioning around 50°C as the environment heated to 80°C and failed to record video until it cooled to 60°C, where it regained all functionality for the duration of the test. Although part of the test plan, neither a hot nor cold soak was conducted. The results suggest that either the manufacturer's temperature rating of -40°C to 80°C does not reflect the operational

temperature range of the camera, or the external temperature measured by thermocouples does not accurately reflect the camera's operating temperature.

1. Test Objective

The primary objective of the test was to characterize the TIC EDU in a thermal vacuum environment to the manufacturer's temperature rating of -40°C to 80°C. The secondary objective was to demonstrate the operability of the TIC EDU camera in a simulated extreme temperature soak at -40°C and 80°C.

2. Pass/Fail Criteria

Passing criteria included obtaining video from the TIC EDU at every five degrees in the rated temperature range. Additionally, it included qualitatively assessing the TIC EDU video to be the same, functioning nominally without degradation at each extreme temperature level.

3. Testing Plan

The TVAC test used the following five steps to execute the objective of the test. The first step was to heat the TIC EDU from ambient temperature to the maximum temperature of 80°C, conducting a functional test of the TIC EDU every five degrees. The second step was to hold the TIC EDU at a temperature of 80°C for one hour. The third step was to cool the TIC EDU to -40°C, conducting a functional test of the TIC EDU every five degrees. The fourth step was to hold the TIC EDU at a temperature of -40°C for one hour. The fifth and final step was to return the TIC EDU to ambient temperature, conducting a functional test of the TIC EDU every five degrees. The same functional test steps from the vibration test applied to the thermal vacuum test, shown in Table 2. Figure 35 shows the intended test profile with the five steps labelled.

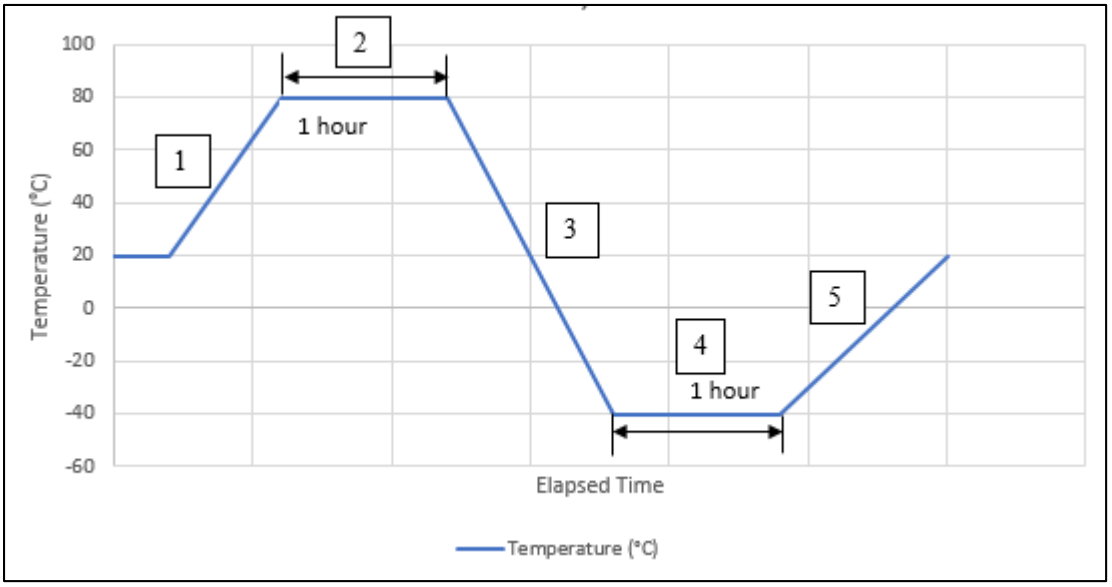

Figure 35. First TVAC Test Intended Test Profile

4. Test Setup

The TVAC test setup inside the chamber includes the IR source and camera placement, power and interface cabling, and thermocouple placement. Figure 36 shows an overall look inside the TVAC chamber, further examined in greater detail throughout the remainder of this section.

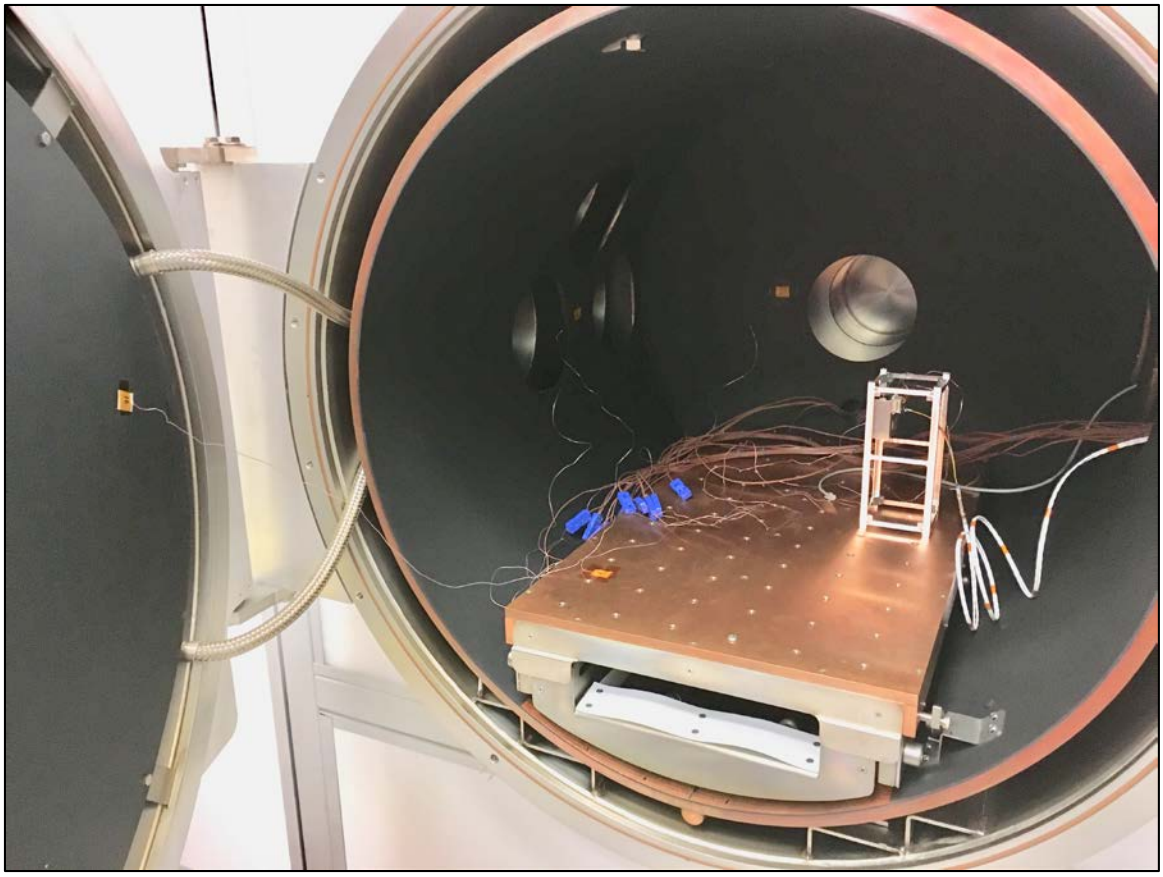

Figure 36. First TVAC Test Overall Setup

a. TIC EDU and IR Source

The TIC EDU was positioned to face a portion of the chamber wall where both the TVAC shroud and port blank resided in the TIC EDU's field of view. Two strips of material with different emissivities, a black piece of electrical tape and white ribbon, were placed on the port blank. The intention of the setup was for the TIC EDU to be able to image the differential between the strips on the port blank, the port blank itself, and the shroud. The TIC EDU was attached to an aluminum mount which was connected to a 2U aluminum CubeSat HAB frame. Figure 37 shows a picture of the test setup, including the port blank with the two strips and the TIC EDU mount on the 2U CubeSat HAB frame.

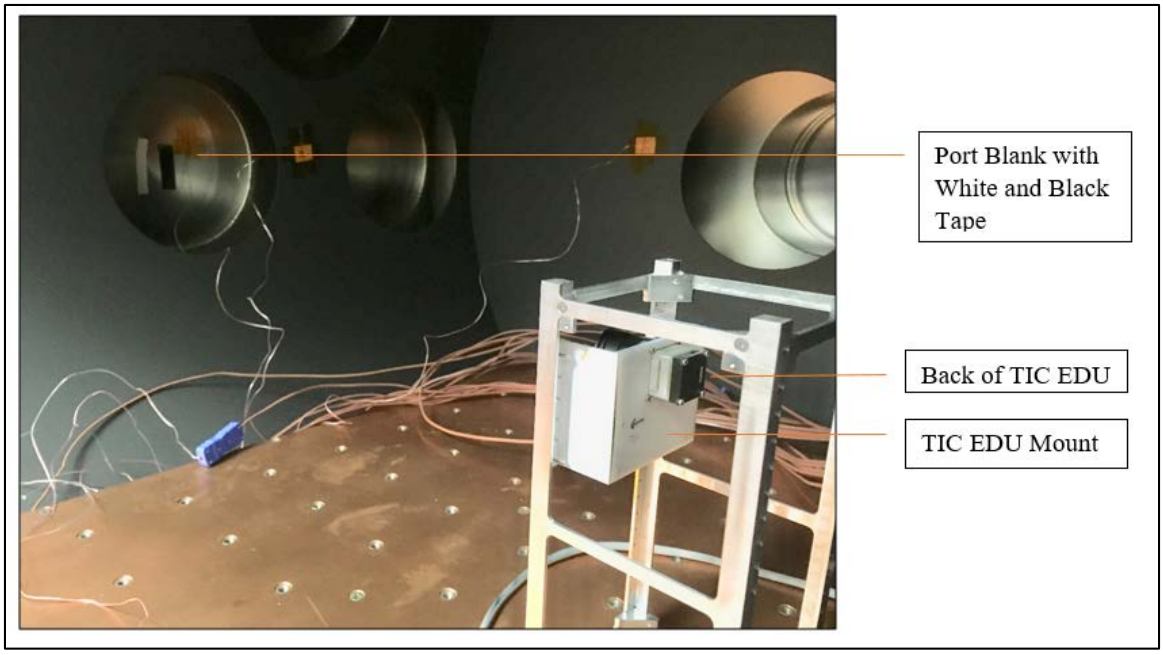

Figure 37. First TVAC Test Setup of TIC EDU and IR Source

b. Cabling

The test setup required cabling inside and outside of the chamber for command and control purposes. The TIC EDU received power through a USB connection. Outside the chamber, a Raspberry Pi powered a desktop computer screen which connected to the TIC EDU by USB. Figure 38 shows the test setup and the necessary cabling to power the TIC EDU from inside the chamber while controlling from outside.

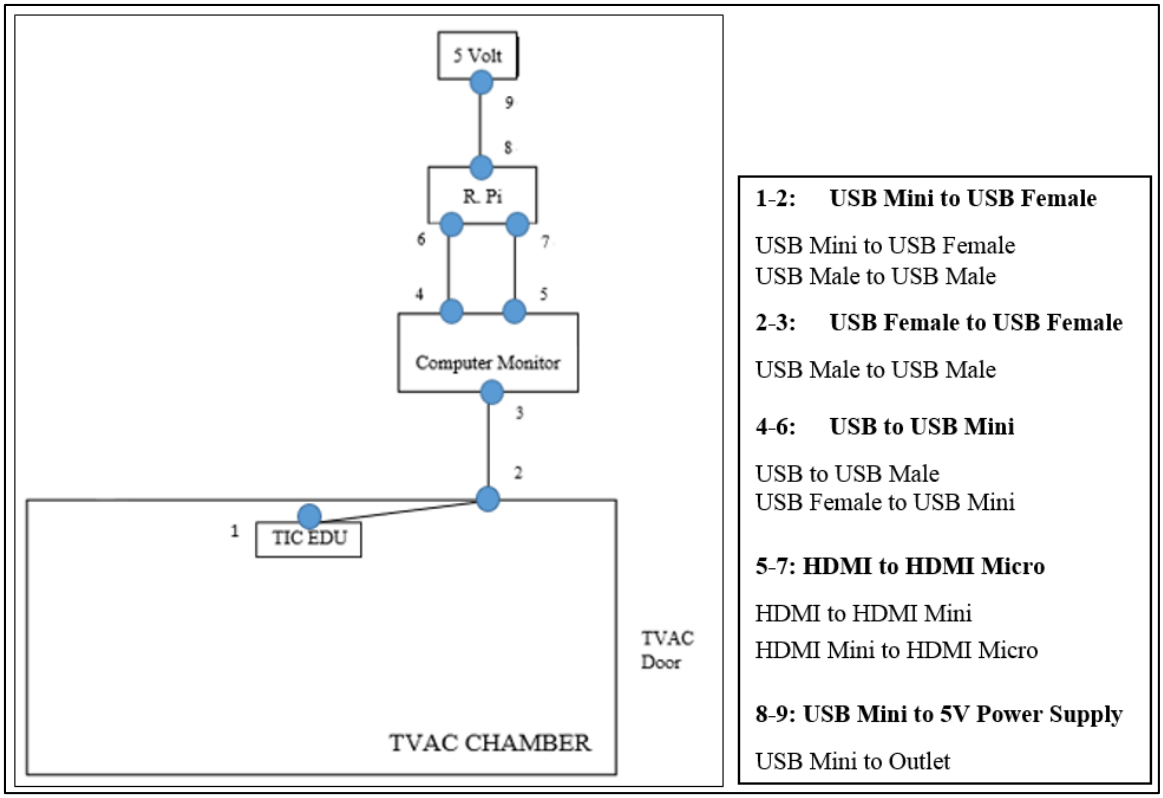

Figure 38. First TVAC Test Setup and Cabling Requirements

c. Thermocouples

A total of nine thermocouples were used. The thermocouples were placed throughout the chamber to record the temperature of the platen, chamber door, shroud, chamber wall, port blank, TIC EDU, and TIC EDU mount, as reflected in Table 9. The thermocouple numbers do not start linearly at number one because of user setup. Of the twenty-four thermocouples available, the nine assigned were chosen at random and placed throughout the chamber. The remaining fifteen thermocouples were unused. Figure 39 shows the thermocouples throughout the TVAC chamber and Figure 40 shows, specifically, the thermocouples on the TIC EDU.

Table 9. First TVAC Test Thermocouple Numbers and Placement

Thermocouple Number	Thermocouple Placement
2	Platen
3	Port Blank
4	Back Wall of Chamber
5	Back of Camera
6	Left Side of Camera
8	Back of Mount
10	Shroud
11	Front of Mount
16	Chamber Door

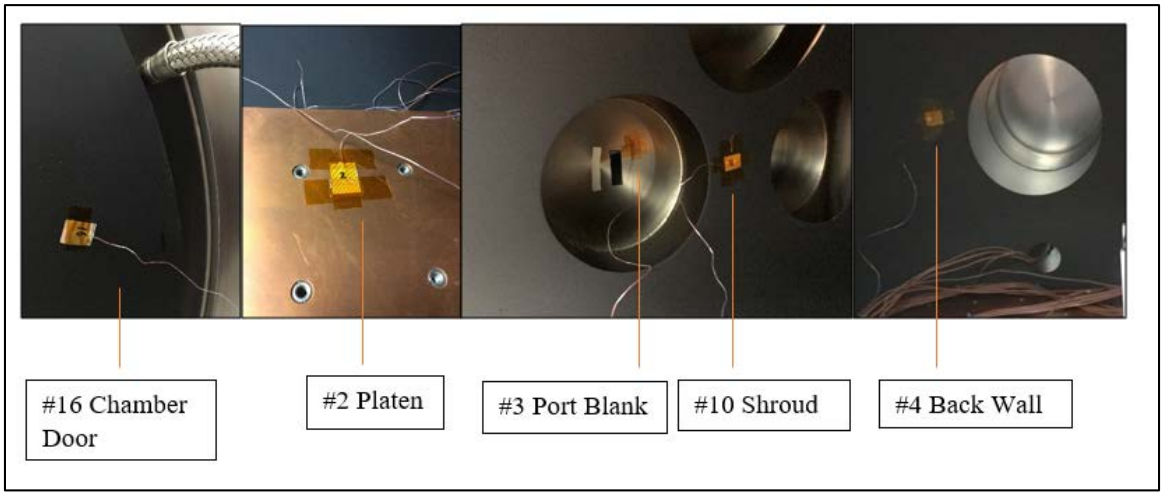

Figure 39. First TVAC Test Setup of Thermocouples

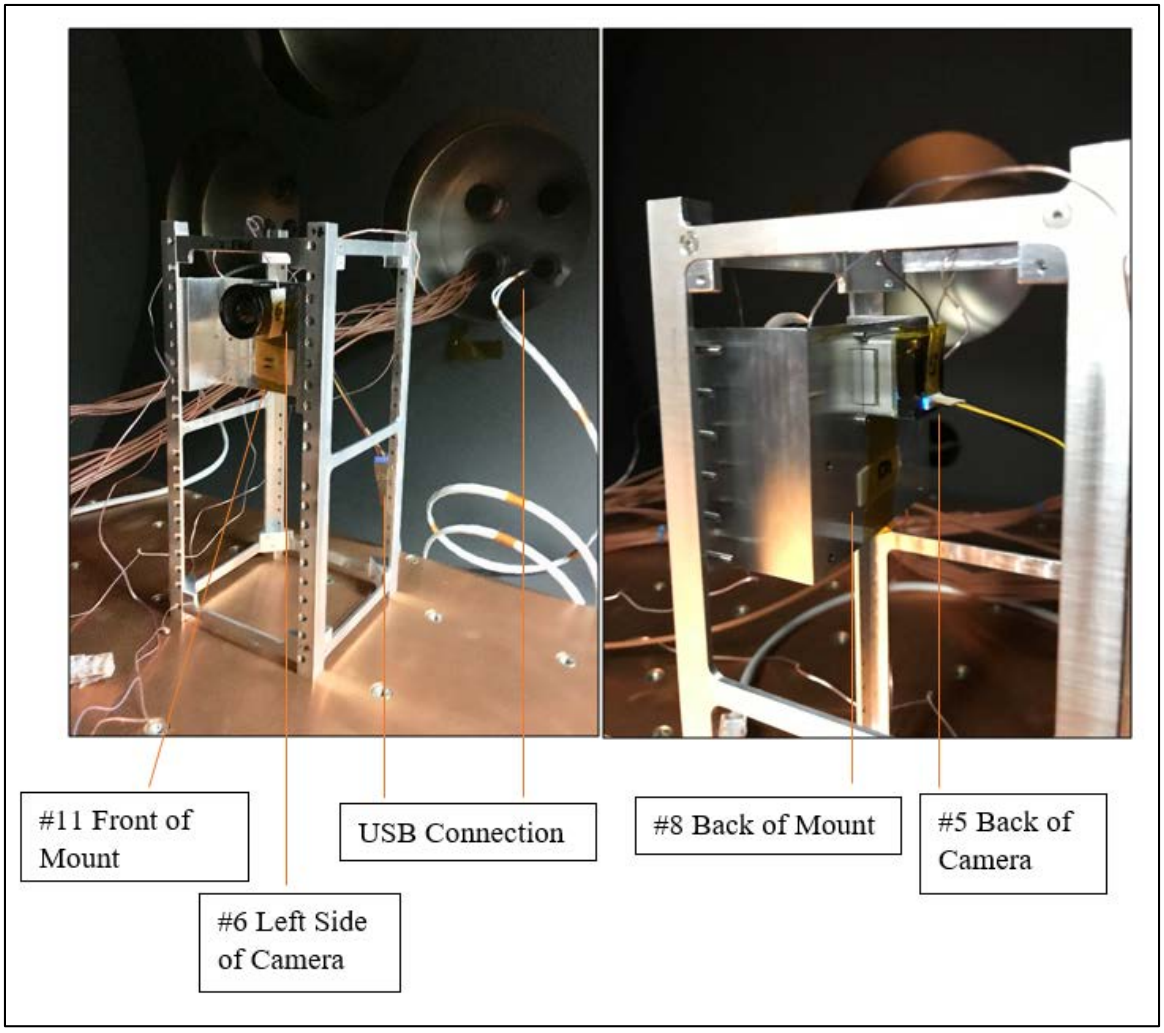

Figure 40. First TVAC Test Thermocouples on the TIC EDU

5. Discussion

The total elapsed time of the TVAC test was five hours and nineteen minutes. No significant images were taken which could distinguish the shroud, the tapes, and the chamber wall from one other. The thermocouple on the back of the TIC EDU failed from the onset of the test, so the thermocouple on the side of the TIC EDU was used as the primary source of information to determine the temperature of the camera. Additionally, the thermocouple on the port blank failed from the onset of the test, which made it difficult to determine the temperature differential between the port blank and the shroud. Due to the height of the HAB frame and the location of the TIC EDU mount relative to the platen, it

was expected that the TIC EDU would take considerable time to heat. Contrary to expectation, the camera heated very quickly. The cooling process took significantly longer, though. Figure 41 depicts the overall temperature profile of the TVAC test, showing the temperature from the thermocouple on the left side of the camera relative to the elapsed time.

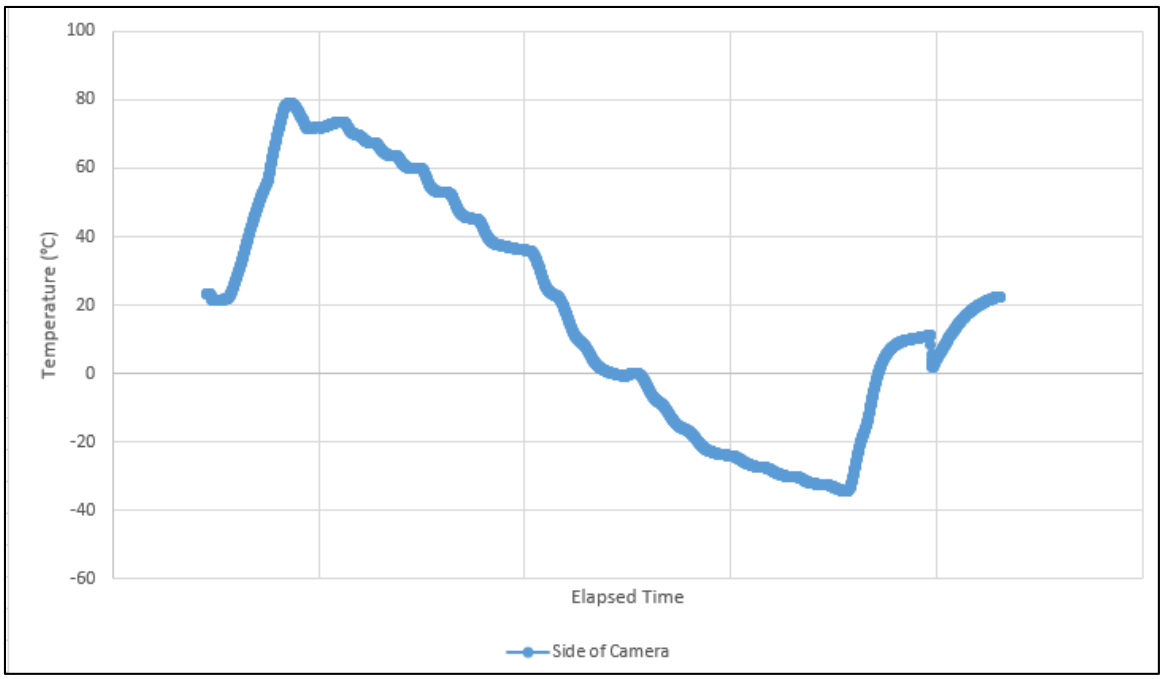

Figure 41. First TVAC Test Overall Temperature Profile of the Temperature of the Left Side of the Camera Relative to the Elapsed Time

a. Temperature Ramp—Ambient to 80°C

The first step of the TVAC test was to heat the environment from ambient temperature to 80°C. Since it was expected that the TIC EDU would not heat quickly, the chamber temperature was set immediately to 80°C. The platen heated quickly, as did the TIC EDU. A successful functional test occurred at 37°C, but the next functional test at 48°C failed, meaning TIC EDU could not successfully record a video. As the temperature rose, the camera continued to fail the functional tests by not successfully recording video. It was evident that the camera received the command (Step 4 of Table 2), but the camera would respond with zero byte packages, meaning no data was recorded. Two power cycles

and some troubleshooting proved ineffective in resolving the issue. Due to the TIC EDU not successfully recording video, a one-hour soak at 80°C was not conducted. Table 10 shows a summarized timeline of events of heating the TIC EDU from ambient temperature to 80°C, and Figure 42 graphically shows the temperature of the platen and the left side of the camera relative to the elapsed time.

Table 10. Timeline of Events from Ambient Temperature to 80°C

Time	Action	TIC EDU Temp	Functional Test
+0 min	Start Vacuum	23°C	Passed
+6 min	Set Chamber to 80C	23°C	N/A
+14 min	N/A	37°C	Passed
+18 min	N/A	48°C	Failed
+22 min	Set Chamber to 120C	57°C	N/A
+29 min	N/A	77°C	Failed

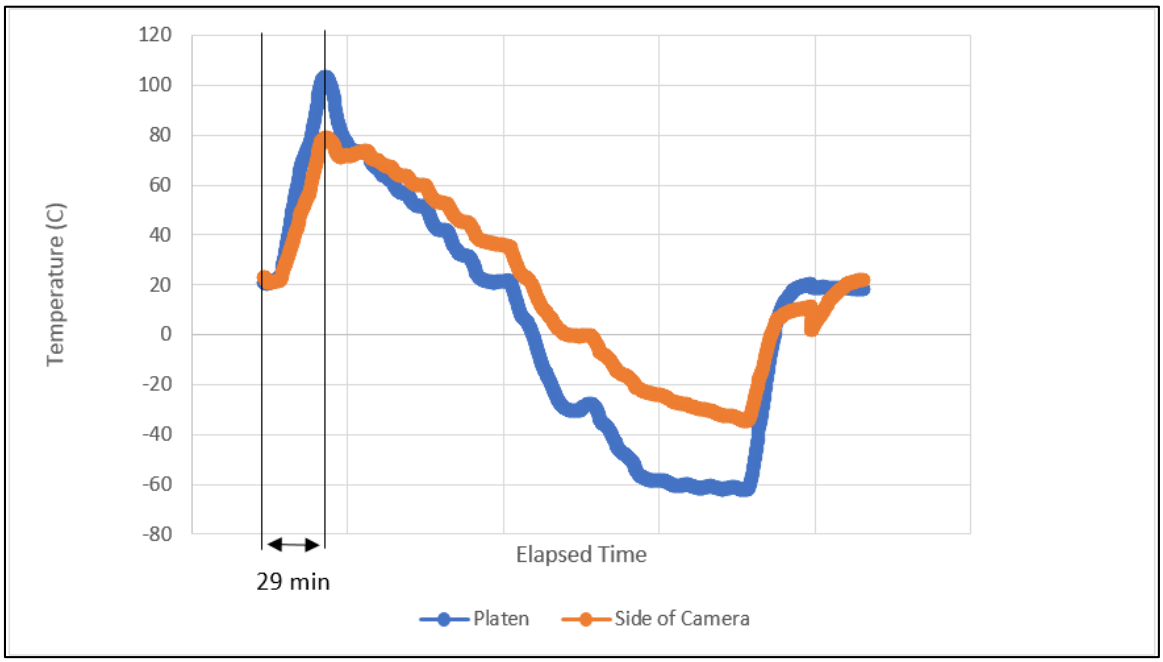

Figure 42. Temperature of Platen and the Left Side of the Camera Relative to Elapsed Time from Ambient Temperature to 80°C

b. Temperature Drop—80°C to -40°C

As the environment cooled to -40°C, a functional test was conducted on the TIC EDU every five degrees. The TIC EDU passed the first functional test since it had stopped working at 60°C, 118 minutes into the test. Table 11 shows a summarized timeline of events as the TIC EDU cooled from 80°C to the first few successful functional tests.

Table 11. Timeline of Events from 80°C to 60°C

Time	Action	TIC EDU Temp	Functional Test
+92 min	Set Chamber to 65°C	73°C	Failed
+98 min	Set Chamber to 60°C	70°C	N/A
+101 min	N/A	68°C	Failed
+105 min	Set Chamber to 55°C	66°C	Failed
+110 min	Conducted Power Cycle	N/A	N/A
+114 min	Set Chamber to 50°C	64°C	Failed
+118 min	N/A	60°C	Passed
+129 min	N/A	56°C	Passed
+152 min	N/A	41°C	Passed

After the TIC regained functionality at 60°C, it continued to perform well and it passed the functional tests throughout the cool portion of the testing. Due to the amount of time it required to cool the TIC EDU and the amount of liquid nitrogen (LN2) available, the camera did not reach -40°C, but instead only reached -35°C. A cold soak was not conducted. Figure 43 shows the temperature of the platen and the left side of the camera relative to the elapsed time as the environment was cooled to -40°C.

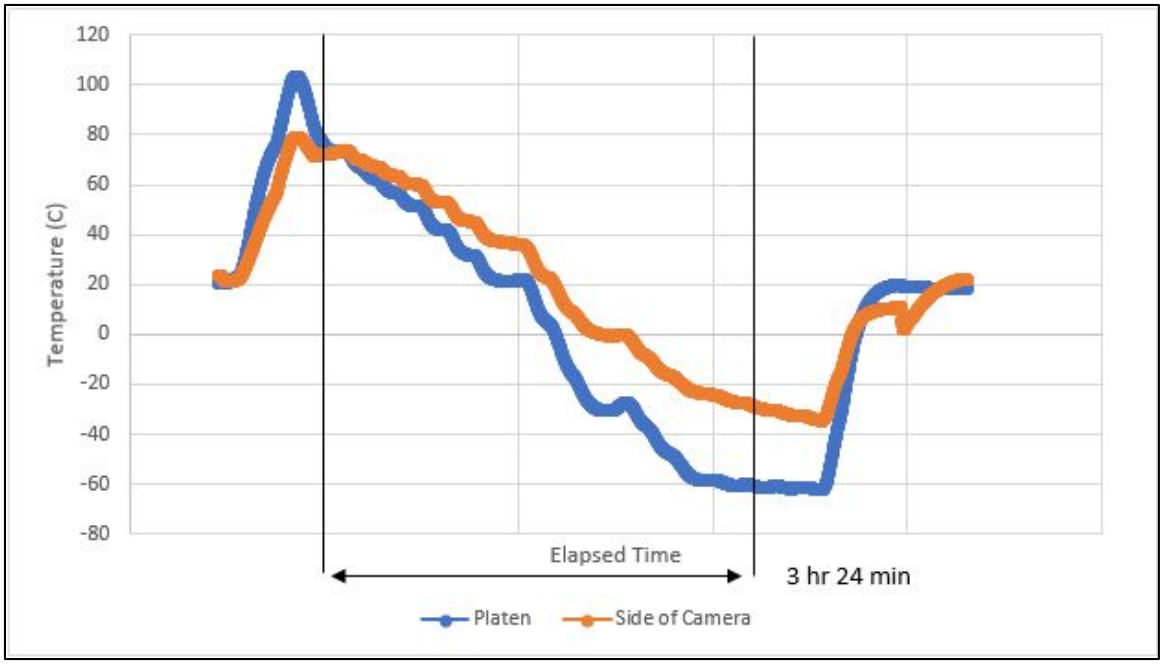

Figure 43. Temperature of Platen and the Left Side of the Camera Relative to Elapsed Time from 80°C to -40°C

c. Imagery

An active IR source was not used for imaging because it was expected that a temperature differential would be detected between the strips, port blank, and shroud. The imagery from the camera did not detect any differential or image anything significant. One possibility for the lack of detection of anything in the imagery is because the source was not distinguishable enough in the short distance. Due to the focal length of the camera, it is possible the camera was too close to focus on the port blank and strips of material. A second possibility is that there was not a significant differential to image. Due to the failure of the port blank thermocouple from the onset of the test, a temperature comparison of the port blank and shroud is difficult to analyze because the port blank thermocouple temperature read-out remained at room temperature the entire test.

6. Results and Recommendations

Overall, the TVAC test provided critical lessons learned for implementation on a future TVAC test. A heat soak was not conducted due to the camera not being able to take videos, and a cold soak was not conducted due to time and LN2 constraints. The camera's poor performance in hot temperatures suggests that either the manufacturer's temperature ratings reflect survival temperatures and not operational temperatures, or that the internal temperature of the camera was higher than the external temperature measured by a thermocouple.

Four recommendations from the results of the first TVAC test suggest the need for a follow-on test. The first recommendation is to acquire a means to better record the temperature of the camera, whether through a better placed thermocouple or software from the manufacturer to read internal temperature. The second recommendation is to modify the test setup so that the TIC EDU cools more quickly. A third recommendation is to increase the redundancy in thermocouple placement to account for failed thermocouples. A fourth and final recommendation is to acquire more LN2 and conduct a cold soak, even if a hot soak is not possible due to the camera not functioning at warmer temperatures.

E. SECOND THERMAL VACUUM TEST

The TIC EDU performed well and passed the criteria established for the second TVAC test. With an added ability to read the internal temperature of the camera's focal FPA, the camera functioned without degradation throughout the entire test as the internal temperature cooled to -40°C and heated to 80°C. An active IR source proved to be a much better source, evidenced by the imagery acquired during testing. Additionally, a one-hour soak at each extreme temperature was conducted successfully.

1. Test Objective

The first objective of the test was to characterize the IR camera in a thermal vacuum environment from -40°C to failure, which was expected around 60°C. The second objective was to demonstrate the operability of the IR camera in a simulated extreme temperature

soak at -40°C. The third objective was to qualitatively compare images taken of the active IR source by the IR camera at two different power levels.

2. Pass/Fail Criteria

Passing criteria included obtaining images at every five degrees from -40°C to failure. It also included seeing a qualitative difference in the images taken of the active IR source at the two different power levels, 10 V and 25 V.

3. Testing Plan

The TVAC test used the following four steps to execute the objective of the test. The first step was to cool the TIC EDU from ambient temperature to -40°C, conducting a functional test of the camera every five degrees. The second step was to hold the TIC EDU for one-hour at -40°C. The third step was to heat the TIC EDU to failure, conducting a functional test of the camera at every five degrees. The fourth and final step was to return the TIC EDU to ambient temperature. Figure 44 shows the intended test profile with the corresponding steps labeled and Table 12 outlines the steps of a functional test.

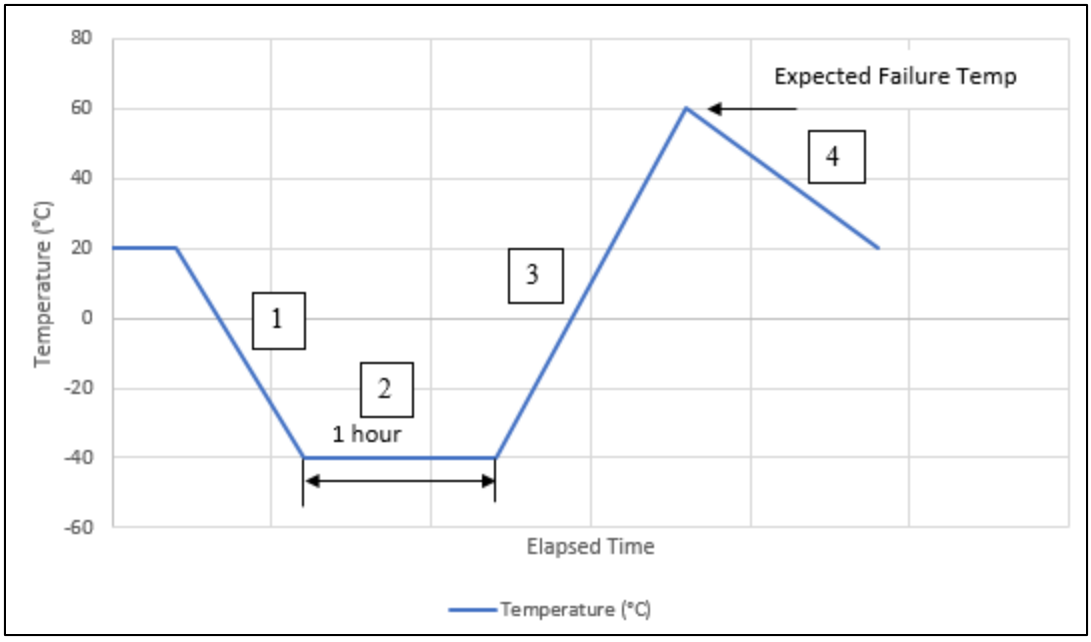

Figure 44. Second TVAC Test Intended Test Profile

Table 12. Steps of the Functional Test for the FLIR BOSON Software

Step	Action
1	Set the active IR source to 10 V. Capture image.
2	Set the active IR source to 25 V. Capture image.

4. Test Setup

Four significant changes were made to the test setup from the first TVAC test. The first was the addition of an active IR source. The second was the placement of the source as far as possible from the TIC EDU to improve focus. The third was the use of a copper mount to hold the base of the TIC EDU directly on the platen to promote thermal conduction. The fourth was the use of a laptop with software from the manufacturer to interface with the TIC EDU and read the internal FPA temperature instead of using a Raspberry Pi. Figure 45 shows an overall look inside the TVAC chamber, further examined in greater detail throughout the rest of the section, and Figure 46 shows the FLIR BOSON software interface.

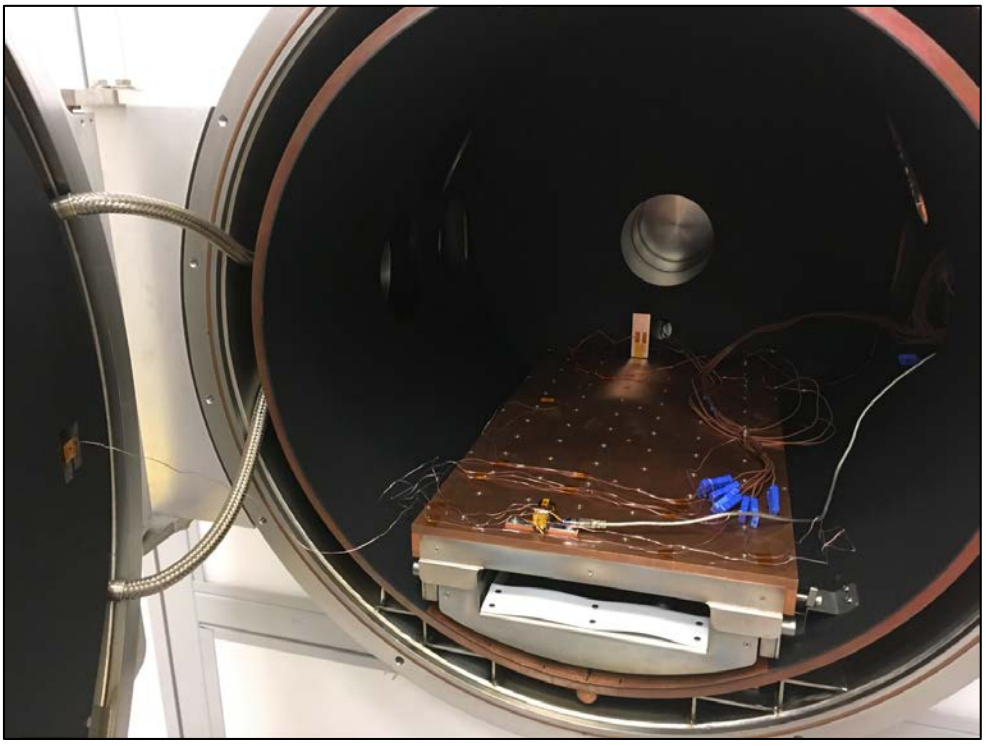

Figure 45. Second TVAC Test Setup of TIC EDU and IR Source

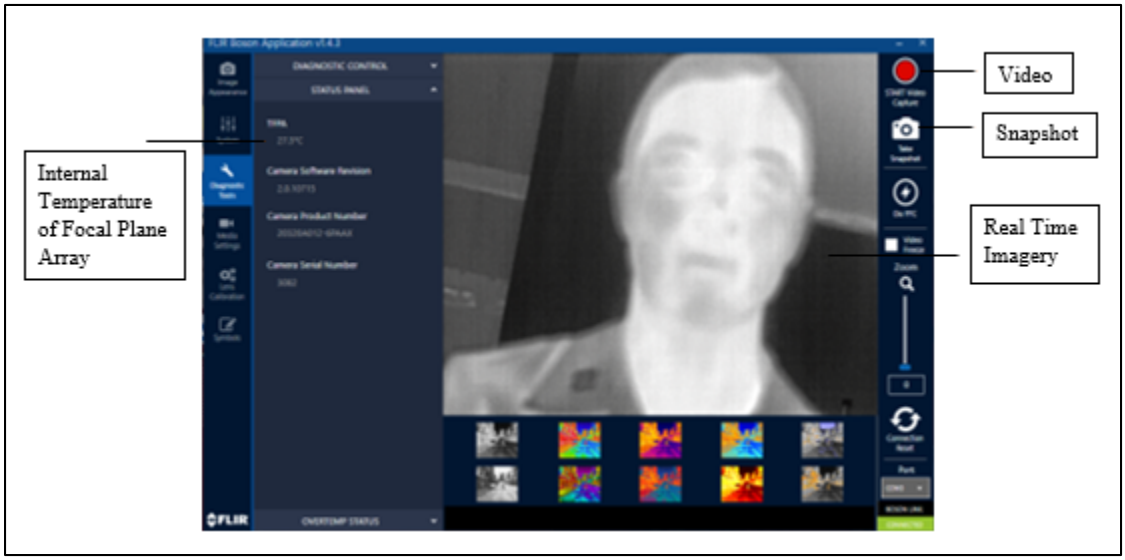

Figure 46. FLIR BOSON Software Interface

a. TIC EDU and IR Source

The TIC EDU was positioned as close to the chamber door as possible, while the active IR source was placed as far away as possible to create the greatest separation between the camera and the IR source. The distance between the camera and IR source was approximately 33 inches. Both items were attached to the platen using 1/4-20 screws. The active IR source was placed on an aluminum L-bracket within the field of view of the camera. A strip of aluminum tape was placed in the middle of the IR source in order to create a differential to be seen in the imagery, as shown in Figure 47. The TIC EDU was placed on one piece of copper with a second piece of copper holding the base of the TIC EDU. Two aluminum washers were used to hold the setup in place, as shown in Figure 48.

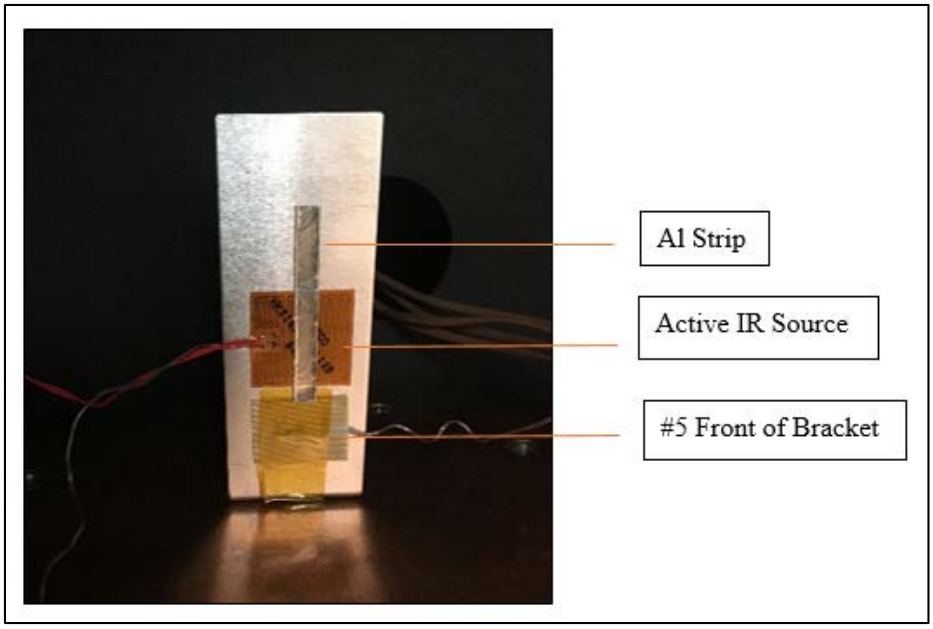

Figure 47. Second TVAC Test Setup of IR Source with Al Strip and Thermocouple

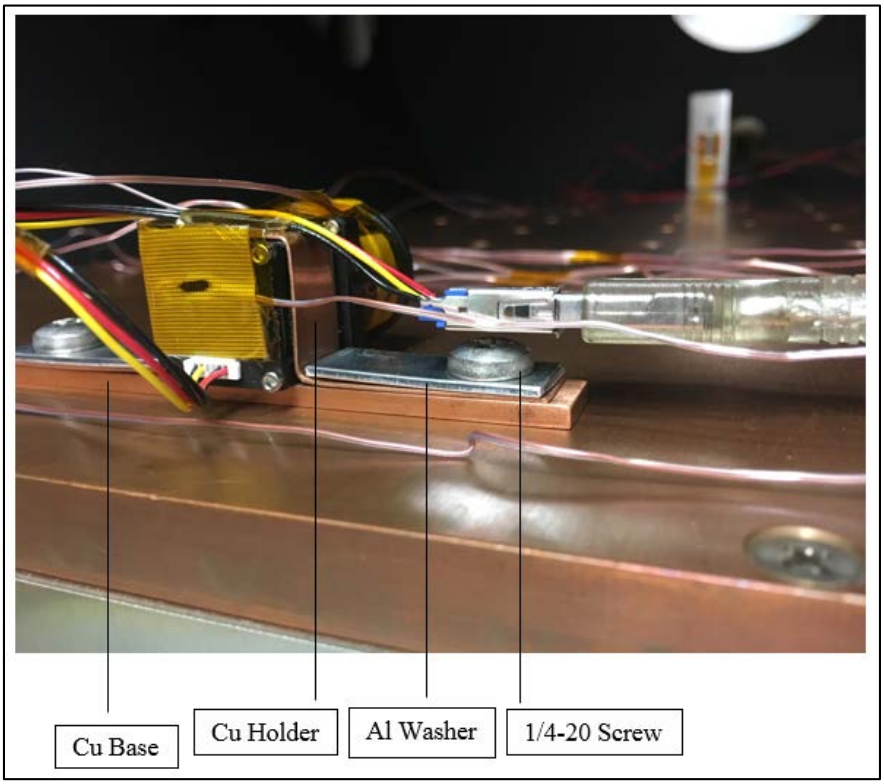

Figure 48. Second TVAC Test Setup of TIC EDU on Copper Mount

b. Cabling

The test setup required cabling inside and outside the chamber for command and control purposes of the TIC EDU and the active IR source. The TIC EDU received power through a USB connection. Outside the chamber, the USB cable was plugged into a laptop to run the FLIR BOSON software. The active IR source was powered through BNC cabling connected to a power supply outside the chamber. Figure 49 shows the test setup and the necessary cabling to power the TIC EDU and IR source while commanding them both from the outside. Figure 50 shows a picture of the setup from test day.

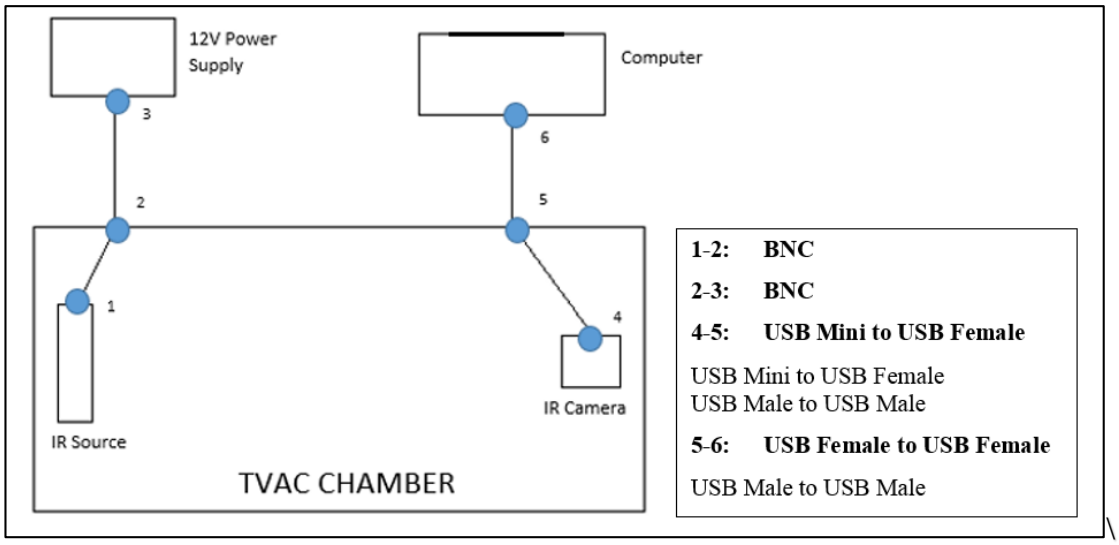

Figure 49. Second TVAC Test Setup and Cabling Requirements

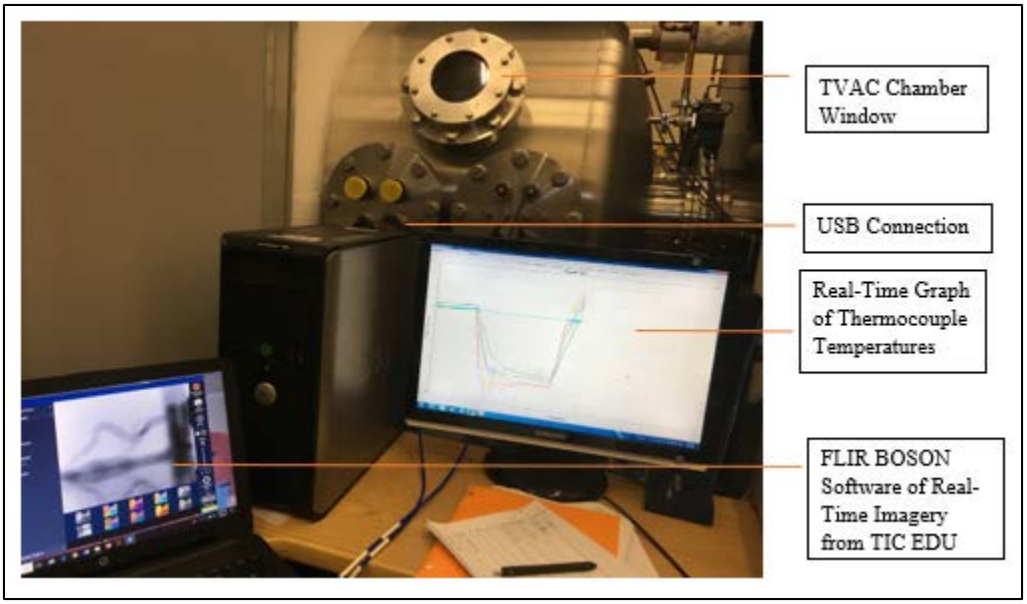

Figure 50. Second TVAC Test Setup and Cabling Picture from Test Day

c. Thermocouples

A total of eight thermocouples were used. The thermocouples were placed on the TIC EDU, active IR source, platen, and chamber wall, as reflected in Table 13. Figure 51 shows the thermocouples on the TIC EDU.

Table 13. Second TVAC Test Thermocouple Numbers and Placement

Thermocouple Number	Thermocouple Placement
1	Back of Camera
2	Chamber Door
3	Top of Camera
4	Platen
5	Front of L Bracket
6	Left Side of Camera
7	Right Side of Camera
8	Back of L Bracket

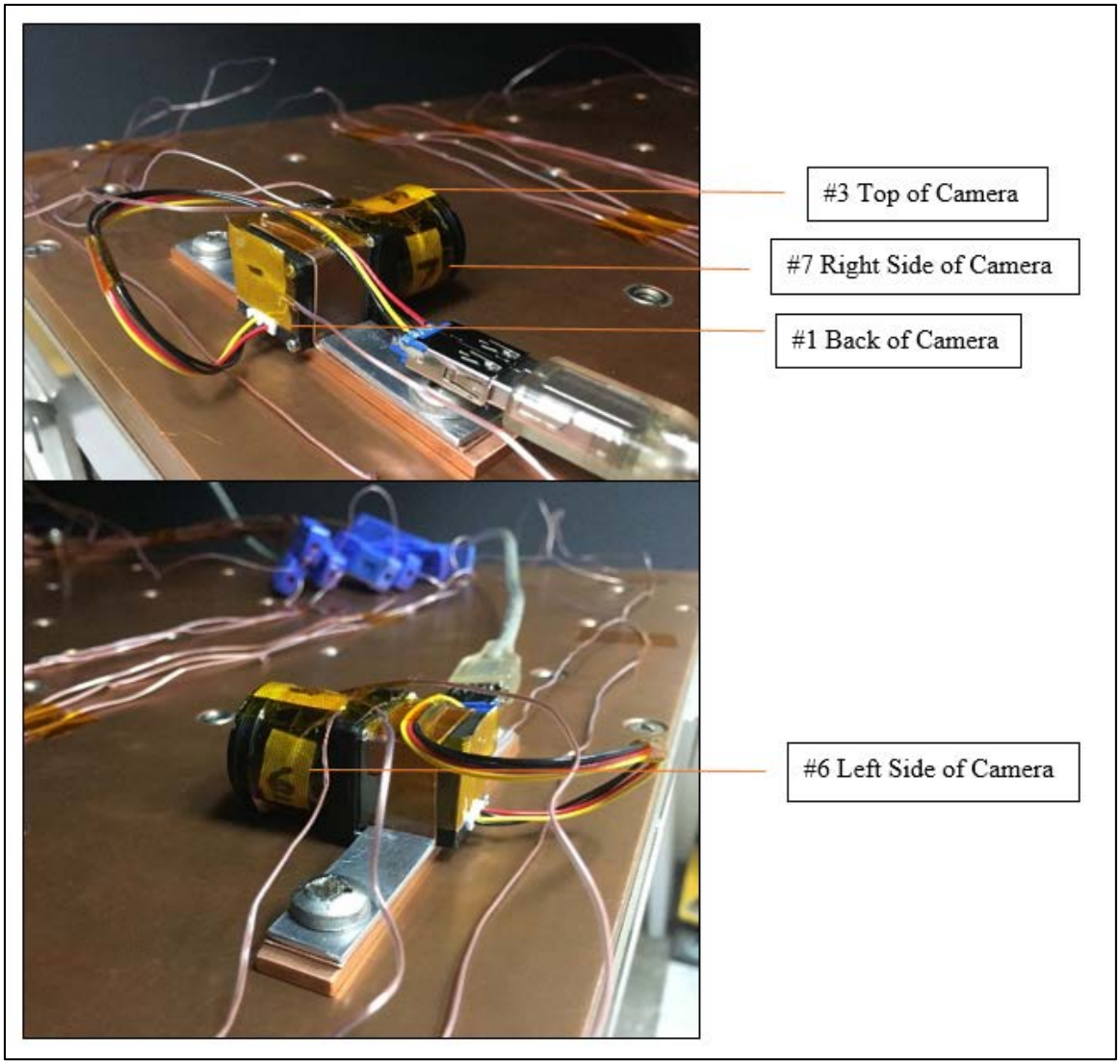

Figure 51. Second TVAC Test Setup of Thermocouples on the TIC EDU

5. Discussion

The total elapsed time of the TVAC test was five hours and twenty-two minutes. By monitoring the internal temperature of the TIC EDU, the test was able to successfully cool the camera to -40°C for a one-hour cold soak and heat the camera to 80°C for a one-hour hot soak. Contrary to expectations based on previous test results, the camera, when internal temperature was monitored, functioned properly past the 60°C prediction. Images were successfully taken every five degrees for the entire duration of the test. The thermocouple on the right side of the camera failed from the onset of the test, but the

thermocouples on the left side of the camera and on the back functioned properly. Additionally, the FLIR BOSON software successfully provided a read-out of the internal FPA temperature of the camera. The test setup with the copper plates significantly improved the TIC EDU's ability to heat and cool quickly. Figure 52 depicts the overall temperature profile of the TVAC test, showing the internal temperature of the camera and the external temperature of the left side of the camera relative to the elapsed time.

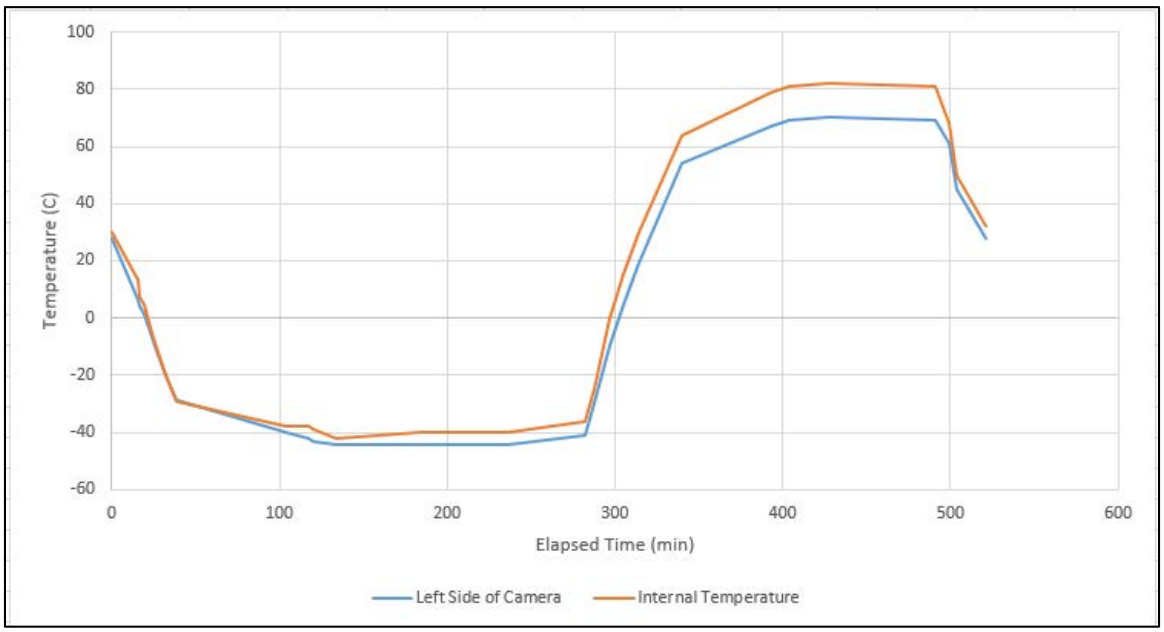

Figure 52. Second TVAC Test Overall Temperature Profile Showing the Internal Temperature of the TIC EDU Relative to Elapsed Time

a. Internal Temperature vs. External Temperature of the Camera

The internal temperature of the camera mirrored the external temperature read-out of the thermocouple in the cold environment, but in the hot environment, the internal temperature of the camera was significantly higher. The internal temperature not only heated more quickly than the external, but it also remained ten degrees Celsius hotter throughout the hot soak at 80°C. Figure 52 shows the left side of the camera and the internal temperature of the camera relative to the elapsed time.

b. Imagery Discussion

The IR camera was able to successfully take images and videos throughout the entire TVAC test. The brightness of the active IR source was detectable between the 10 V and 25 V images. The expectation was for the TIC EDU to image the IR source more clearly at colder temperatures because of semiconductor physics. The expectation proved true as the camera resolved the aluminum strip on the IR source and the wires of the IR source with better focus at colder temperatures. Figure 53 depicts the temperature of the left side of the camera and the temperature of the heat strip used as the active IR source. Figure 51 shows the location of the thermocouple on the left side of the camera and Figure 47 shows the location of the thermocouple near the heat strip. The heating and cooling of the IR source between 10 V and 25 V is easily distinguishable, especially during the temperature soaks. Figure 54 shows the baseline imagery at ambient temperature with the active IR source at 0 V, 10 V, and 25 V. Figure 55 shows the imagery at -40°C at 10 V and 25 V, and Figure 56 shows the imagery at 80°C at 10 V and 25 V. In Figures 53 and 54, a reflection shows to the right of the active IR source that was not present at ambient temperature testing.

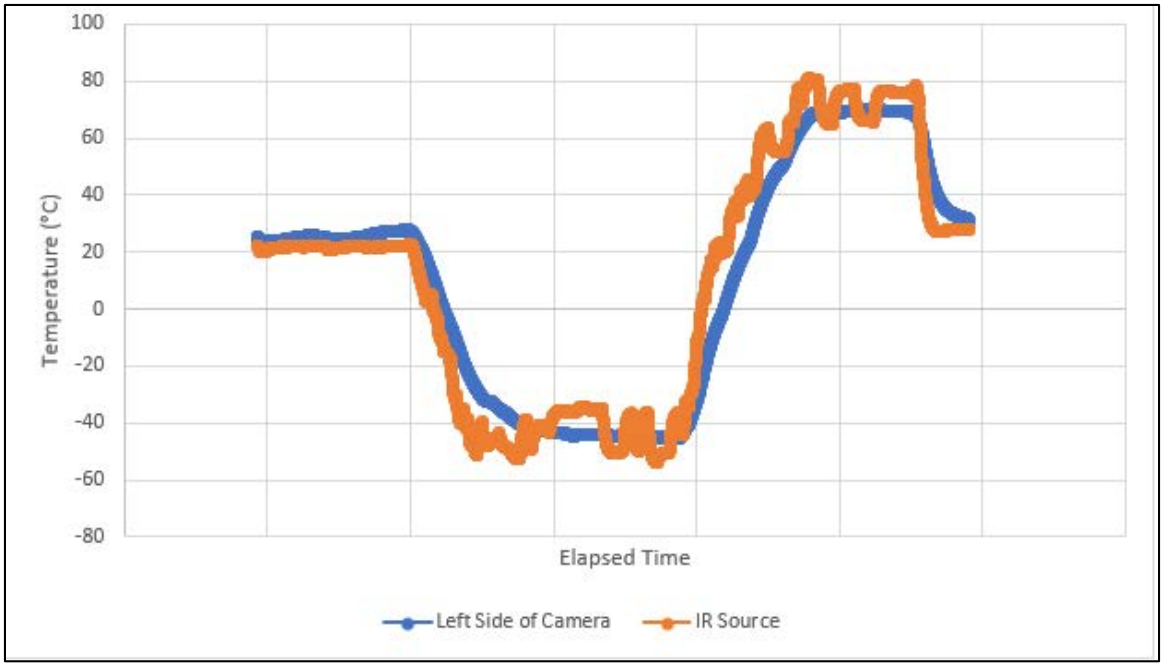

Figure 53. Second TVAC Test the Left Side of the Camera and the Active IR Source Temperature Relative to Elapsed Time

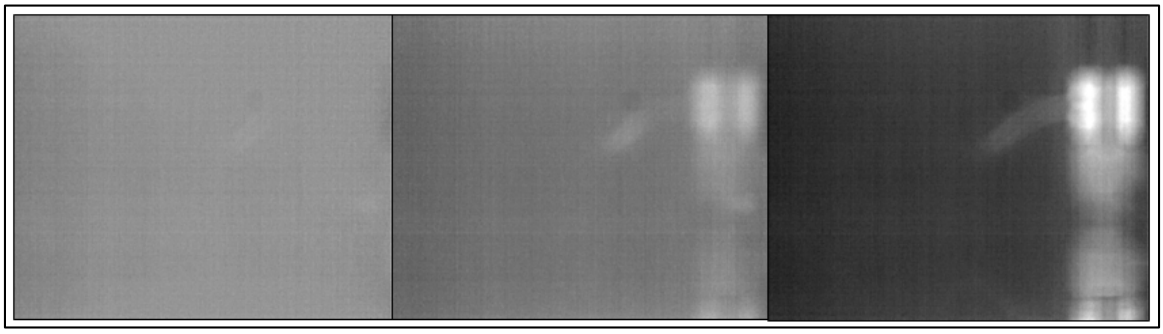

Figure 54. Second TVAC Test TIC EDU Imagery at Ambient Temperature with the Active IR Source at 0 V, 10 V, and 25 V

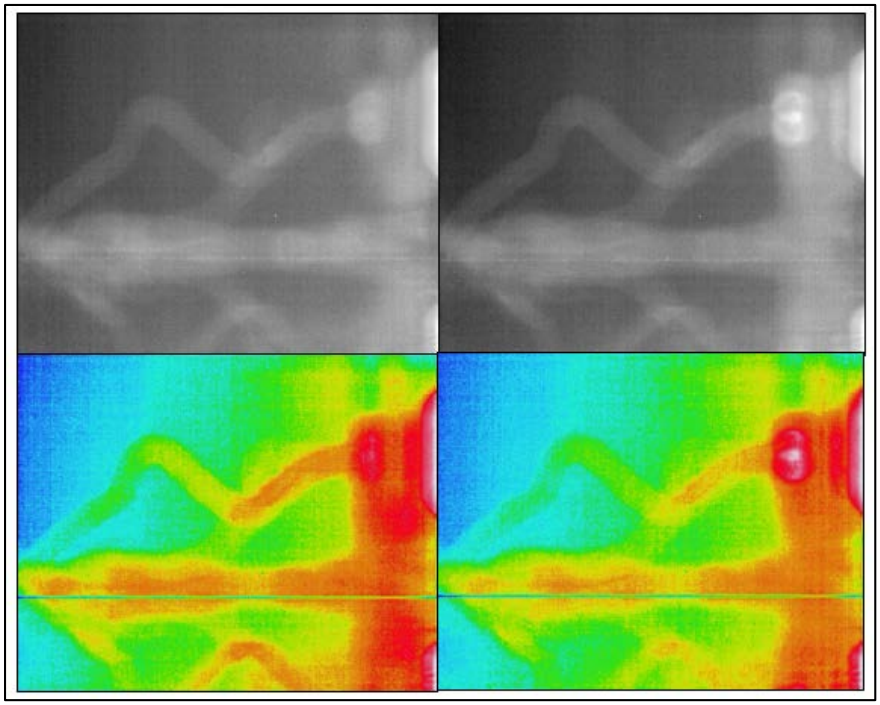

Figure 55. Second TVAC Test TIC EDU Imagery at -40°C with the Active IR Source at 10 V (Left Images) and 25 V (Right Images)

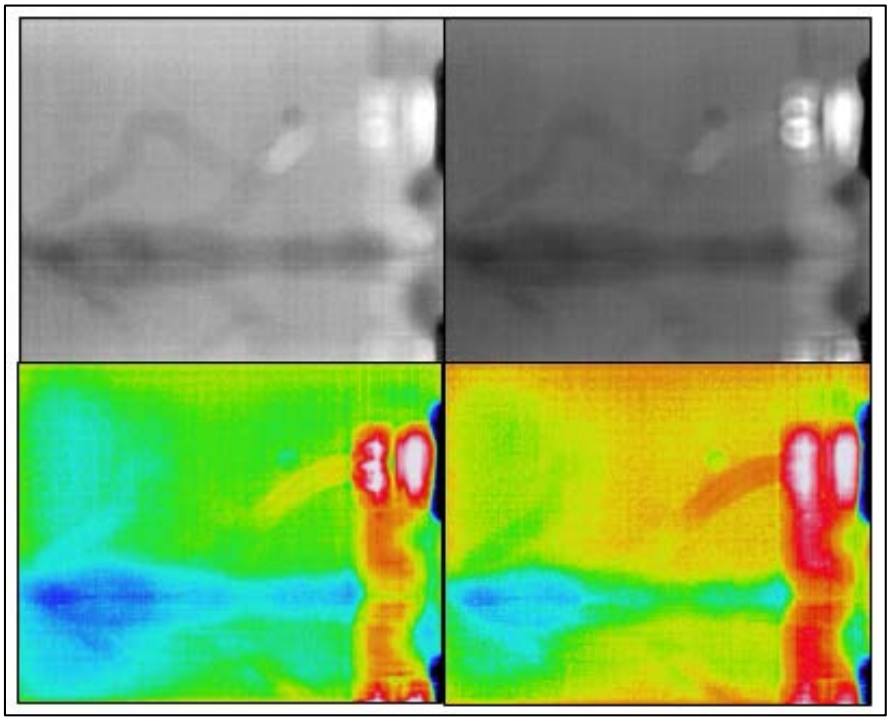

Figure 56. Second TVAC Test TIC EDU Imagery at 80°C with the Active IR Source at 10 V (Left Images) and 25 V (Right Images)

6. Results and Recommendations

The data comparison of the two thermal vacuum tests shows the FPA inside the camera is hotter than the case and sensitive to heating. In the first TVAC test, the camera stopped functioning at 50°C, the measured external temperature of the camera, due to the rapid heating of the chamber. Even when the chamber slowly heated, as in the second TVAC test, the FPA heated faster than any other portion of the camera and remained more than ten degrees Celsius hotter throughout the entire heat soak. The sensitivity of the FPA to heat implies specific thermal considerations for when in the space environment. The TVAC tests show the TIC payload requires a means of thermal control to ensure temperatures remain conducive to camera functionality. A critical consideration is the rate at which the FPA heats when in sunlight. The camera should remain below the max temperature operability rating, and must not be subjected to temperature surges. The thermal vacuum tests of the TIC EDU demonstrate the need for an internal temperature read-out. The external temperature of the camera fails to accurately represent the FPA temperature and therefore, is not an accurate representation of the camera's operating temperature. An internal temperature read-out allows for accurate data analysis during acceptance testing as well as assists in trouble-shooting on-orbit anomalies.

Overall, the lessons learned from the first TVAC test were successfully implemented in the second TVAC test. With a modified test setup with copper plates, an acquired software to read the internal temperature of the camera, an increased distance between the IR source and the camera, and an active IR source, the second TVAC test went significantly better. The results show that the manufacturer's ratings were in reference to the internal operating temperature of the IR camera, and the FPA is sensitive to heating. The TVAC tests showed the value of being able to measure the internal temperature of the camera and increased the confidence in the survivability of the TIC EDU for the space environment.

F. SUMMARY OF TIC EDU DEVELOPMENT TESTING

The development tests conducted on the TIC EDU provided a means to establish confidence in the mission objective of integrating a TIC as a CubeSat payload and to develop procedures and guidelines for future acceptance testing of the flight hardware. Four results from the developmental testing present critical implications regarding the TIC's performance in the launch and space environment. Firstly, the presence of a bus should increase the rigidity of the satellite structure and decrease the amplitude of the frequency on the payload during vibration. Secondly, the survival of the TIC EDU through vibration testing establishes confidence in a COTS camera's ability to survive the launch environment. Specifically, its survival focuses the vibration testing of the flight hardware TIC on the workmanship of the THz lens, not the COTS camera itself. Thirdly, the FPA of the camera heats quickly when subjected to a warm environment, showing sensitivity to temperature surges. Fourthly, the internal temperature of the FPA directly relates to the camera's operability, and therefore, necessitates the ability to read the internal temperature in order to monitor the camera's functionality. Overall, the testing served as a means of verification to establish confidence, within the SSAG and with the project sponsor, that the TIC will withstand and function in the launch and space environment.

V. INTEGRATION PLAN

This section examines the integration plan of the flight hardware TIC onto the SSAG-developed HAB bus. The development tests conducted on the TIC EDU generated a baseline understanding of the integration process without harming the actual flight hardware. The guidelines, procedures, and challenges identified through the TIC EDU testing assisted in the transition of integrating the actual flight hardware. The integration plan presents the camera selected as the flight hardware TIC, compares the flight hardware TIC to the TIC EDU, and examines the flight hardware TIC's interface requirements with the SSAG-developed HAB bus.

A. FLIGHT HARDWARE TIC BACKGROUND

The camera selected as the flight hardware TIC is the Tamarisk 640 thermal imaging camera. Characteristics of the camera include a 640 x 480 array format, 17-micron meter pixel pitch micro-bolometer, 30 Hz frame rate, and an operational temperature rating of -40°C to 80°C [39]. Of the two Tamarisk 640 cameras purchased, one camera is a 7.5 mm focal length with a 90 degree HFOV, and the second camera is a 50 mm focal length with a 12.4 degree HFOV. Unique to the camera is the ability to remove and swap the lens, a characteristic which solidified its selection as the flight hardware. The purchase of two cameras supports the Sensor Research Laboratory's ability to integrate a terahertz lens and to test and develop the terahertz imaging capability with cameras varying in focal length and field of view. Figure 57 reflects the specifications of the Tamarisk 640.

Figure 57. Tamarisk 640 Specifications. Source: [39].

B. TIC EDU AND FLIGHT HARDWARE TIC COMPARISON

The most significant difference between the TIC EDU and flight hardware TIC is the Tamarisk 640's swappable lens. Additional differences include the effective frame rates, array formats, pixel sizes, electrical controls, and volumetric sizes. The array format increases from 320 x 256 to 640 x 480. The effective frame rate more than triples from 9 frames per second to 30, and the pixel size rises from 12 to 17 micron meters. The flight hardware TIC requires 3 to 5.5 V of input voltage and dissipates 1.2 Watts (W) of power,

as opposed to the TIC EDU's power requirement of 3.3 V and power dissipation of 580 mW. Furthermore, the Tamarisk 640 cameras require more space and weigh more at 100 g and 295 g, as opposed to the TIC EDU's smaller size and mass of 43 g. Both the mechanical and electrical interfaces of the Tamarisk 640 are explored more in the following section. Table 14 summarizes the camera specifications of the TIC EDU and flight hardware TIC.

Table 14. TIC EDU and Flight Hardware TIC Comparison of Specifications. Adapted from [37], [39].

Imaging	**TIC EDU**	**Flight Hardware TIC**
Sensor Technology	Uncooled VOx microbolometer	Uncooled VOx microbolometer
Array Format	320 x 256	640 x 480
Effective Frame Rate	9 Hz	30 Hz
Field of View	12° HFOV	90° HFOV & 12.4° HFOV
Pixel Size	12 micron meter	17 micron meter
Thermal Sensitivity	<40 mK	<50 mK
Focal Length	18 mm	7.5 mm & 50 mm
Electrical		
Input Voltage	3.3 V	3 - 5.5 V
Power Dissipation	<580 mW	< 1.2 W
Video Channels	CMOS, USB 2.0	NTSC, PAL, CMOS
Control Channels	UART, USB	UART, RS-232, USB 2.0
Mechanical		
Size (with lens)	21 x 21 x 45 mm, 19.8 cm^3	46 x 40 x 39 mm, 71.8 cm^3 & 58 x 58 x 86 mm, 289.3 cm^3
Weight (with lens)	43 g	100 g & 295 g
Environmental		
Operating Temp	-40°C to 80°C	-40°C to 80°C

The specifications of the flight hardware TIC predicate certain implications based on its similarities and differences with the TIC EDU. The identical operating temperatures of the TIC EDU and flight hardware TIC imply similar thermal behaviors, including the sensitivity of the FPA to temperature surges and the criticality of an internal temperature read-out. Another similarity is USB control, which aids in the continuity of testing setup

and design. The mechanical and electrical interfaces must account for the differences in the cameras, as discussed in the following section.

C. INTERFACE REQUIREMENTS

Three accessories were purchased along with the two different Tamarisk 640 cameras which allows for three different operational setups. The first two setups permit immediate access to the camera for familiarity and testing without the need for cabling or software development. The third setup considers the requirements for operating from the HAB bus, but necessitates both cabling and software development.

The feature board, feature board basic cable, and connector kit accessories purchased from the manufacturer create two setup options for immediate familiarization and testing of the Tamarisk 640 camera. The "feature board" [40] accessory interfaces with the base configuration of the camera through a 60-pin connector. Figure 58 shows the base configuration of the camera and Figure 59 shows the base configuration with the feature board.

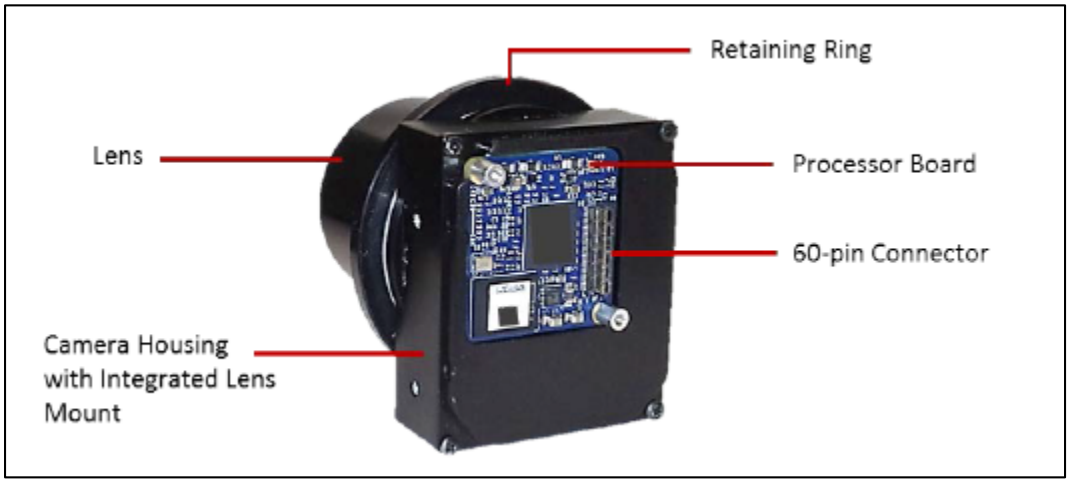

Figure 58. Tamarisk 640 Base Configuration with 60-Pin Connector. Source: [40].

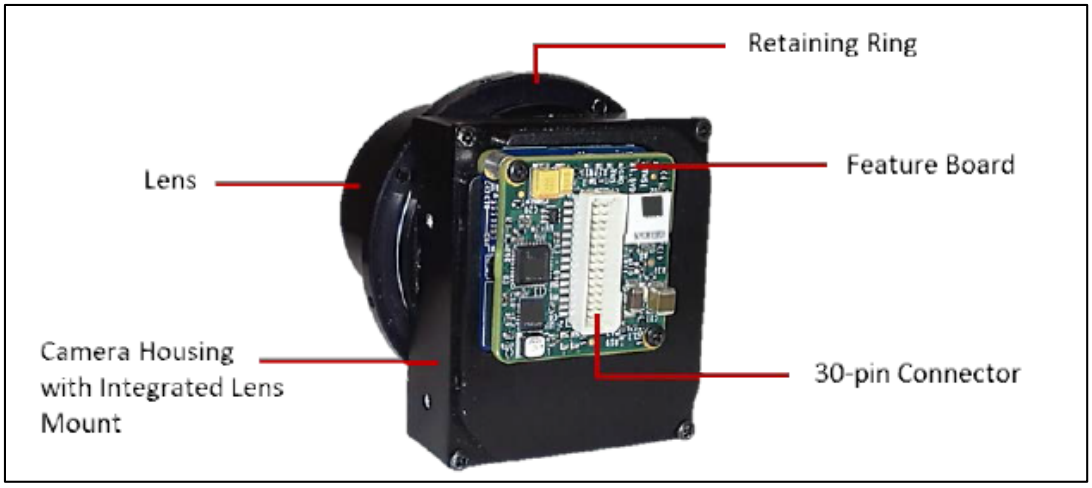

Figure 59. Tamarisk 640 Base Configuration and Feature Board with 30-Pin Connector. Source: [40].

Building off the feature board, the "feature board basic cable" [41] and the "connector kit" [42] accessories allow for two setups of immediate camera control through a computer connected to the internet. The Software Interface Control Document [43] provides the needed commands for camera control through USB and RS-232 when connected to a computer. The feature board basic cable provides a power, video, and USB connection for the camera, shown in Figure 60. The cable supports analog video through BNC and camera control through USB. The cable interfaces to the camera through the 30-pin connector on the feature board.

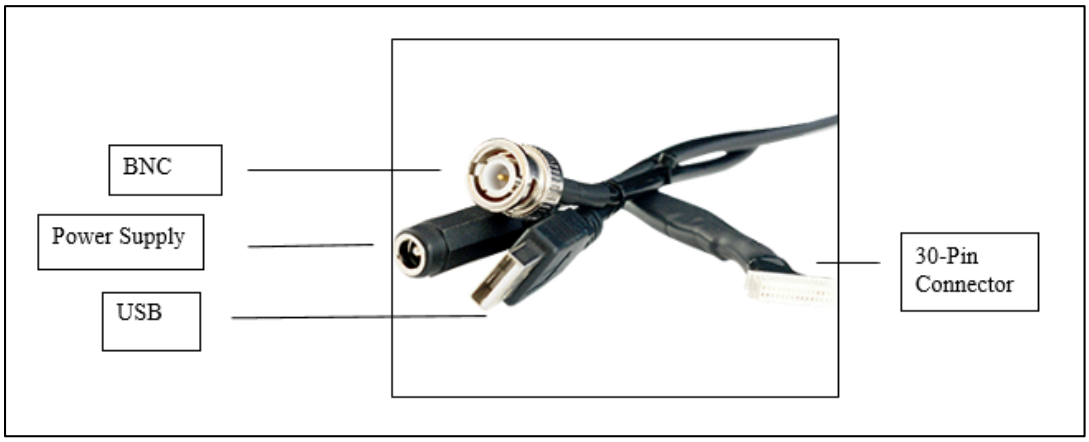

Figure 60. Tamarisk 640 Feature Board Basic Cable. Adapted from [41].

The connector kit also interfaces with the camera through the 30-pin connector on the feature board to provide RS-232, power, mini-USB, and BNC-video. Figure 61 shows the connector kit and Figure 62 shows the setup with the camera, base configuration, feature board, 30-pin connector, and connector kit. The feature board basic cable, feature board, and connector kit allow for immediate access to the camera for familiarity and testing.

Figure 61. Tamarisk 640 Connector Kit. Adapted from [42].

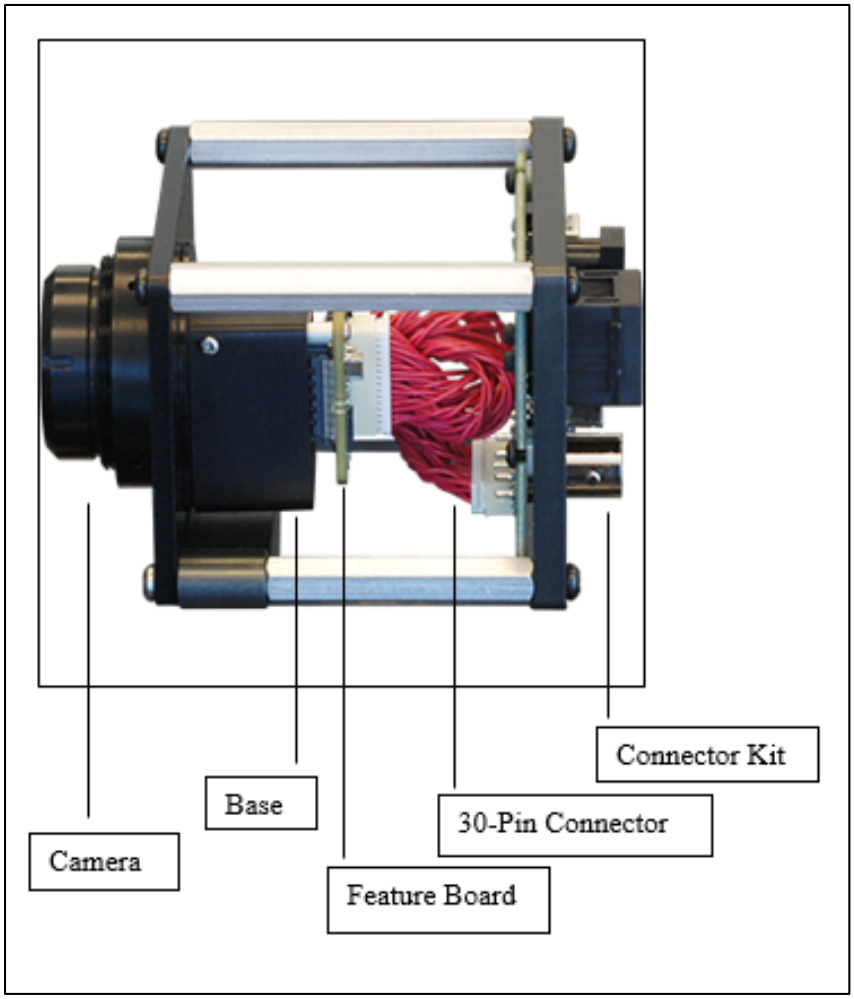

Figure 62. Side View of Tamarisk 640 Feature Board, 30-Pin Connector, and Connector Kit. Adapted from [42].

The third setup interfaces the Tamarisk 640 camera with the HAB bus. The setup requires the development of a custom-made cable, similar to the feature board basic cable, made of space grade materials with power, BNC-video, and RS-232 connections. Additionally, the setup requires an internet protocol (IP) video encoder and level shift for video and control purposes. The following section describes the mechanical and electrical interface requirements of the Tamarisk 640 camera with the HAB bus. The mechanical interface presents the volumetric size and weight, along with the necessary CAD models for mounting the flight hardware TIC on the HAB frame. The electrical interface comments on the power, video, and control cabling considerations.

1. Mechanical Interface

Two mechanical interfaces include the weight of the camera and the volumetric dimensions. The camera's weight of 100 g or 295 g falls under the weight limit of 1.8 kg for HAB flights. The camera's volumetric dimensions of either 46 x 40 x 39 mm or 58 x 58 x 86 mm fit within the 95 x 95 x 100 mm payload envelope of a 1U CubeSat structure. The base dimensions of the Tamarisk 640 camera remain the same for both sizes, but the overall dimensions change depending on the size of the lens. The addition of the feature board also adds 7.5 mm of length to the depth of the base [39]. Figure 63 shows the dimensions of the Tamarisk 640 base, without the lens.

Figure 63. Tamarisk 640 Camera Base Dimensions without the Lens. Source: [39].

The CAD model for the TIC EDU required alterations to accommodate the bigger dimensions and heavier weights of the flight hardware TIC. The most significant change pertains to the extension of the mount to attach to both faces of the HAB frame. The extra mounting holes support the heavier weight of the cameras. Additional modifications include changing the height from 60 mm to 100 mm and the width from 30 mm to 60 mm. The extra space allows for the larger lens and volumetric dimensions of the Tamarisk 640 in comparison to the FLIR BOSON 320. Figures 64 and 65 show the Tamarisk 640 50 mm camera with the dimensions of 58 x 58 x 93.5, which accounts for the 7.5 mm increase in

the depth for the feature board, mounted on a 2U HAB frame. The 93.5 mm depth of the camera does not allow much space for cabling, but the lens dimensions will likely change after modifications from the Sensor Research Laboratory. The CAD model with the 50mm camera shows the worst case layout and orientation inside the CubeSat frame.

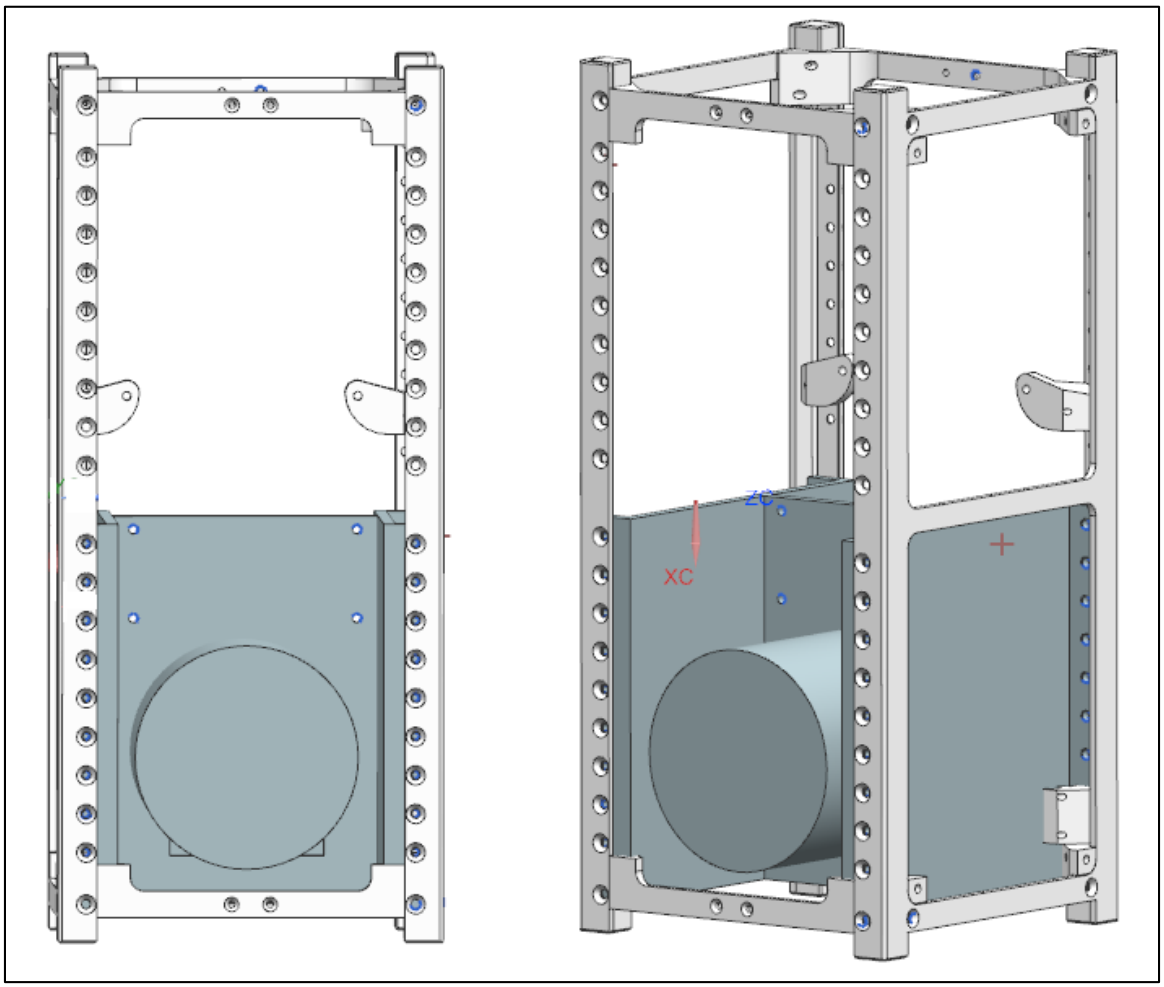

Figure 64. Front View of the Flight Hardware TIC CAD Model on a 2U HAB Frame with Tamarisk 640 58 x 58 x 93.5 mm Camera

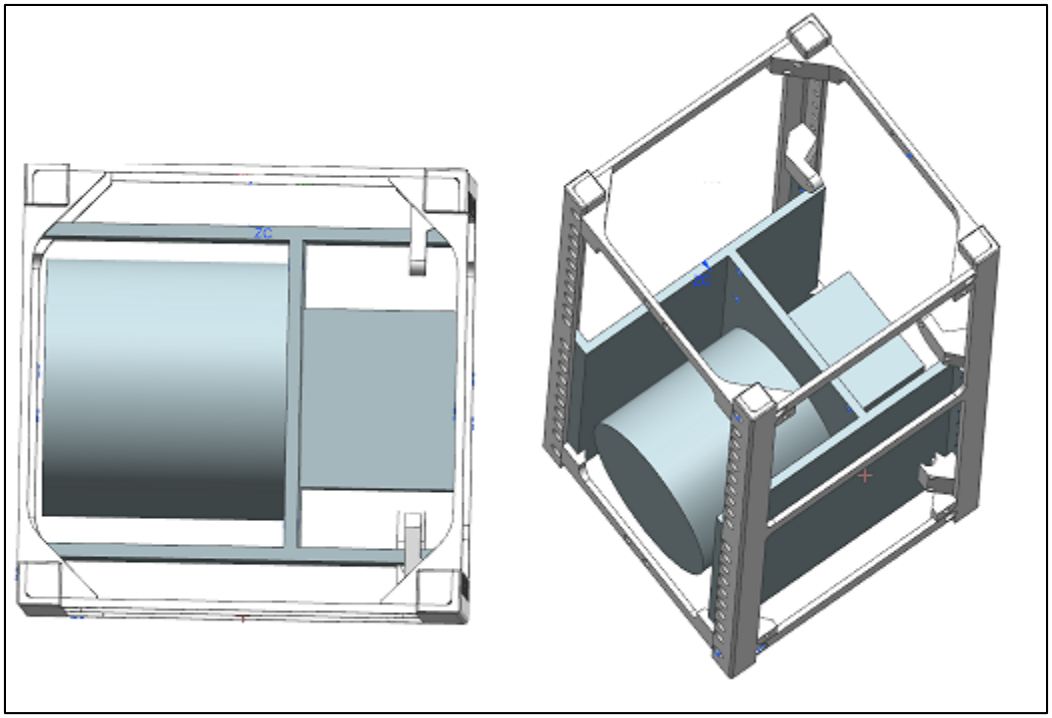

Figure 65. Top View of the Flight Hardware TIC CAD Model on the 2U HAB Frame with Tamarisk 640 58 x 58 x 93.5 mm Camera

2. Electrical Interface

The electrical interface of the Tamarisk 640 camera with the HAB bus includes power, video, and control. A custom-made cable, similar in design to the feature board basic cable, will interface the Tamarisk 640 camera with the HAB bus and be made of space grade materials. The cable will connect to the camera through the 30-pin connector on the feature board and interface with the EPS and C&DH through a power, BNC-video, and RS-232 connector.

The Tamarisk 640 camera requires 3 to 5.5 V of power [39], achievable through the HAB bus EPS which supplies 5 V [35]. For video, the camera will use the custom-made cable and an IP video encoder to convert analog video through BNC to a network package through Ethernet to the Raspberry Pi of the C&DH. A standard IP video encoder requires 12 V of power at 0.5 amperes (A) [44], provided by the EPS through a point of load (POL) up-converter. For control, the camera will use the custom-made cable and a level shift to convert a 1.8 V RS-232 input into a 3.3 V RS-232 output for the Raspberry

Pi of the C&DH [40]. Figure 66 shows the block diagram of the electrical interfaces for the flight hardware TIC with the major subsystems of the HAB bus.

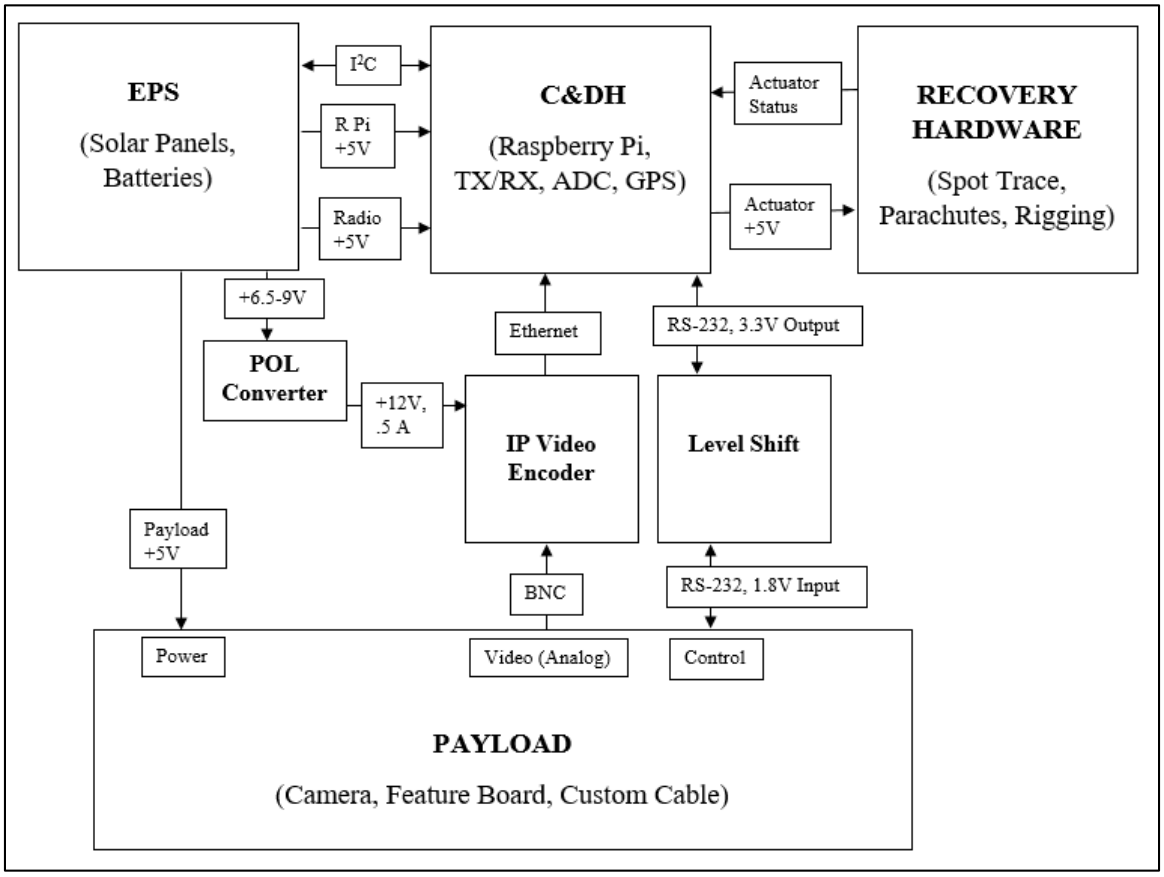

Figure 66. Block Diagram of the Flight Hardware TIC's Interfaces with the HAB Bus Subsystems

In summary, the camera selected as the flight hardware TIC is the Tamarisk 640 thermal imaging camera. The distinguishing characteristics of the camera from the TIC EDU include its swappable lens, larger volume, heavier weight, and 640 x 480 array format. Two cameras with different focal lengths and field of view were purchased to support testing for the Sensor Research Laboratory. The additional purchase of the feature board, feature board basic cable, and connector kit accessories allow for immediate use and familiarization. Overall, the integration of the flight hardware TIC onto the HAB bus

necessitates an upgraded mount for the mechanical interface and cabling and software development for the electrical interface.

VI. CONCLUSION

Terahertz imaging, although an emerging technology, may provide new and unique capabilities for the space domain. With the potential to reveal physical phenomena never seen before in that region of the electromagnetic spectrum and the ability to penetrate most materials except metal, a TIC as a CubeSat payload shows great promise. The objective to flight qualify a TIC as a CubeSat payload in the near future exemplifies the operationally responsive nature of the CubeSat platform to demonstrate evolving technologies. Furthermore, the project benefits the field of terahertz science and technology by bringing terahertz imaging to the space medium for the first time.

This thesis focused on two areas of research. Firstly, it investigated the potential uses of a TIC payload. It determined two potential applications of a TIC payload to be on-orbit satellite inspection and far away space object detection. Secondly, it conducted development testing with a TIC EDU to commence the integration and flight qualification effort. The vibration and thermal vacuum testing of the TIC EDU established confidence in the design and in the feasibility of the mission objective. Overall, this thesis accomplished focused research objectives of national interest by supporting DoD Space efforts in the utilization of very small satellites.

Based on the survival of the TIC EDU, a FLIR BOSON 320 thermal imaging camera, the SSAG and project sponsor can confidently move forward with the selection of the Tamarisk 640 thermal imaging camera as the flight hardware TIC. The vibration testing of the TIC EDU verified the survival of a COTS camera in the launch environment. In particular, the results focus the need to vibration test the workmanship of the THz lens incorporated onto the TIC, not the Tamarisk 640 camera itself. The thermal vacuum testing of the TIC EDU showed the sensitivity of the camera's FPA to heating and the importance of monitoring the internal temperature to ensure operability. With the knowledge of how the TIC EDU operates, the lessons learned establish the foundation for flight hardware integration, qualification, and acceptance.

Further research includes developing a concept of operations (CONOPS) for a satellite with a TIC payload and completing the flight qualification process. Follow-on work entails integrating and testing the custom THz lens onto the Tamarisk 640 camera, maintaining compatibility with other buses in addition to the SSAG-developed HAB bus, performing system level acceptance testing of the payload flight unit, and integrating the flight hardware onto the bus selected for flight. These areas of further research are made possible by the research and testing accomplished by this thesis.

APPENDIX A. HAND-WRITTEN LOG FROM FIRST TVAC TEST

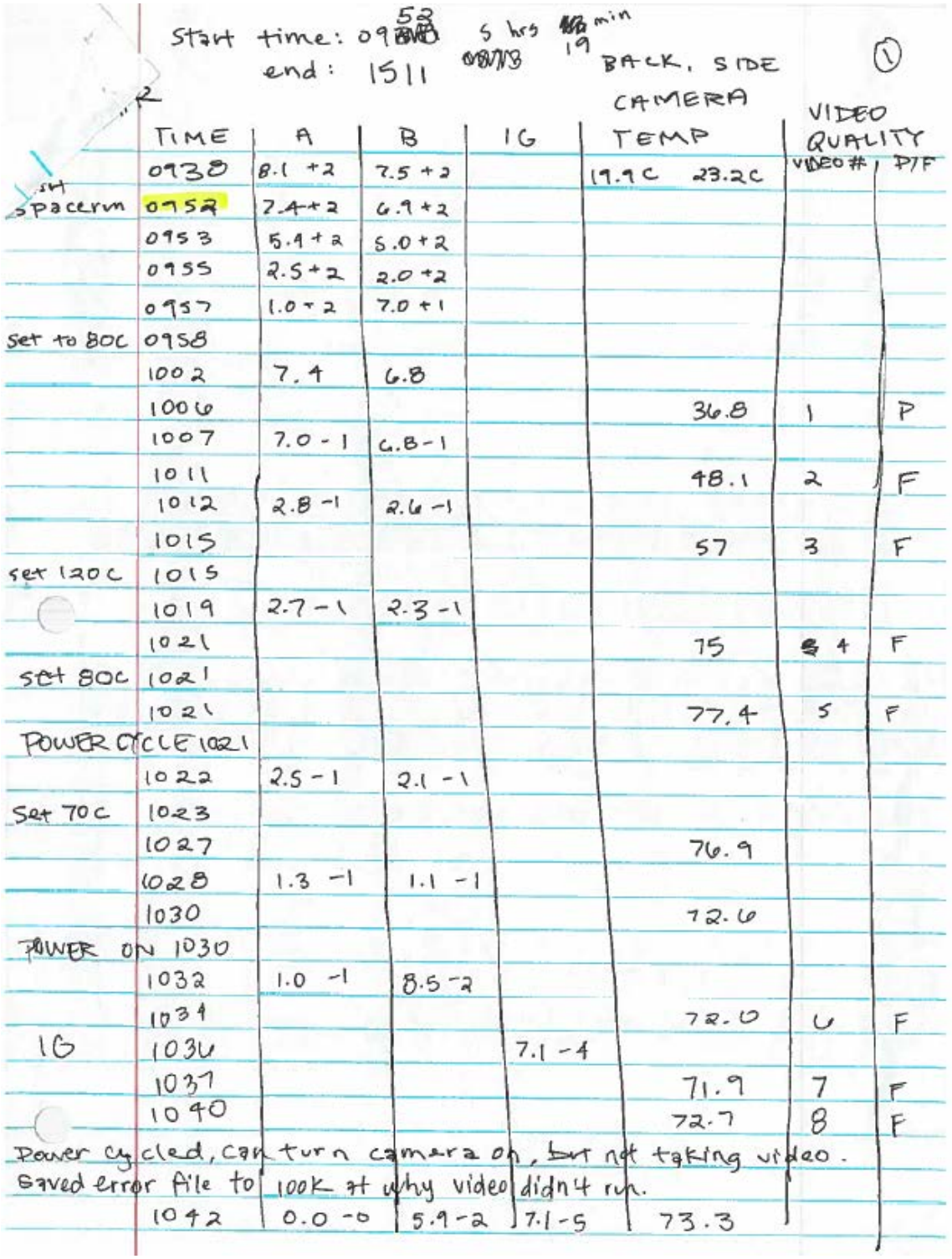

Start time: 0952 5 hrs 19 min
end: 1511
BACK, SIDE CAMERA ①

	TIME	A	B	IG	TEMP	VIDEO QUALITY VIDEO #	P/F
	0938	8.1 +2	7.5 +2		19.9C 23.2C		
set spacerm	0952	7.4+2	6.9+2				
	0953	5.1+2	5.0+2				
	0955	2.5+2	2.0+2				
	0957	1.0+2	7.0+1				
set to 80C	0958						
	1002	7.4	6.8				
	1006				36.8	1	P
	1007	7.0 -1	6.8-1				
	1011				48.1	2	F
	1012	2.8 -1	2.6 -1				
	1015				57	3	F
set 120C	1015						
	1019	2.7 -1	2.3 -1				
	1021				75	4	F
set 80C	1021						
	1021				77.4	5	F
POWER CYCLE 1021							
	1022	2.5 -1	2.1 -1				
Set 70C	1023						
	1027				76.9		
	1028	1.3 -1	1.1 -1				
	1030				72.6		
POWER ON 1030							
	1032	1.0 -1	8.5-2				
	1034				72.0	6	F
IG	1036			7.1 -4			
	1037				71.9	7	F
	1040				72.7	8	F
Power cycled, can turn camera on, but not taking video. Saved error file to look at why video didn't run.							
	1042	0.0 -0	5.9-2	7.1-5	73.3		

PASSES: 1, 10, 12, 15, 16, 17, 18, 19, 20 (2)

* OD b/w blank & shroud

	TIME	A	B	16	SIDE TEMP	# VIDEO	P/F
Set 65	1044						
	1045	0.0 -0	5.3 -2	6.1$_8$ -5	73.7		
Set 60	1050				69.9		
	1053	0.0 -0	3.7 -2	3.4 -5	68.4		
Set 55	1057						
	1100				65.6	9	F
	1102 disconnected HDMI to camera Different error. Confirming suspicion camera is ON, just not working.						
Set 50	1106						
	1107	0.0 - 0	2.7 - 2	2.1 - 5	63.6		
	1110				60.8	10	P
	1112					11	F
Set 40	1116						
	1121				55.9	12	P
	1121		2.0 - 2	1.2 -5			
Set 30	1127						
	1130				50.8	13	F
	1135				45.9	14	F
Set 20	1138						
	1143				40.9	15	P
	1144			5.5 - 6			
	1153				36.8	16	P
Set 0	1201			3.9 - 6			
	1205				30.8	17	P
	1207				25.8	18	P
	1209			3.0 - 6			
Set -25	1211						
	1214				20.8	19	P
	1215		9.3 - 3	2.4 - 6			
	1216				15.8	20	P

	TIME	A	B	IG	TEMP	# VIDEO	P/F
	1219				11.2	21	P
SET-40	1221						
	1225				5.9	22	P
	1231				0.9	23	P Perfect!
SET -60	1237						
SET -25	1238						
	SETTING TO -25 TO NOT OPEN LN2 VALVE						
	1239 - 1242						
	CHANGED LN2 CANISTER						
SET -40	1243						
	1248			1.2-6			
	1249				-5.0	24	P Perfect
SET -50	1252						
	1255				-9.2	25	P Perfect
	1300				-14.8	26	P Perfect
SET -60	1302						
	1307			9.1-7			
	1308				-19.2	27	P Perfect
	1325				-24.6	28	P Perfect
	1341				-29.2	29	P Perfect (line formed)
	1405			7.3-7			
	1406				-34.1	30	P Perfect (line)
SET -10	1408						
	1412				-30.1	31	P Perf (line)
	1413				-25.6	32	P Perf (line)
SET 20 1417	1415				-20.9	33	P Perf (line)
	1417				-15.9	34	P Perf (line)
	1417		5.7-3	1.7-6			
	1418				-10.8	35	P Perf (line)
EE SPACE RUN	1419						
ENED HANDLES	1420						
	1420				-5.2	36	P Perf No LINE

④

- vibe test I did was worse case

	TIME	A	B	16	TEMP	VIDEO	
	1422				0.5	37	P Perf
	1422		4.5 -3	4.2 -5			
	1424				4.2	38	P Perf
SHOULD HAVE BEEN EARLIER	1426		4.3 -3	7.1 -5			
	1431				9.2	39	P Perf
	1432		4.4 -3	1.2 -4			
HAMBER VENT ON	1443						
	1446	7.6 +1	1.8 -1				
ET TEMP OFF	1449						
	1449				11.0	40	P
	1452	2.3 +2	1.5				
	1504				20.5	41	P
HAMBER ENT OFF	1511	7.7 +2	4.1 +2				
URN OFF & CAMERA	1511						

APPENDIX B. HAND-WRITTEN LOG FROM SECOND TVAC TEST

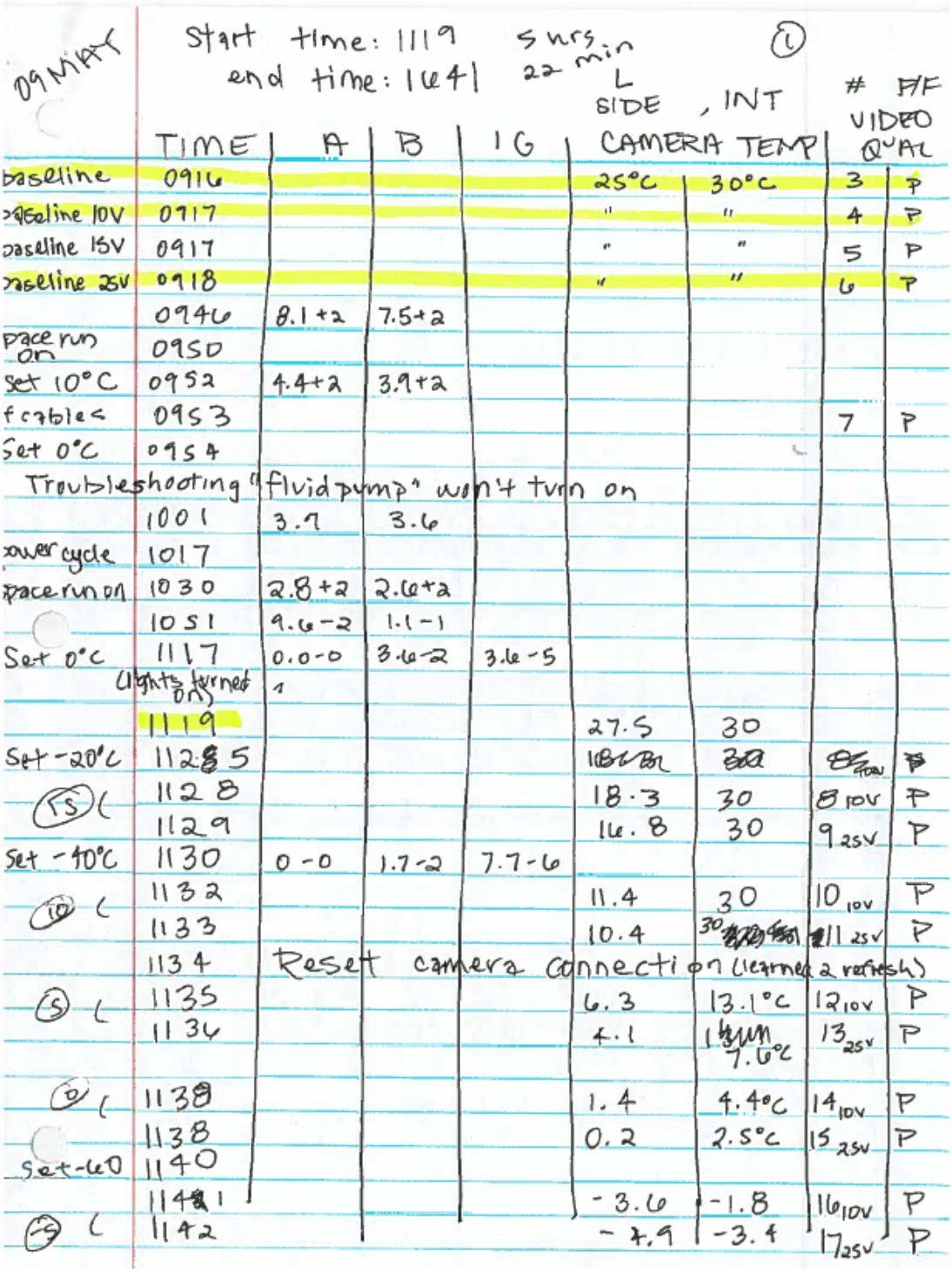

09 MAY

Start time: 1119 5 hrs 22 min (1)
end time: 1641

	TIME	A	B	IG	CAMERA TEMP L SIDE	CAMERA TEMP INT	# FF VIDEO QUAL	
baseline	0916				25°C	30°C	3	P
baseline 10V	0917				"	"	4	P
baseline 15V	0917				"	"	5	P
baseline 25V	0918				"	"	6	P
	0946	8.1+2	7.5+2					
pace run on	0950							
set 10°C	0952	4.4+2	3.9+2					
f cables	0953						7	P
Set 0°C	0954							
Troubleshooting "fluid pump" won't turn on								
	1001	3.7	3.6					
power cycle	1017							
pace run on	1030	2.8+2	2.6+2					
	1051	9.6-2	1.1-1					
Set 0°C	1117	0.0-0	3.6-2	3.6-5				
	Lights turned on	1						
	1119				27.5	30		
Set -20°C	1128 5				[illegible]	[illegible]	[illegible]	[illegible]
(5)	1128				18.3	30	8 10V	P
	1129				16.8	30	9 25V	P
Set -40°C	1130	0-0	1.7-2	7.7-6				
(10)	1132				11.4	30	10 10V	P
	1133				10.4	30 [illegible]	11 25V	P
	1134	Reset camera connection (learned 2 refresh)						
(5)	1135				6.3	13.1°C	12 10V	P
	1136				4.1	13 then 7.6°C	13 25V	P
(0)	1138				1.4	4.4°C	14 10V	P
	1138				0.2	2.5°C	15 25V	P
Set -60	1140							
	1141				-3.6	-1.8	16 10V	P
(-5)	1142				-4.9	-3.4	17 25V	P

09MAY — ②

	TIME	A	B	IG	L SIDE CAMERA TEMP	INT TEMP	# VIDEO QUAL	D/F
	1142			4.3-6				
-10	1144				-8.7	-7.6	18_{10V}	P
	1145				-10.0	-8.6	19_{25V}	P
-15	1148				-14.7	-13.7	20_{10}	P
	1148				-15.5	-14.7	21_{25V}	P
-20	1151				-19.4	-19	22_{10}	P
	1151				-20.2	-20	23_{25}	P
-25	1154				-24.1	-24.5	24_{10}	P
	1155				-24.7	-25.2	25_{25}	P
	1155			2.9-6				
-30	1158				-28.1	-28.6	26_{10}	P
	1158				-28.5	-29.1	27_{25}	P
SET-42	1200							
-40	1203			4.1-6				
-50	1205							
	1208			2.5-6				
-35	1210				-34.3	-32.4	28_{10}	P
	1210				-34.5	-32.6	29_{25}	P
SET-55	1213			2.3-6				
-40	1223				-40.1	-37.8	30_{10}	P
	1223				-40.4	-38	31_{25}	P
Set -50	1226							
	COMMENCED SOAK				1226	-39		
SET -52	1232				-41.7	-38.8		
	1234				-41.8	-38.5		
SET -53	1236				-42.1	-38.5		
	1237					-38.6		
	1238					-38.8		
	1239				-42.8	-39	32_{10}	P
	1240				-42.9	-39.2	33_{25}	P
	1241	commenced video				-39.3		
	1242	stopped video				-39.5	Capture-2 25V	P

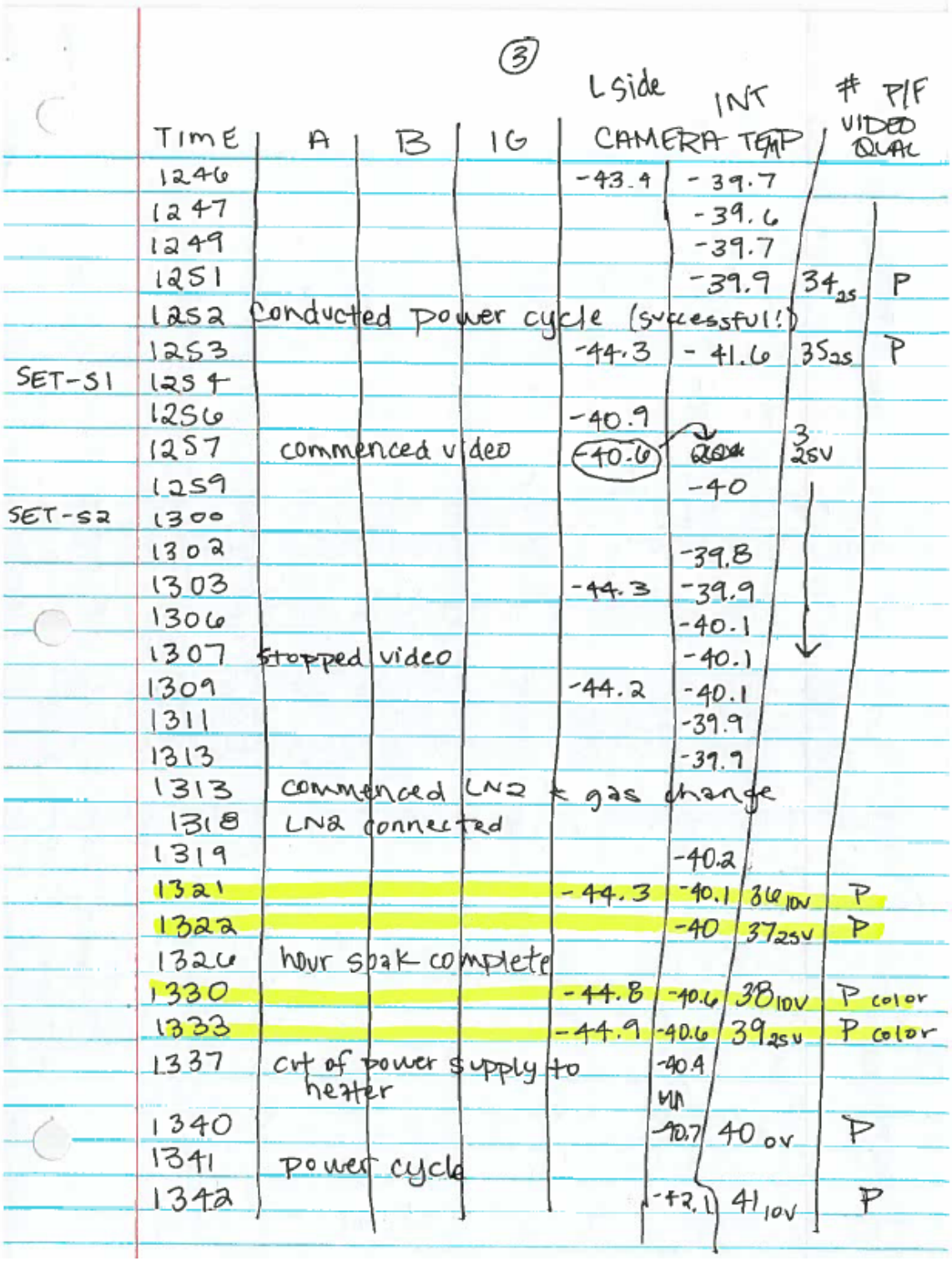

	TIME	A	B	IG	L Side CAMERA	INT TEMP	#	P/F VIDEO QUAL
	1246				-43.4	-39.7		
	1247					-39.6		
	1249					-39.7		
	1251					-39.9	34_{2S}	P
	1252	conducted power cycle (successful!)						
	1253				-44.3	-41.6	35_{2S}	P
SET-S1	1254							
	1256				-40.9			
	1257	commenced video			-40.6		3 $_{25V}$	
	1259					-40		
SET-S2	1300							
	1302					-39.8		
	1303				-44.3	-39.9		
	1306					-40.1		
	1307	stopped video				-40.1		
	1309				-44.2	-40.1		
	1311					-39.9		
	1313					-39.7		
	1313	commenced LN2 + gas change						
	1318	LN2 connected						
	1319					-40.2		
	1321				-44.3	-40.1	36_{10V}	P
	1322					-40	37_{25V}	P
	1326	hour soak complete						
	1330				-44.8	-40.6	38_{10V}	P color
	1333				-44.9	-40.6	39_{25V}	P color
	1337	cut of power supply to heater				-40.4		
	1340					-40.7	40_{0V}	P
	1341	power cycle						
	1342					-42.1	41_{10V}	P

(4)

	TIME	A	B	IG	CAMERA TEMP		VIDEO QUAL	
	1354	Gas changed						
Set -30	1355							
(-40)	1358			3.1-6	-43.7	-39.9	42_{10}	P
	1359				-42.5	-38.9	43_{25}	P
Set -10	1401							
(-35)	1401				-40.6	-36.2	44_{10}	P
	1402				-40.0	-35.5	45_{25}	P
(-30)	1404				-35.6	-31.5	46_{10}	P
	1405				-34.8	-30.1	47_{25}	P
Set 10	1406							
(-25)	1407				-31.3	-25.7	48_{10}	P
	1407				-30.3	-24.7	49_{25}	P
(-20)	1408				-27.2	-21.8	50_{10}	P
	1409				-25.4	-19.7	51_{25}	P
(-15)	1410				-22.2	-16	52_{10}	P
	1411				-21.2	-14.6	53_{25}	P
(-10)	1411				-18.4	-11.9	54_{10}	P
	1412				-17.7	-10.2	55_{25}	P
(-5)	1413				-14.4	-6.1	56_{10}	P
	1414				-13.4	-4.8	57_{25}	P
(0)	1416				-10.4	-0.6	58_{10}	P
	1416				-9.3	0.8	[illegible]	
	1416			1.5-5			59_{10}	
(5)	1417				-6.8	4.1	[illegible]	P
	1418				-5.5	5.9	60_{25}	P
SET 30	1420							
(10)	1420				-2.6	9.2	61_{10}	P
	1421				-2.0	9.8	62_{25}	P
(15)	1424				3.7	14.3	63_{10}	P
	1424				4.6	15.5	64_{25}	P
(20)	1426				8.5	19.1	65_{10}	P
	27				9.2	19.9	66_{25}	P
SET 50	1429							

	TIME	A	B	IG	L CAMERA TEMP	INT	(5) # VIDEO	P/F QUAL
(25)	1430				13.6	24.7	67_{10}	P
	30				14.4	25.4	68_{25}	P
(30)	33				18.5	29.7	69_{10}	P
	33				19.0	30.3	[illegible]	[illegible]
(35)	37				23.2	34.4	70_{10}	P
	37				24.1	35	71_{25}	P
(40)	1440				30.6	39.4	72_{10}	P
	41				31.4	40.8	73_{25}	P
(45)	44				37.3	47	74_{10}	P
	44				37.9	48	75_{25}	P
(50)	46				40	50.3	[illegible]	[illegible]
	46				40.4	51	76_{25}	P
(55)	48				43.3	54.3	77_{10}	P
	49				43.6	54.7	78_{25}	P
(60)	1453				47.9	59.4	79_{10}	P
	53				48.3	59.9	80_{25}	P
SET 65	1456							
(65)	1459				53.9	64	[illegible]	[illegible]
	1459				54.8	64.7	81_{25}	P
(70)	1503				59.2	69.2	82_{10}	P
	1503				59.6	69.7	83_{25}	P
(75)	1507				63.8	74.8	84_{10}	P
	1508				64.3	75.5	85_{25}	P
(80)	1512				67.4	79	86_{10}	P
	1512				67.5	80	87_{25}	P
	Note: Platen at 75.2 °C!							
SET 62	1512	COMMENCE SOAK						
	1514					81	88_{25}	P
	1516				68.9	81.8	89_{25}	P
	"				"	"	90_{10}	P
	1520					81.7		
	1523					81		

(6)

	TIME	A	B	IG	CAMERA TEMP		VIDEO QUAL	
	1523	Conducted power cycle						
	1525			68.9	78.7	91_{10}		P
	25			68.8	79	92_{25}		P
	1526	commenced video			79.4	4_{25}		P
	27			68.9	79.9			
	30				80.3			
	35			69.6	80.7			
	36	stopped video			80.9	↓		
	1538			69.7	80.9	93_{25}		P color
	1538			69.8	81	94_{10}		P color
SET 61	1543							
	1547			70.1	81.5			
	49			70.0	81.5	95_{10}		P
	"			"	"	96_{25}		P
	52				81.4			
	1601			69.5	80.9			
	1610			69.2	80.6	97_{25}		P
SET 21	1612	hour soak complete						
	1612	unlatched chamber ~~hour soak complete~~						
	1612	space run off						
	1613	chamber vent on						
	1614				78.5			
	1615	~~turned off heater~~			75.1	98_{25}		P
	1616	turned off heater						
	1618			60.7	67.6			
	1620				58.3			
	1623				49.3	99_{0V}		P
	1625	turned off temp controller						
	1640	chamber vent off						
		Closed chamber door						
	1640				38.1			
	1641	powered off tyac						

LIST OF REFERENCES

[1] W. L. Chan, J. Deibel and D. M. Mittleman, "Imaging with terahertz radiation," *Rep. Prog. Phy.*, vol. 70, pp. 1325–1379, Jul. 2007. [Online]. doi:10.1088/0034-4885/70/8/R02

[2] M. J. Fitch and R. Osiander, "Terahertz waves for communications and sensing," *John Hopkins APL Technical Digest*, vol. 25, no. 4, pp. 348–355, 2004. [Online]. Available: http://techdigest.jhuapl.edu/TD/td2504/Fitch.pdf

[3] B. B. Hu and M. C. Nuss, "Imaging with terahertz waves," *Opt. Lett.*, vol. 20, no. 16, pp. 1716–1718, Aug. 1995. [Online]. doi:10.1364/OL.20.001716

[4] K. K. Ahi, N. Asadizanjani, S. Shahbazmohamadi, M. M. Tehranipoor and M. Anwar, "Terahertz characterization of electronic components and comparison of terahertz imaging with x-ray imaging techniques," *Proc. of SPIE – The Int. Soc. for Opt. Eng.*, vol. 9483, Apr. 2015. [Online]. doi:10.1117/12.2183128

[5] R. Parascandola, "NYPD's pricey, controversial 'T-Ray' gun sensors sit idle, but that's OK with cops," New York Daily News, February 21, 2017. [Online]. Available: http://beta.nydailynews.com/new-york/nypd-t-ray-gun-sensors-sit-idle-cops-article-1.2978581

[6] C. C. Venturini, "Improving mission success of CubeSats," Aerospace Corp., El Segundo, CA, USA, Aerospace Report No. TOR-2017-01689, 2017. [Online]. Available: file:///E:/Thesis/Resources/TOR-2017-01689_-_Improving_Mission_Success_of_CubeSats.pdf

[7] M. Swartwout, CubeSat Database, 2018. [Online]. Available: https://sites.google.com/a/slu.edu/swartwout/home/cubesat-database

[8] C. T. Chaplain, "Space acquisitions: DoD continues to face challenges of delayed delivery of critical space capabilities and fragmented leadership," Washington, DC, USA, GAO Report No. GAO-17-619T, 2017.

[9] S. Siceloff, "CubeSat launchers expected to open research opportunities for all," NASA, Oct. 14, 2015. [Online]. Available: https://www.nasa.gov/feature/cubesat-launchers-expected-to-open-research-opportunities-for-all

[10] S. J. Kline, A. Writt, A. Forbes, J. Yungbluth, and K. Herren, "High Altitude Balloon (HAB) experiment, 2017," October 5, 2017. [Online]. Available: https://cle.nps.edu/portal/site/5acee35b-3423-4630-81d4-9e2ccdc0c5d4

[11] M. S. Correa de Souza, “NPS terahertz project: IR HAB flight testing and integration,” M.S. thesis, Space Sys. Academic Group, NPS, Monterey, CA, USA, 2018.

[12] S. J. Kline, “Flight qualifications of a terahertz imaging camera as a CubeSat payload,” M.S. thesis, Space Sys. Academic Group, NPS, Monterey, CA, USA, 2018.

[13] X. Yang, X. Zhao, K. Yang, Y. Liu, Y. Liu, W. Fu, and Y. Luo, “Biomedical applications of terahertz spectroscopy and imaging,” *Trends in Biotechnology*, vol. 34, no. 10, pp. 810–824, October 2016. [Online]. doi:10.1016/j.tibtech.2016.04.008

[14] K. Kuroo, R. Hasegawa, T. Tanabe and Y. Oyama, “Terahertz application for non-destructive inspection of coated Al electrical conductive wires,” *J. Imaging*, vol. 3, no. 3, article 27, Jul. 2017. [Online]. doi:10.3390/jimaging3030027

[15] B. Weeden, “Dancing in the dark redux: Recent Russian rendezvous and proximity operations in space,” *The Space Review*, October 5, 2015. [Online]. Available: http://www.thespacereview.com/article/2839/1

[16] M. Neufeld, “The world’s first space rendezvous,” National Air and Space Museum, December 15, 2015. [Online]. Available: airandspace.si.edu/stories/editorial/world%E2%80%99s-first-space-rendezvous

[17] “Space rendezvous: Tomorrow’s technology will build on historical breakthroughs,” NASA Engineering & Safety Center Technical Update, 2015. [Online]. https://www.nasa.gov/sites/default/files/atoms/files/techupdate-2015-onepage.pdf

[18] “GSSAP satellite overview,” Spaceflight 101. Accessed February 12, 2018. [Online]. Available: http://spaceflight101.com/spacecraft/gssap/

[19] M. Gruss, “Secretive ANGELS satellite part of new space experiments,” *Space News*, April 14, 2016. [Online]. Available: http://spacenews.com/secretive-angels-satellite-part-of-new-space-experiments/

[20] L. David, “Military micro-sat explores space inspection, servicing technologies,” Space.com, July 22, 2005. [Online]. Available: https://www.space.com/1336-military-micro-sat-explores-space-inspection-servicing-technologies.html

[21] C. Henry, “ViviSat launching first MEV for in-orbit servicing in 2018,” Via Satellite, March 24, 2016. [Online]. Available: http://www.satellitetoday.com/innovation/2016/03/24/vivisat-launching-first-mev-for-in-orbit-servicing-in-2018/

[22] “ViviSat,” U.S. Space. Accessed February 15, 2018. [Online]. Available: http://www.usspacellc.com/in-orbit-servicing/vivisat

[23] "Space Systems/Loral to support DARPA on revolutionary hosted payload concept," LORAL, July 25, 2012. [Online]. Available: http://www.loral.com/News/Loral-News/News-details/2012/Space-Systems-Loral-to-Support-DARPA-on-Revolutionary-Hosted-Payload-Concept/default.aspx

[24] "India trying to reconnect with most powerful communications satellite: ISRO," Reuters, April 2, 2018. [Online]. Available: https://www.reuters.com/article/us-space-launch-india/india-trying-to-reconnect-with-most-powerful-communications-satellite-isro-idUSKCN1H9118

[25] S. Clark, "Spacewatch: India loses contact with communications satellite," *The Guardian*, April 5, 2018. [Online]. Available: https://www.theguardian.com/science/2018/apr/05/spacewatch-india-loses-contact-with-communications-satellite

[26] J. Allen, "Ultraviolet radiation: How it affects life on earth," NASA Earth Observatory, September 6, 2011. [Online]. Available: https://earthobservatory.nasa.gov/Features/UVB/

[27] "Space camera blazes new terahertz trails," European Space Agency, February 11, 2003. [Online]. Available: http://www.esa.int/Our_Activities/Space_Engineering_Technology/TTP2/Space_camera_blazes_new_terahertz_trails.

[28] D. Zimdars, J. A. Valdmanis, J. S. White, G. Stuk, S. Williamson, W. P. Winfree and E. I. Madaras, "Technology and applications of terahertz imaging non-destructive examination: Inspection of space shuttle sprayed on foam insulation," *AIP Conf. Proc.*, vol. 760, no. 570, pp. 570–577, 2005. [Online]. doi:10.1063/1.1916726

[29] L. J. Hansen and C. H. Pollock, "Spacecraft computer systems," in *Space Mission Analysis and Design*, W. J. Larson and J. R. Wertz, Eds. El Segundo, CA, USA: Microcosm Press and Dordrecht, NED: Kluwer Academic Publishers, 2005, p. 671.

[30] *General Environment Verification Standard (GEVS)*, GSFC-STD-7000A, April 22, 2013.

[31] *Space and Missile Systems Center Standard*, SMC-S-016, September 5, 2014.

[32] W. F. Tosney and S. Pavlica, "Satellite verification planning: Best practices and pitfalls related to testing," *Proceedings of the 5th International Symposium on Environmental Testing for Space Programmes*, ESA SP-558, Jun. 2004. [Online]. Available: http://adsbit.harvard.edu/cgi-bin/nph-iarticle_query?bibcode=2004ESASP.558..243T&db_key=AST&page_ind=0&plate_select=NO&data_type=GIF&type=SCREEN_GIF&classic=YES

[33] B. Chesley, R. Lutz and R. F. Brodsky, “Space Payload Design and Sizing,” in *Space Mission Analysis and Design*, W. J. Larson and J. R. Wertz, Eds. El Segundo, CA, USA: Microcosm Press and Dordrecht, NED: Kluwer Academic Publishers, 2005, pp. 241.

[34] Code of Federal Regulations, Title 14, Chap. 1, Subchap. F, Part 101.1.i. May 21, 2018. [Online]. Available: https://www.ecfr.gov/cgi-bin/text-idx?rgn=div5 &node=14:2.0.1.3.15#se14.2.101_131

[35] “High-Altitude Balloon (HAB) Bus Interface Control Document,” working paper, Space Sys. Academic Group, NPS, Monterey, CA, USA, October 30, 2017.

[36] T. Sarafin, P. Doukas, L. Demchak, and M. Browning, “Part 1: Introduction to vibration testing,” in *Vibration Testing of Small Satellites*. Colorado: Instar Engineering and Consulting, Inc, 2017.

[37] “FLIR BOSON 320 18mm lens thermal imaging camera,” OEM Cameras. Accessed December 12, 2017. [Online]. Available: http://www.oemcameras.com/flir-boson-320x256-18mm.htm

[38] D. J. Ewins, *Modal Testing: Theory, Practice, and Application*. Baldock, Hertfordshire, England; Philadelphia, PA: Research Studies Press, 2000.

[39] DRS Technologies: A Finmeccanica Company, *Tamarisk Infrared solutions that fit*, MR-2013-01-654_Rev06, 2012. [Online]. Available: www.drsinfrared.com/ portals/0/docs/datasheets/TamariskFamily_Datasheet_MR-2013-01-654_Rev06.pdf

[40] DRS Technologies: A Finmeccanica Company, *Tamarisk 640 17 µm 640x480 long wave infrared camera electrical interface control document*, 1014845 RevC, 2013. [Online]. Available: https://www.sierraolympic.com/images/uploads/documents/1014845-Tamarisk640_Electrical_Interface_Control_Document_RevCb.pdf

[41] “Tamarisk Feature Board Basic Cable,” Sierra Olympic Technologies Inc. Accessed on May 21, 2018. [Online]. Available: https://www.sierraolympic.com/ products/details/tamarisk-feature-board-basic-cable

[42] “Tamarisk 640 Connector Kit,” Sierra Olympic Technologies Inc. Accessed on May 25, 2018. [Online]. Available: https://www.sierraolympic.com/products/ details/tamarisk-640-connector-kit-all

[43] DRS Technologies: A Finmeccanica Company, *Tamarisk 640 17 µm 640x480 long wave infrared camera software interface control document*, 1014844 RevC, 2013. [Online]. Available: https://www.sierraolympic.com/images/uploads/ documents/1014844-Tamarisk640_Software_Interface_Control_Document_ RevCb.pdf

[44] Grandstream Networks, Inc., *GXV3500 User Manuel*, Firmware Version 1.0.1.94, 2016. [Online]. Available: http://www.grandstream.com/sites/default/files/Resources/gxv3500_user_manual.pdf

THIS PAGE INTENTIONALLY LEFT BLANK

INITIAL DISTRIBUTION LIST

1. Defense Technical Information Center
   Ft. Belvoir, Virginia

2. Dudley Knox Library
   Naval Postgraduate School
   Monterey, California